

A STUDY OF SUPERSONIC FLOW PAST VIBRATING  
SHELLS AND CASCADES

Christian William Brix

Library  
Naval Postgraduate School  
Monterey, California 93940

# NAVAL POSTGRADUATE SCHOOL

## Monterey, California



# THESIS

A STUDY OF SUPERSONIC FLOW  
PAST VIBRATING SHELLS AND CASCADES

by

Christian William Brix, Jr.

Thesis Advisor:

M. F. Platzer

June 1973

T154909

*Approved for public release; distribution unlimited.*



A Study of Supersonic Flow  
Past Vibrating Shells and Cascades

by

Christian William Brix, Jr.  
Lieutenant, United States Navy  
M.S., Naval Postgraduate School, 1972

Submitted in partial fulfillment of the  
requirements for the degree of

AERONAUTICAL ENGINEER

from the

NAVAL POSTGRADUATE SCHOOL  
June 1973



## ABSTRACT

Supersonic flow past oscillating cylindrical shells and oscillating flat-plate cascades is analyzed using linearized characteristics methods. Pressure distributions and generalized aerodynamic forces are computed for arbitrary radius to length ratios, axial and circumferential wave numbers, Mach numbers, and reduced frequencies. Excellent agreement is obtained with a previous solution of the complete unsteady linearized potential equation by Dowell and Widnall using Laplace transform techniques. Also, pressure distributions are computed for flat-plate cascades with subsonic leading edge locus for arbitrary solidity, stagger angle, frequency, and interblade phase angle. For comparison, a two-blade solution is developed using the method of singularities. Good agreement is obtained for this special case.





## TABLE OF CONTENTS

	Page
I. INTRODUCTION .....	10
II. PROBLEM FORMULATION .....	12
III. THE METHOD OF CHARACTERISTICS .....	19
A. CYLINDRICAL SHELL .....	19
B. CASCADE .....	24
C. THE SAUER-HEINZ PROCEDURE .....	38
IV. COMPUTATIONAL PROCEDURE .....	42
A. CYLINDRICAL SHELL .....	42
B. CASCADE .....	44
C. SAUER-HEINZ .....	49
V. RESULTS AND COMPARISONS .....	52
A. CYLINDRICAL SHELL .....	52
B. CASCADE .....	67
VI. CONCLUSIONS AND RECOMMENDATIONS .....	78
A. CYLINDRICAL SHELL .....	78
B. CASCADE .....	78
APPENDIX A - Cylindrical Shell Program Variables.....	80
APPENDIX B - Cylindrical Shell Flow Diagram.....	82
APPENDIX C - Cascade Program Variables.....	84
APPENDIX D - Cascade Program Flow Diagram.....	88
APPENDIX E - Sauer-Heinz Program Variables.....	90
APPENDIX F - Sauer-Heinz Program Flow Diagram.....	92



	Page
APPENDIX G - Infinite Length Cylinder Theory.....	93
APPENDIX H - Method of Singularities.....	95
APPENDIX I - Program Listings.....	100
LIST OF REFERENCES.....	129
INITIAL DISTRIBUTION LIST.....	131
FORM DD 1473.....	132



## LIST OF ILLUSTRATIONS

Fig.	
1.	Cascade Configuration..... 13
2.	Cylinder Geometry..... 13
3.	Cylindrical Shell Characteristics Network..... 20
4.	General Flow Field Molecule..... 28
5.	Upper Surface Molecule..... 31
6.	Lower Surface Molecule..... 32
7.	New Blade Molecule..... 35
8.	Wake Molecule..... 36
9.	Sauer-Heinz Characteristic Network..... 41
10.	Cascade Computational Area..... 45
11. - 16.	
	Generalized Aerodynamic Force vs. Circumferential Mode Number..... 53
17. - 24.	
	Generalized Aerodynamic Force vs. Radius to Length Ratio..... 59
25.	Pressure Distribution Over Wavy-Walled Cylinder. 68
26. - 29.	
	Cascade Pressure Coefficient Difference vs. Fraction Chord..... 69
30. - 32.	
	Pressure Coefficient Difference vs. Fraction Chord..... 75
H-1	Method of Singularities Configuration..... 95



## LIST OF SYMBOLS

$A_1$	See Equation (G-3)
$C$	Teipel complex velocity of sound perturbation amplitude.
$c$	Velocity of sound perturbation
$\bar{c}$	Local velocity of sound
$c_\infty$	Free-stream velocity of sound
$\hat{c}$	Blade chord
$C_p$	Coefficient of pressure
$\bar{C}_p$	Pressure coefficient amplitude
$d$	Interblade distance
$e$	2.718282
$H_n^{(2)}$	Hankel function of the second kind, order $n$
$h$	Radial deflection (shell) Blade chord line (cascade)
$i$	The square root of minus one
$J_n$	Bessel function of the first kind, order $n$
$k$	Reduced frequency
$L$	Cylinder length
$M$	Free-stream Mach number
$m$	Axial mode number
$N$	Number of blades
$n$	Circumferential mode number
$P$	Non-dimensional complex pressure perturbation amplitude
$p$	Pressure
$p_\infty$	Free-stream pressure





$R$	Radius to length ratio
$r$	Radial coordinate
$S$	Entropy
$\Delta s$	Increment of distance along a characteristic
$T$	Temperature
$t$	Time
$U$	Teipel complex streamwise velocity perturbation amplitude
$u$	Streamwise velocity perturbation
$\bar{u}$	Local streamwise velocity
$u_{\infty}$	Free-stream velocity
$V$	Teipel complex normal velocity perturbation amplitude
$v$	Normal velocity perturbation
$W$	Velocity in the z-direction
$w$	z-direction velocity perturbation
$x, y, z$	Rectangular coordinates
$x, r, \theta$	Cylindrical coordinates
$x_0$	Elastic axis position
$Y_n$	Bessel function of the second kind, order $n$
$Z(x)$	Radial deflection amplitude
$\alpha$	Mach angle
$\beta$	Stagger angle
$\delta$	Interblade phase angle
$\xi, \eta$	Characteristic coordinates
$v$	Grid fineness ratio
$\rho$	Local density
$\rho_{\infty}$	Free-stream density



$\phi$	Velocity perturbation amplitude
$\phi$	Velocity potential amplitude
$\psi_m(x)$	Stream-wise mode shape
$\psi_1$	See Equation (G-3)
$\omega$	Circular frequency
$\pi$	3.141593 .



### ACKNOWLEDGMENT

This thesis was written with the close support and continual assistance of Associate Professor M. F. Platzer.



## I. INTRODUCTION

Supersonic flutter of skin panels first occurred on the German V-2 missile and has become of increasing engineering importance in recent years with the development of supersonic flight vehicles. Panel flutter, for example, was found to occur on the X-15 Rocket Aircraft and Saturn Space Launch Vehicle. An integral part of the flutter analysis of such panels is the determination of the oscillatory pressure distribution. A number of approaches have been formulated which resulted mostly in approximation theories. A detailed review of the state of the art can be found in Reference 6. Only one "exact" approach was worked out by Dowell and Widnall using the complete linearized unsteady potential equation (Ref. 2). However, this approach requires rather complicated and time-consuming complex integration techniques.

In the present work a method of characteristics procedure is developed to determine supersonic flow past vibrating panels and cylindrical shells resulting in a rapid computation of the pressure distribution and generalized aerodynamic forces.

A second flutter problem has also become of considerable interest very recently. Due to the continuing trend toward higher tip speeds in modern jet engine fans and compressors, the possibility of supersonic blade flutter has become of considerable concern. A recent review of this problem area





has been given in "A Workshop on Aeroelasticity in Turbo-machines" (Ref. 13).

In the present study the method of characteristics is applied to compute supersonic flow past a finite flat plate cascade with subsonic leading edge locus. In the past, cascade studies have proved to be a useful tool for the understanding of the complicated three-dimensional, incompressible or subsonic flow through an actual compressor stage. Although it is doubtful that the much more complex mixed transonic-supersonic flow can be modeled by a two-dimensional cascade idealization, the analysis of an infinitely thin flat plate cascade may point the way toward a fuller understanding. The method of characteristics again proved to be a convenient tool for the analysis of supersonic flow past oscillating cascades.



## II. PROBLEM FORMULATION

Inviscid adiabatic flow of a gas along the positive x-axis is considered which is perturbed by either A) an airfoil cascade executing small pitch oscillations (Fig. 1) or B) small amplitude vibrations of the surface of a circular cylinder whose axis is aligned with the free-stream direction (Fig. 2).

The following basic equations hold:

The equation of state for a perfect gas,

$$p = \rho RT \quad (1)$$

the conservation equation for mass,

$$\frac{D\rho}{Dt} + \rho \left( \frac{\partial \bar{u}}{\partial x} + \frac{\partial v}{\partial y} + \frac{\partial w}{\partial z} \right) = 0 \quad (2)$$

the conservation of momentum

$$\frac{D\bar{u}}{Dt} + \frac{1}{\rho} \frac{\partial p}{\partial x} = 0$$

$$\frac{Dv}{Dt} + \frac{1}{\rho} \frac{\partial p}{\partial y} = 0$$

$$\frac{Dw}{Dt} + \frac{1}{\rho} \frac{\partial p}{\partial z} = 0$$

and the conservation of energy

$$\frac{Ds}{Dt} = 0$$

where  $\frac{D}{Dt}$  is the substantial derivative and  $s$  is the entropy of the fluid particle.

The assumption of small amplitude vibrations makes it possible to introduce the small perturbation concept.



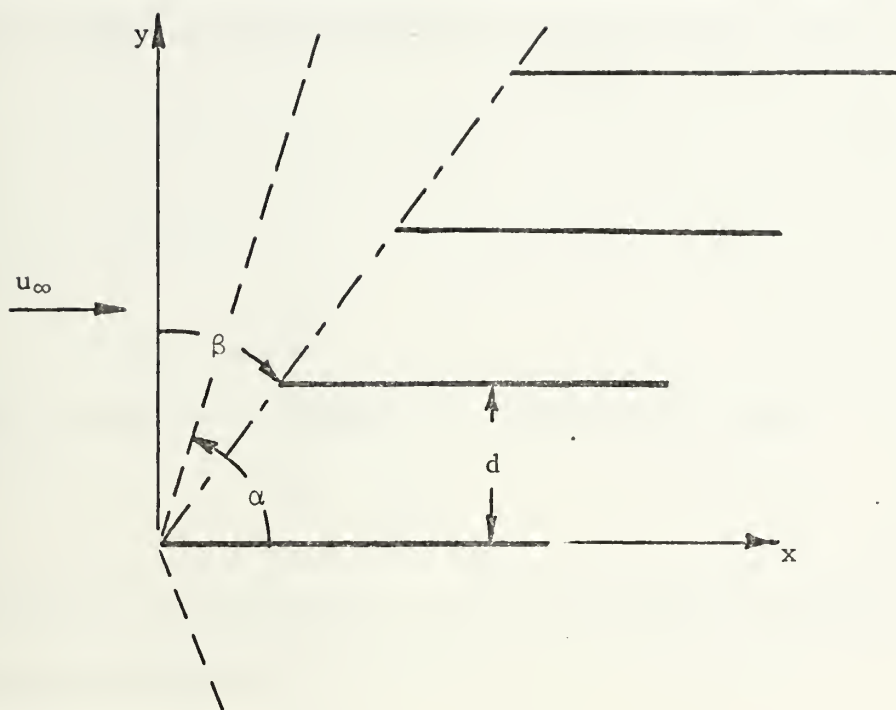


Figure 1. Cascade Configuration

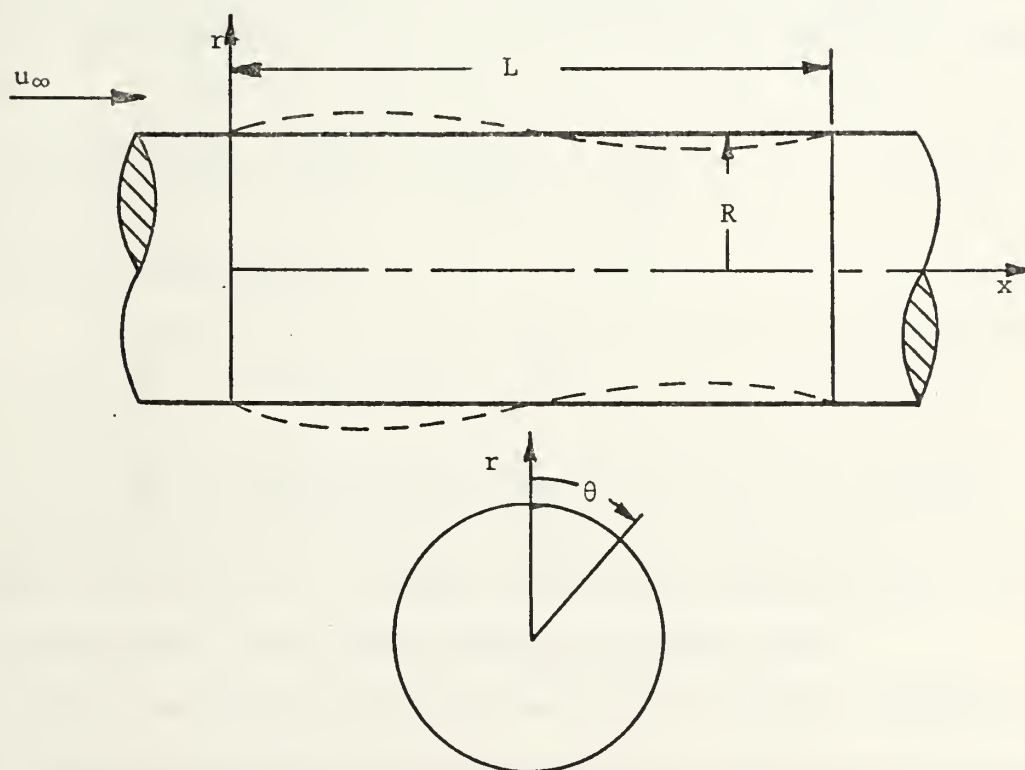


Figure 2. Cylinder Geometry



Therefore, all flow quantities are assumed as small perturbations linearly superimposed on free-stream quantities, i.e.,

$$\bar{u} = u_{\infty} + u \quad (5)$$

$$V = v \quad (6)$$

$$W = w \quad (7)$$

$$\bar{c} = c_{\infty} + c \quad (8)$$

and the pressure and density perturbations are:

$$\Delta p = p - p_{\infty} \quad (9)$$

$$\Delta \rho = \rho - \rho_{\infty} \quad (10)$$

The pressure perturbation can be expressed by the velocity of sound perturbation, i.e.,

$$p - p_{\infty} = \frac{2}{\gamma - 1} \rho_{\infty} c_{\infty} (\bar{c} - c_{\infty}) \quad (11)$$

Specializing to planar flow, one has for the continuity equation:

$$\frac{2}{\gamma - 1} \frac{\partial c}{\partial t} + \frac{2}{\gamma - 1} u_{\infty} \frac{\partial c}{\partial x} + c_{\infty} \frac{\partial u}{\partial x} + c_{\infty} \frac{\partial v}{\partial y} = 0 \quad (12)$$

and the Euler equations:

$$\frac{\partial u}{\partial t} + u_{\infty} \frac{\partial u}{\partial x} + \frac{2}{\gamma - 1} c_{\infty} \frac{\partial c}{\partial x} = 0 \quad (13a)$$

$$\frac{\partial v}{\partial t} + u_{\infty} \frac{\partial v}{\partial x} + \frac{2}{\gamma - 1} c_{\infty} \frac{\partial c}{\partial y} = 0 \quad (13b)$$

Equations (12) and (13) are the governing equations for the case of supersonic flow past oscillating cascades.

For the case of supersonic flow past vibrating cylindrical shells, the equivalent single equation for the perturbation





potential,  $\phi(x, r, \theta, t)$  in cylindrical coordinates was taken as the more convenient basic governing equation, i.e.,

$$(1-M^2)\phi_{xx} + \phi_{rr} + \frac{1}{r}\phi_r + \frac{1}{r^2}\phi_{\theta\theta} - 2\frac{M}{c_\infty}\phi_{xt} - \frac{1}{c_\infty^2}\phi_{tt} = 0 \quad (14)$$

For a derivation of this equation reference is made to one of the standard texts, e.g., Bisplinghof, Ashley, and Halfman, "Aeroelasticity", (Ref. 1).

For a complete formulation, proper initial and boundary conditions must be prescribed. The most important ones are A) the flow on the body surface must be tangent at any instant in time and B) Sommerfeld's radiation condition must be satisfied, i.e., waves must propagate away from sources of disturbance.

After properly linearizing the general flow tangency condition, (see Ref. 1) one obtains for the flow tangency condition on a thin airfoil, performing a time dependent small amplitude motion about the  $y=0$  plane,

$$v = \frac{\partial h}{\partial t} + u_\infty \frac{\partial h}{\partial x} \quad \text{at } y=0 \quad (15)$$

where  $h(x, t)$  is the equation of the airfoil chord line.

For the vibrating cylindrical shell the flow tangency condition over the flexible portion becomes

$$\begin{aligned} \phi_r \Big|_{r=R} &= \frac{\partial h}{\partial t} + u_\infty \frac{\partial h}{\partial x} & 0 \leq x \leq 1 \\ \phi_r \Big|_{r=R} &= 0 & x < 0 \end{aligned} \quad (16)$$



where  $h(x, \theta, t)$  in this case describes the radial shell deflection.

With the assumption of a perturbation potential, the momentum equations, equations (3), may be integrated to

$$\frac{\partial \phi}{\partial t} + \frac{u_{\infty}^2}{2} + u_{\infty} \frac{\partial \phi}{\partial x} + \int \frac{dp}{\rho} = c(t) \quad (17)$$

assuming uniform parallel flow far upstream,

$$c(t) = \frac{u_{\infty}^2}{2} \quad (18)$$

Also, the density-pressure relationship can be expanded as

$$\rho(p) = \rho_{\infty} + \left(\frac{d\rho}{dp}\right)(p - p_{\infty}) + \frac{1}{2} \left(\frac{d^2\rho}{dp^2}\right)(p - p_{\infty})^2 + \dots \quad (19)$$

therefore,

$$\int_{p_{\infty}}^p \frac{dp}{\rho(p)} = \frac{1}{\rho_{\infty}} \int_{p_{\infty}}^p \left[ 1 - \frac{p - p_{\infty}}{p_{\infty} \gamma} \right] dp \approx \frac{p - p_{\infty}}{\rho_{\infty}} \quad (20)$$

Hence, the perturbation pressure can be expressed in terms of the perturbation potential, i.e.,

$$p - p_{\infty} = -\rho_{\infty} \left[ \frac{\partial \phi}{\partial t} + u_{\infty} \frac{\partial \phi}{\partial x} \right] \quad (21)$$

In pressure coefficient form this becomes

$$C_p = \frac{p - p_{\infty}}{\frac{1}{2} \rho_{\infty} u_{\infty}^2} = -\frac{2}{u_{\infty}^2} \phi_t - \frac{2}{u_{\infty}} \phi_x \quad (22)$$

For further analysis it is convenient to use non-dimensional quantities. Introducing for the oscillating cascade case the blade chord as the unit of length one has the following non-dimensional coordinates:



$$\bar{x} = \frac{x}{\hat{c}}, \quad \bar{y} = \frac{y}{\hat{c}}, \quad \bar{t} = \frac{t}{\hat{c}} \frac{u_\infty}{\hat{c}} \quad (23)$$

Furthermore, introducing the assumption of harmonic time-dependence, one can define a reduced frequency

$$k = \frac{\omega \hat{c}}{u_\infty} \quad (24)$$

where  $\omega$  is the circular frequency of blade oscillation.

Following previous work by Teipel (Ref. 3) for single blade oscillations the non-dimensional complex amplitude functions

$$U(\bar{x}, \bar{y}) e^{i\omega t} = \frac{u}{u_\infty} \quad (25)$$

$$V(\bar{x}, \bar{y}) e^{i\omega t} = \frac{1}{\sqrt{M^2 - 1}} \frac{v}{u_\infty} \quad (26)$$

$$C(\bar{x}, \bar{y}) e^{i\omega t} = \frac{2}{\gamma - 1} \frac{1}{M^2} \frac{c}{c_\infty} \quad (27)$$

are introduced. Substituting these equations into the continuity and Euler equations (12) and (13) gives

$$\frac{\partial U}{\partial x} + \sqrt{M^2 - 1} \frac{\partial V}{\partial y} + M^2 \frac{\partial C}{\partial x} + ikM^2 C = 0 \quad (28)$$

$$\frac{\partial U}{\partial x} + \frac{\partial C}{\partial x} + ikU = 0 \quad (29)$$

$$\frac{\partial V}{\partial x} + \frac{1}{\sqrt{M^2 - 1}} \frac{\partial C}{\partial y} + ikV = 0 \quad (30)$$

where the overbar on  $x$  and  $y$  is being dropped for convenience in the subsequent analysis.

Introducing similar non-dimensional variables with distances referred to flexible cylinder length, velocities to free-stream speed and time to cylinder length divided by free-stream speed, one obtains the equation for the non-dimensional perturbation potential, i.e.,



$$(1-M^2)\phi_{xx} + \phi_{rr} + \frac{1}{r^2}\phi_{\theta\theta} - 2M^2\phi_{xt} - M^2\phi_{tt} = 0 \quad (31)$$

subject to the boundary condition

$$\begin{aligned} \phi_r \Big|_{r=R} &= \frac{\partial h}{\partial t} + \frac{\partial h}{\partial x} & 0 \leq x \leq 1 \\ &= 0 & x < 0 \end{aligned} \quad (32)$$

If the radial shell deflection is assumed as

$$h(x, \theta, t) = Z(x) \cos n\theta \cdot e^{ikt} \quad (33)$$

where  $k$  is now referred to cylinder length, i.e.,

$$k = \frac{\omega L}{u_\infty} \quad (34)$$

Then the velocity potential must also have the form,

$$\phi(x, r, \theta, t) = \phi(x, r) \cos n\theta \cdot e^{ikt} \quad (35)$$

Substitution of equation (35) into equation (31) then gives

$$(1-M^2)\phi_{xx} + \phi_{rr} + \frac{1}{r}\phi_r - \frac{n^2}{r^2}\phi - 2ikM^2\phi_x + k^2M^2\phi = 0 \quad (36)$$

subject to

$$\begin{aligned} \phi_r \Big|_{r=R} &= \frac{\partial Z}{\partial x} + ikZ & 0 \leq x \leq 1 \\ &= 0 & x < 0 \end{aligned} \quad (37)$$

The pressure coefficient in terms of the non-dimensional velocity potential is

$$C_p = -2[ik\phi + \phi_x] \quad (38)$$

and the pressure coefficient amplitude is

$$\bar{C}_p = -2[ik\phi + \phi_x] \quad (38a)$$

These are the basic equations used in the subsequent cylindrical shell vibration analysis.





### III. THE METHOD OF CHARACTERISTICS

#### A. CYLINDRICAL SHELL

In Section II, equation (36) was developed as the partial differential equation for  $\phi(x,r)$  that requires solution subject to the boundary condition, equation (37). The following developments are based on a previous paper by Platzer, Brix, and Webster, (Ref. 7).

If  $M > 1$ , equation (30) is hyperbolic and has real characteristics, which satisfy the ordinary differential equation

$$(M^2 - 1)dr^2 - dx^2 = 0 \quad (39)$$

An arbitrary function  $F(x,r)$  has the following derivatives along the two characteristics:

$$\frac{dF}{ds} = F_x \cdot \frac{dx}{ds} + F_r \frac{dr}{ds} = \frac{\sqrt{M^2 - 1}}{M} F_x \pm \frac{1}{M} F_r \quad (40)$$

where  $ds$  is the differential arc-length along the characteristic  $ds^2 = M^2 dr^2$  and

$$\frac{dx}{ds} = \frac{\sqrt{M^2 - 1}}{M} \quad (41)$$

and

$$\frac{dr}{ds} = \pm \frac{1}{M} \quad (42)$$

Letting  $s_1$  be the arc-length of the left-running Mach line and  $s_2$  the arc-length of the right-running Mach line, one obtains for the first derivatives,

$$F_1 = \frac{\sqrt{M^2 - 1}}{M} F_x + \frac{1}{M} F_r \quad (43)$$



and

$$F_2 = \frac{\sqrt{M^2-1}}{M} F_x - \frac{1}{M} F_r \quad (44)$$

and for the second derivatives

$$-F_{12} = \frac{dF_1}{ds_2} = \frac{1}{M^2} [(1-M^2)F_{xx} + F_{rr}] = -F_{21} \quad (45)$$

Therefore, equation (30) can be written as

$$\frac{d\phi_1}{ds_2} = \frac{\phi_1 - \phi_2}{2rM} - \frac{ikM}{\sqrt{M^2-1}} (\phi_1 + \phi_2) + (k^2 - \frac{n^2}{r^2 M^2}) \phi \quad (46)$$

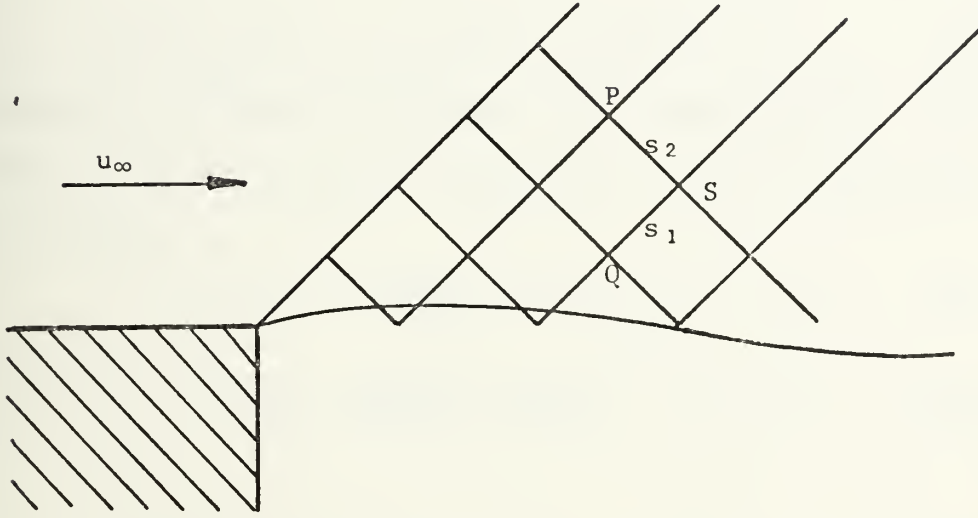


Figure 3. Cylindrical Shell Characteristics Network

The finite difference form of this equation for the points P and S (see Figure 3) on the right-running Mach line is

$$\frac{\phi_1(S) - \phi_1(P)}{\Delta s} = \frac{\phi_1 - \phi_2}{2rM} - \frac{ikM}{\sqrt{M^2-1}} (\phi_1 + \phi_2) + (k^2 - \frac{n^2}{r^2 M^2}) \phi \quad (47)$$

Similarly, for the points Q and S on the left-running Mach line one obtains

$$\frac{\phi_2(S) - \phi_2(Q)}{\Delta s} = \frac{\phi_1 - \phi_2}{2rM} - \frac{ikM}{\sqrt{M^2-1}} (\phi_1 + \phi_2) + (k^2 - \frac{n^2}{r^2 M^2}) \phi \quad (48)$$



Now solving for the values of  $\phi_1$  and  $\phi_2$  at S from the known values at P and Q (Figure 3) the entire flow field may be computed point by point. For this purpose the values for  $\phi_1$  and  $\phi_2$  in equation (47) are averaged between P and S, i.e.,

$$\phi_1 = \frac{\phi_1(P) + \phi_1(S)}{2} \quad (49)$$

$$\phi_2 = \frac{\phi_2(P) + \phi_2(S)}{2} \quad (50)$$

and

$$\phi(S) = \phi(P) + \frac{1}{2} [\phi_2(P) + \phi_2(S)] \Delta s \quad (51)$$

is obtained by integration along the right-running Mach line.

Similarly,  $\phi_1$  and  $\phi_2$  in equation (48) are averaged between Q and S

$$\phi_1 = \frac{\phi_1(Q) + \phi_1(S)}{2} \quad (52)$$

$$\phi_2 = \frac{\phi_2(Q) + \phi_2(S)}{2} \quad (53)$$

and

$$\phi(S) = \phi(Q) + \frac{1}{2} [\phi_1(Q) + \phi_1(S)] \Delta s \quad (54)$$

This results in a system of two equations for  $\phi_1(S)$  and  $\phi_2(S)$ , i.e.,

$$A\phi_1(S) + B\phi_2(S) = C \quad (55)$$

$$D\phi_1(S) + E\phi_2(S) = F \quad (56)$$



where

$$A = 1 - \frac{\Delta s}{4Mr(S)} + \frac{ikM\Delta s}{2\sqrt{M^2-1}} \quad (57)$$

$$B = \frac{\Delta s}{4Mr(S)} + \frac{ikM\Delta s}{2\sqrt{M^2-1}} - \frac{\Delta s^2}{4} \left( k^2 - \frac{n^2}{M^2 r^2(S)} \right) \quad (58)$$

$$\begin{aligned} C = & \phi_1(P) \left[ 1 + \frac{\Delta s}{4Mr(P)} - \frac{ikM\Delta s}{2\sqrt{M^2-1}} \right] \\ & + \phi_2(P) \left[ -\frac{\Delta s}{4Mr(P)} - \frac{ikM\Delta s}{2\sqrt{M^2-1}} + \frac{\Delta s^2}{4} \left( k^2 - \frac{n^2}{M^2 r^2(S)} \right) \right] \end{aligned} \quad (59)$$

$$D = \frac{\Delta s}{4Mr(S)} - \frac{ikM\Delta s}{2\sqrt{M^2-1}} + \frac{\Delta s^2}{4} \left( k^2 - \frac{n^2}{M^2 r^2(S)} \right) \quad (60)$$

$$E = -1 - \frac{\Delta s}{4Mr(S)} - \frac{ikM\Delta s}{2\sqrt{M^2-1}} \quad (61)$$

$$\begin{aligned} F = & \phi_2(Q) \left[ -1 + \frac{\Delta s}{4Mr(Q)} + \frac{ikM\Delta s}{2\sqrt{M^2-1}} \right] \\ & + \phi_1(Q) \left[ -\frac{\Delta s}{4r(Q)M} + \frac{ikM\Delta s}{2\sqrt{M^2-1}} - \frac{\Delta s^2}{4} \left( k^2 - \frac{n^2}{M^2 r^2(S)} \right) \right] \\ & + \phi(Q) \left[ -\frac{\Delta s}{2} \left( k^2 - \frac{n^2}{r^2(S)M^2} \right) - \frac{\Delta s}{2} \left( k^2 - \frac{n^2}{M^2 r^2(Q)} \right) \right] \end{aligned} \quad (62)$$

The above procedure will suffice for the computation of  $\phi$  and its derivatives at a general flow field point, but needs to be modified to obtain the values on the initial Mach line and along the cylinder surface.

On the initial Mach line (Figure 3) it is known that  $\phi = \phi_1 = 0$ . Hence, equation (56) becomes

$$E\phi_2(S) = F \quad (63)$$





where E is known from equation (61) and F simplifies to

$$F = \phi_2(Q) \left[ -1 + \frac{\Delta s}{4Mr(Q)} + \frac{ikM\Delta s}{2\sqrt{M^2-1}} \right] \quad (64)$$

On the cylinder surface the normal velocity is prescribed, i.e.,

$$\phi_r = \frac{M}{2} (\phi_1 - \phi_2) = \frac{\partial Z}{\partial x} + ikZ \quad (65)$$

whereas equation (55) must hold along the right-running Mach line. The values for  $\phi_1$  and  $\phi_2$  on the surface are then found from

$$\phi_1(S) = \frac{C + \frac{2}{M} \left( \frac{\partial Z}{\partial x} + ikZ \right) B}{A + B} \quad (66)$$

and

$$\phi_2(S) = \frac{C - \frac{2}{M} \left( \frac{\partial Z}{\partial x} + ikZ \right) B}{A + B} \quad (67)$$

The pressure distribution over the vibrating cylindrical shell is obtained from the linearized pressure amplitude, equation (38a), and the generalized aerodynamic force  $Q_{mr}$  is found from

$$Q_{mr} = \frac{1}{2} \int_0^1 \bar{C}_{pm}(x) \psi_r(x) dx \quad (68)$$

where

$$Z(x) = \sum_m A_m \psi_m(x) \quad (69)$$

and  $\bar{C}_{pm}(x)$  is the aerodynamic pressure amplitude due to the deflection  $\psi_m(x)$ .

These equations were programmed in Fortran IV. The program description appears in Section IV-A.



## B. CASCADE

In Section II equations (28) - (30) were developed as the governing system of partial differential equations for the analysis of the cascade problem. A solution of these equations can be obtained using the method of characteristics. The following development of this method is largely based on the previous work by Teipel (Ref. 3) and Chalkley (Ref. 9), where further details can be found.

Transforming the system into a new coordinate system,  $\xi(x,y)$  and  $\eta(x,y)$ , and considering now a system of three simultaneous equations in unknowns  $U_\xi$ ,  $V_\xi$ , and  $C_\xi$ , the equations may be written

$$\begin{aligned} \xi_x U_\xi + \cot \alpha \xi_y V_\xi + M^2 \xi_x C_\xi = & - U_\eta \eta_y - \cot \alpha V_\eta \eta_y \\ & - M^2 C_\eta \eta_x - ikM^2 C \end{aligned} \quad (70)$$

$$\xi_x U_\xi + \xi_x C_\xi = - U_\eta \eta_x - C_\eta \eta_x - ikU \quad (71)$$

$$\xi_x V_\xi + \tan \alpha \xi_y C_\xi = - V_\eta \eta_x - \tan \alpha C_\eta \eta_y - ikV \quad (72)$$

If  $U_\xi$ ,  $V_\xi$ , and  $C_\xi$  are made indeterminate across lines of  $\eta = \text{constant}$ , the determinant of the matrix of coefficients of the above equations must equal zero, or

$$-\xi_x^3 - \xi_x [\xi_y^2 - M^2 \xi_x^2] = 0 \quad (73)$$

The solutions to this equation give the three characteristic directions in the physical  $(x,y)$  plane:

$$\frac{dy}{dx} = 0 \quad (74)$$

$$\frac{dy}{dx} = \pm \tan \alpha \quad (75)$$



In order to find the compatibility relations of the first derivatives of  $U$ ,  $V$ , and  $C$  along the characteristics, equations (70) - (72) are written along lines of  $\xi = \text{constant}$ ,  $\eta = \text{constant}$ , and along streamlines, that is, for

$$\text{str}(x,y) = \text{constant}, \quad \frac{\partial y}{\partial x} = 0 \quad (76)$$

$$\xi(x,y) = \text{constant}, \quad \frac{\partial y}{\partial x} = \frac{1}{\sqrt{M^2-1}} \quad (77)$$

$$\eta(x,y) = \text{constant}, \quad \frac{\partial y}{\partial x} = \frac{-1}{\sqrt{M^2-1}} \quad (78)$$

If an arbitrary function of  $x$  and  $y$  in the equations is denoted by  $f$  then,  $\frac{\partial f}{\partial x}$  holding  $\text{str}$  constant becomes

$$\left(\frac{\partial f}{\partial x}\right)_{\text{str}} = \frac{\partial f}{\partial x} \quad (79)$$

Likewise,  $\frac{\partial f}{\partial x}$  holding  $\xi$  constant becomes,

$$\left(\frac{\partial f}{\partial x}\right)_{\xi} = \frac{\partial f}{\partial x} + \frac{1}{\sqrt{M^2-1}} \frac{\partial f}{\partial y} \quad (80)$$

and,  $\frac{\partial f}{\partial x}$  holding  $\eta$  constant becomes

$$\left(\frac{\partial f}{\partial x}\right)_{\eta} = \frac{\partial f}{\partial x} = \frac{1}{\sqrt{M^2-1}} \frac{\partial f}{\partial y} \quad (81)$$

Combining these equations and rewriting,

$$\frac{\partial f}{\partial x} = \left(\frac{\partial f}{\partial x}\right)_{\text{str}} \quad (82)$$

$$\frac{\partial f}{\partial x} = \frac{1}{2} \left[ \left(\frac{\partial f}{\partial x}\right)_{\xi} + \left(\frac{\partial f}{\partial x}\right)_{\eta} \right] \quad (83)$$

$$\frac{\partial f}{\partial y} = \frac{1}{2} \sqrt{M^2-1} \left[ \left(\frac{\partial f}{\partial x}\right)_{\xi} - \left(\frac{\partial f}{\partial x}\right)_{\eta} \right] \quad (84)$$

Substituting these relations into the equations of motion gives



$$\begin{aligned} \frac{1}{2} [(\frac{\partial U}{\partial x})_{\xi} + (\frac{\partial U}{\partial x})_{\eta}] + \frac{1}{2} (M^2-1) [(\frac{\partial V}{\partial x})_{\xi} - (\frac{\partial V}{\partial x})_{\eta}] \\ + \frac{1}{2} M^2 [(\frac{\partial C}{\partial x})_{\xi} + (\frac{\partial C}{\partial x})_{\eta}] + ikM^2C = 0 \end{aligned} \quad (85)$$

$$\frac{1}{2} [(\frac{\partial U}{\partial x})_{\xi} + (\frac{\partial U}{\partial x})_{\eta}] + \frac{1}{2} [(\frac{\partial C}{\partial x})_{\xi} + (\frac{\partial C}{\partial x})_{\eta}] + ikU = 0 \quad (86)$$

$$[(\frac{\partial V}{\partial x})_{\xi} + (\frac{\partial V}{\partial x})_{\eta}] + \frac{1}{2} [(\frac{\partial C}{\partial x})_{\xi} - (\frac{\partial C}{\partial x})_{\eta}] + ikV = 0 \quad (87)$$

Subtracting equation (86) from equation (85) gives an equation that is first added to equation (87) and then subtracted from equation (87). The result is two compatibility relations that must be satisfied along lines of constant  $\xi$  and lines of constant  $\eta$ , i.e.,

$$(\frac{\partial V}{\partial x})_{\xi} + (\frac{\partial C}{\partial x})_{\xi} + ik[V + \frac{1}{M^2-1} (M^2C-U)] = 0 \quad (88)$$

$$(\frac{\partial V}{\partial x})_{\eta} - (\frac{\partial C}{\partial x})_{\eta} + ik[V - \frac{1}{M^2-1} (M^2C-U)] = 0 \quad (89)$$

The third compatibility relation is obtained by considering equation (86) along a streamline

$$(\frac{\partial U}{\partial x})_{\text{str}} + (\frac{\partial C}{\partial x})_{\text{str}} + ikU = 0 \quad (90)$$

If irrotational flow is assumed, the equation of irrotationality

$$\frac{\partial u}{\partial y} - \frac{\partial v}{\partial x} = 0 \quad (91)$$

may be substituted for the second equation of motion in the system. With the assumption of simple harmonic motion, it may be written in terms of Teipel's amplitude functions,

$$\frac{\partial U}{\partial y} - \sqrt{M^2-1} \frac{\partial V}{\partial x} = 0 \quad (92)$$

The non-dimensional system of equations can then be written as,





$$\frac{\partial U}{\partial x} + \sqrt{M^2 - 1} \frac{\partial V}{\partial y} + M^2 \frac{\partial C}{\partial x} + ikM^2 C = 0 \quad (93)$$

$$\frac{\partial U}{\partial x} + \frac{\partial C}{\partial x} + ikU = 0 \quad (94)$$

$$\frac{\partial U}{\partial y} - \sqrt{M^2 - 1} \frac{\partial V}{\partial x} = 0 \quad (95)$$

By transforming equations (93) - (95) to the arbitrary coordinate system,  $\xi$  and  $\eta$ , the system can be considered one of simultaneous equations in  $U_\xi$ ,  $V_\xi$ , and  $C_\xi$ . By making any of these derivatives indeterminate, the results of setting the determinant of the matrix of their coefficients equal to zero are equations (74) and (75), the characteristic directions.

By writing the equations of motion, as before, along lines of  $\xi = \text{constant}$  and  $\eta = \text{constant}$  and performing the same algebraic manipulations, the two compatibility relations can be determined:

$$\left(\frac{\partial U}{\partial x}\right)_\xi - \left(\frac{\partial V}{\partial x}\right)_\xi + ik \frac{M^2}{M^2 - 1} (U - C) = 0 \quad (96)$$

$$\left(\frac{\partial U}{\partial x}\right)_\eta + \left(\frac{\partial V}{\partial x}\right)_\eta + ik \frac{M^2}{M^2 - 1} (U - C) = 0 \quad (97)$$

The third compatibility relation is, as before,

$$\left(\frac{\partial U}{\partial x}\right)_{\text{str}} + \left(\frac{\partial C}{\partial x}\right)_{\text{str}} + ikU = 0 \quad (90)$$

The equations of motion are now reduced to a system containing only derivatives with respect to  $x$ . It is, thus, possible to solve these equations using finite differences in the following manner: separating the real from the imaginary parts, the equations can be written,



$$\left(\frac{\partial U_R}{\partial x}\right)_{str} + \left(\frac{\partial C_R}{\partial x}\right)_{str} - kU_I = 0 \quad (98)$$

$$\left(\frac{\partial U_I}{\partial x}\right)_{str} + \left(\frac{\partial C_I}{\partial x}\right)_{str} + kU_R = 0 \quad (99)$$

$$\left(\frac{\partial U_R}{\partial x}\right)_{\xi} - \left(\frac{\partial V_R}{\partial x}\right)_{\xi} - k \frac{M^2}{M^2-1} (U_I - C_I) = 0 \quad (100)$$

$$\left(\frac{\partial U_I}{\partial x}\right)_{\xi} - \left(\frac{\partial V_I}{\partial x}\right)_{\xi} + k \frac{M^2}{M^2-1} (U_R - C_R) = 0 \quad (101)$$

$$\left(\frac{\partial U_R}{\partial x}\right)_{\eta} + \left(\frac{\partial V_R}{\partial x}\right)_{\eta} - k \frac{M^2}{M^2-1} (U_I - C_I) = 0 \quad (102)$$

$$\left(\frac{\partial U_I}{\partial x}\right)_{\eta} + \left(\frac{\partial V_I}{\partial x}\right)_{\eta} + k \frac{M^2}{M^2-1} (U_R - C_R) = 0 \quad (103)$$

To write these equations in finite difference form the computational molecule shown in Figure 4 will be used. With the velocity values all known at  $P_{11}$ ,  $P_{12}$ , and  $P_{21}$ , all the values at  $P_{22}$  can be calculated. The distance  $\Delta x$  is arbitrary.

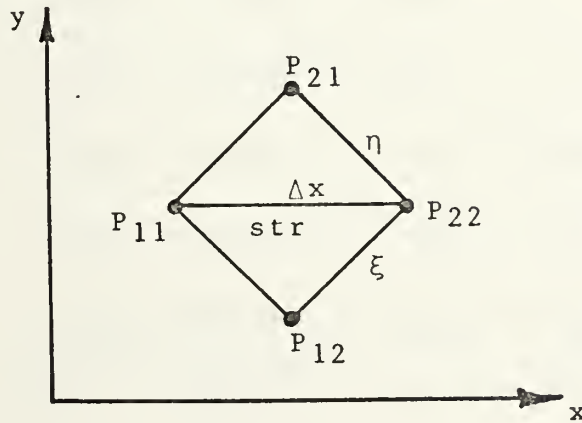


Figure 4. General Flow Field Molecule



If  $F$  is an arbitrary flow quantity, its partial derivatives can be written as

$$\left(\frac{\partial F}{\partial x}\right)_{\text{str}} = \frac{F_{22} - F_{11}}{\Delta x} \quad (104)$$

$$\left(\frac{\partial F}{\partial x}\right)_{\xi} = \frac{F_{22} - F_{12}}{\frac{1}{2} \Delta x} \quad (105)$$

$$\left(\frac{\partial F}{\partial x}\right)_{\eta} = \frac{F_{22} - F_{21}}{\frac{1}{2} \Delta x} \quad (106)$$

The values of the flow quantities in the equations are averages, such that

$$(F)_{\text{str}} = \frac{1}{2} (F_{11} + F_{22}) \quad (107)$$

$$(F)_{\xi} = \frac{1}{2} (F_{12} + F_{22}) \quad (108)$$

$$(F)_{\eta} = \frac{1}{2} (F_{21} + F_{22}) \quad (109)$$

With these relations substituted into equations (98) - (103), the system becomes after some algebraic manipulation,

$$U_{22R} + C_{22R} - A_I U_{22I} = K_{12R} \quad (110)$$

$$U_{22I} + C_{22I} + A_I U_{22R} = K_{12I} \quad (111)$$

$$U_{22R} - V_{22R} + B_I (C_{22I} - U_{22I}) = K_{34R} \quad (112)$$

$$U_{22I} - V_{22I} + B_I (U_{22R} - C_{22R}) = K_{34I} \quad (113)$$

$$U_{22R} + V_{22R} + B_I (C_{22I} - U_{22I}) = K_{56R} \quad (114)$$

$$U_{22I} + V_{22I} + B_I (U_{22R} - C_{22R}) = K_{56I} \quad (115)$$

where

$$K_{12R} = U_{11R} + C_{11R} + A_I U_{11I} \quad (116)$$

$$K_{12I} = U_{11I} + C_{11I} - A_I U_{11R} \quad (117)$$



$$K_{34R} = U_{12R} - V_{12R} + B_I (U_{12I} - C_{12I}) \quad (118)$$

$$K_{34I} = U_{12I} - V_{12I} - B_I (U_{12R} - C_{12R}) \quad (119)$$

$$K_{56R} = U_{21R} + V_{21R} + B_I (U_{21I} - C_{21I}) \quad (120)$$

$$K_{56I} = U_{21I} + V_{21I} - B_I (U_{21R} - C_{21R}) \quad (121)$$

and

$$A_I = \frac{1}{2} k \Delta x \quad (122)$$

$$B_I = \frac{1}{4} k \frac{M^2}{M^2 - 1} \Delta x \quad (123)$$

As shown in Teipel (Ref. 3), solving these equations gives,

$$U_{22R} = \frac{(1 - A_I B_I) \left[ \frac{1}{2} (K_{34R} + K_{56R}) - B_I K_{12I} \right] + 2B_I \left[ \frac{1}{2} (K_{34I} + K_{56I}) + B_I K_{12R} \right]}{(1 - A_I B_I)^2 + (2B_I)^2} \quad (124)$$

$$U_{22I} = \frac{(1 - A_I B_I) \left[ \frac{1}{2} (K_{34I} + K_{56I}) + B_I K_{12R} \right] - 2B_I \left[ \frac{1}{2} (K_{34R} + K_{56R}) - B_I K_{12I} \right]}{(1 - A_I B_I)^2 + (2B_I)^2} \quad (125)$$

$$V_{22R} = \frac{1}{2} (K_{56R} - K_{34R}) \quad (126)$$

$$V_{22I} = \frac{1}{2} (K_{56I} - K_{34I}) \quad (127)$$

$$C_{22R} = K_{12R} - U_{22R} + A_I U_{22I} \quad (128)$$

$$C_{22I} = K_{12I} - U_{22I} - A_I U_{22R} \quad (129)$$

These are the finite difference equations for a point in the general flow field.

At a point on the upper surface of a cascade blade, the normal velocity  $V_{22}$  is prescribed by the movement of the blade.





This velocity was given in the problem formulation. Here the computational molecule is shown in Figure 5.

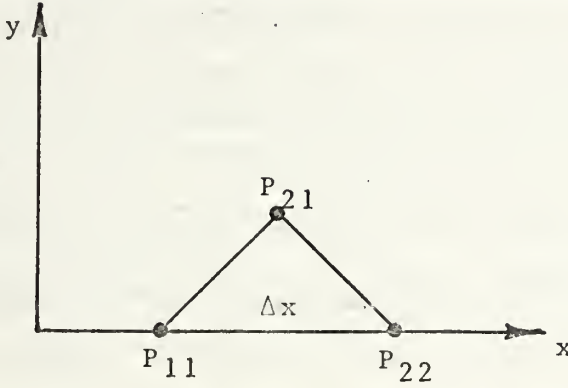


Figure 5. Upper Surface Molecule

The applicable equations are,

$$U_{22R} + C_{22R} - A_I U_{22I} = K_{12R} \quad (130)$$

$$U_{22I} + C_{22I} + A_I U_{22R} = K_{12I} \quad (131)$$

$$U_{22R} - B_I U_{22I} + B_I C_{22I} = K_{56R} - K_{34R} \quad (132)$$

$$U_{22I} + B_I U_{22R} - B_I C_{22R} = K_{56I} - K_{34I} \quad (133)$$

where  $K_{12}$  and  $K_{56}$  are as before, but,

$$K_{34R} = V_{22R} \quad (134)$$

$$K_{34I} = V_{22I} \quad (135)$$

as given by the boundary conditions. Solving for the flow quantities gives

$$U_{22R} = \frac{(1-A_I B_I) [K_{56R} - K_{34R} - B_I K_{12I}] + 2B_I [K_{56I} - K_{34I} + B_I K_{12R}]}{(1-A_I B_I)^2 + (2B_I)^2} \quad (136)$$

$$U_{22I} = \frac{(1-A_I B_I) [K_{56I} - K_{34I} + B_I K_{12R}] - 2B_I [K_{56R} - K_{34R} - B_I K_{12I}]}{(1-A_I B_I)^2 + (2B_I)^2} \quad (137)$$

$$C_{22R} = K_{12R} - U_{22R} + A_I U_{22I} \quad (138)$$



$$C_{22I} = K_{12I} - U_{22I} - A_I U_{22R} \quad (139)$$

and  $V_{22R}$  and  $V_{22I}$  are known from the boundary conditions. These are the finite difference equations for the flow velocities on the upper surface of a cascade blade.

Likewise, at the lower surface of a cascade blade, the normal velocity,  $V_{22}$  is prescribed by the movement of the blade, and was given in the problem formulation. The computational molecule, different from that at the upper surface of the blade, is shown in Figure 6.

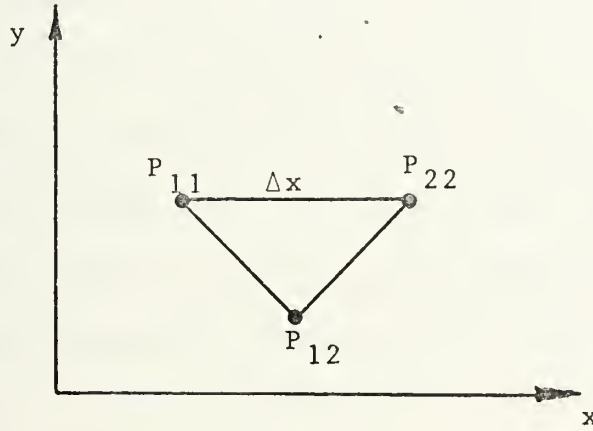


Figure 6. Lower Surface Molecule

Here, the applicable equations are,

$$U_{22R} + C_{22R} - A_I U_{22I} = K_{12R} \quad (140)$$

$$U_{22I} + C_{22I} + A_I U_{22R} = K_{12I} \quad (141)$$

$$U_{22R} - B_I U_{22I} + B_I C_{22I} = K_{56R} + K_{34R} \quad (142)$$

$$U_{22I} + B_I U_{22R} - B_I C_{22R} = K_{56I} + K_{34I} \quad (143)$$

where  $K_{12}$  and  $K_{34}$  are as originally stated, but,

$$K_{56R} = V_{22R} \quad (144)$$

$$K_{56I} = V_{22I} \quad (145)$$



as given by the boundary conditions. Thus, the finite difference equations for the flow velocities at the lower surface of a cascade blade are,

$$U_{22R} = \frac{(1-A_I B_I) [K_{56R} + K_{34R} - B_I K_{12I}] + 2B_I [K_{56I} + K_{34I} + B_I K_{12R}]}{(1-A_I B_I)^2 + (2B_I)^2} \quad (146)$$

$$U_{22I} = \frac{(1-A_I B_I) [K_{56I} + K_{34I} + B_I K_{12R}] - 2B_I [K_{56R} + K_{34R} - B_I K_{12I}]}{(1-A_I B_I)^2 + (2B_I)^2} \quad (147)$$

$$C_{22R} = K_{12R} - U_{22R} + A_I U_{22I} \quad (148)$$

$$C_{22I} = K_{12I} - U_{22I} - A_I U_{22R} \quad (149)$$

where  $V_{22R}$  and  $V_{22I}$  are given from the boundary condition.

To obtain the conditions on the initial left-running Mach line, assume that  $P_{11}$  and  $P_{21}$  as shown in Figure 4 are just in the free-stream and then let  $\Delta x$  shrink to zero.

Since  $K_{12} = K_{56} = 0$  and  $A_I$  and  $B_I$  go to zero as  $\Delta x$  goes to zero, the initial finite difference equations for  $\xi = \text{constant}$  are,

$$U_{22} + C_{22} = 0 \quad (150)$$

$$U_{22} - V_{22} + V_{12} = 0 \quad (151)$$

$$U_{22} + V_{22} = 0 \quad (152)$$

thus,

$$U_{22} = -V_{22} = -C_{22} \quad (153)$$

Equation (96) can be written,

$$\left(\frac{\partial U}{\partial x}\right)_\xi = -ikU \quad (154)$$



Integrating gives,

$$U = U|_{x=0} e^{-ik \frac{M^2}{M^2-1} x} \quad (155)$$

thus,

$$U_{22R} = -V_{22R}(0) \cos \left( k \frac{M^2}{M^2-1} x \right) - V_{22I}(0) \sin \left( k \frac{M^2}{M^2-1} x \right) \quad (156)$$

$$U_{22I} = -V_{22I}(0) \cos \left( k \frac{M^2}{M^2-1} x \right) + V_{22R}(0) \sin \left( k \frac{M^2}{M^2-1} x \right) \quad (157)$$

$$V_{22R} = -U_{22R} \quad (158)$$

$$V_{22I} = -U_{22I} \quad (159)$$

$$C_{22R} = -U_{22R} \quad (160)$$

$$C_{22I} = -U_{22I} \quad (161)$$

For the initial right-running Mach line,  $P_{11}$  and  $P_{12}$  of Figure 4 are assumed to be just in the free-stream and  $\Delta x$  is brought to zero. Since  $K_{12} = K_{34} = 0$ , and  $A_I = B_I = 0$ ,

$$U_{22} + C_{22} = 0 \quad (162)$$

$$U_{22} - V_{22} = 0 \quad (163)$$

$$U_{22} - U_{21} + V_{22} = 0 \quad (164)$$

thus,

$$U_{22} = V_{22} = -C_{22} \quad (165)$$

Equation (97) can then be written,

$$\left( \frac{\partial U}{\partial x} \right)_\eta = -ikU \quad (166)$$

Integrating gives,

$$U = V(0) e^{-ik \frac{M^2}{M^2-1} x} \quad (167)$$





Thus,

$$U_{22R} = V_{22R}(0) \cos \left( k \frac{M^2}{M^2-1} x \right) + V_{22I}(0) \sin \left( k \frac{M^2}{M^2-1} x \right) \quad (168)$$

$$U_{22I} = V_{22I}(0) \cos \left( k \frac{M^2}{M^2-1} x \right) - V_{22R}(0) \sin \left( k \frac{M^2}{M^2-1} x \right) \quad (169)$$

$$V_{22R} = U_{22R} \quad (170)$$

$$C_{22R} = -U_{22R} \quad (171)$$

$$V_{22I} = U_{22I} \quad (172)$$

$$C_{22I} = -U_{22I} \quad (173)$$

At the first position encountered on a blade other than the first blade there are two grid points for which the flow field quantities must be computed; one on the upper surface and one on the lower surface of the blade.

As in Figure 7 the blade is assumed to protrude a very small distance past  $P_{22}$ , thus necessitating the computation of the upper and lower flow velocities at this point. In this case, the equations developed earlier for an upper surface grid point are used for  $P_{22U}$  and those developed for a lower surface grid point are used at  $P_{22L}$ .

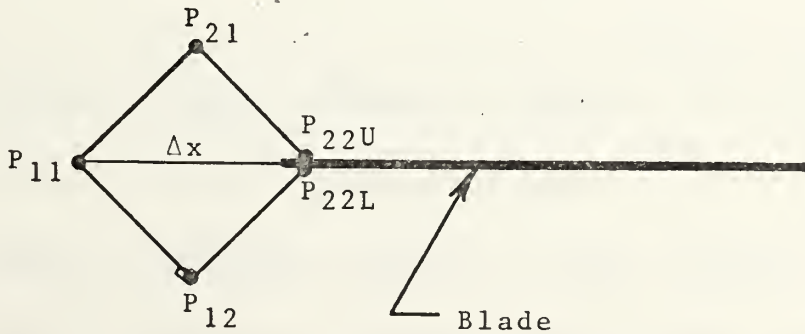


Figure 7. New Blade Molecule



At a position just aft of a blade there are also two grid points to be accounted for; one above and one below the slip plane in the wake. As in Figure 8 the point  $P_{22}$  is assumed to be a very small distance aft of the blade's trailing edge.

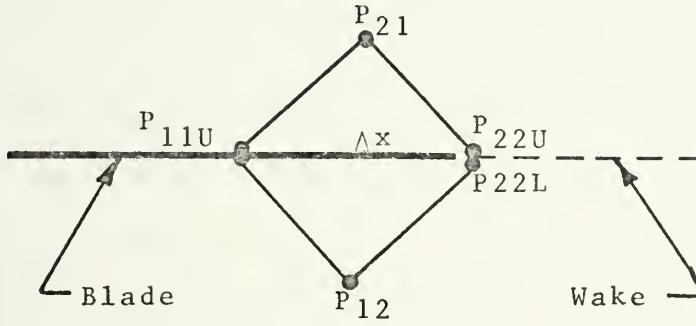


Figure 8. Wake Molecule

At this position the equations for an upper blade grid point apply to  $P_{22U}$  and those for a lower grid point apply to  $P_{22L}$ , i.e.,

$$U_{22RU} + C_{22RU} - A_I U_{22IU} = K_{12RU} \quad (174)$$

$$U_{22IU} + C_{22IU} + A_I U_{22RU} = K_{12IU} \quad (175)$$

$$U_{22RU} + B_I (C_{22IU} - U_{22IU}) = K_{56R} - V_{22RU} \quad (176)$$

$$U_{22IU} + B_I (U_{22RU} - C_{22RU}) = K_{56I} - V_{22IU} \quad (177)$$

and

$$U_{22RL} + C_{22RL} - A_I U_{22IL} = K_{12RL} \quad (178)$$

$$U_{22IL} + C_{22IL} + A_I U_{22RL} = K_{12IL} \quad (179)$$

$$U_{22RL} + B_I (C_{22IL} - U_{22IL}) = V_{22RL} + K_{34R} \quad (180)$$

$$U_{22IL} + B_I (U_{22RL} - C_{22RL}) = V_{22IL} + K_{34I} \quad (181)$$



where

$$K_{12RU} = U_{11RU} + C_{11RU} + A_I U_{11IU} \quad (182)$$

$$K_{12IU} = U_{11IU} + C_{11IU} - A_I U_{11RU} \quad (183)$$

$$K_{12RL} = U_{11RL} + C_{11RL} + A_I U_{11IL} \quad (184)$$

$$K_{12IL} = U_{11IL} + C_{11IL} - A_I U_{11RL} \quad (185)$$

$$K_{34R} = U_{12R} - V_{12R} + B_I (U_{12I} - C_{12I}) \quad (186)$$

$$K_{34I} = U_{12I} - V_{12I} - B_I (U_{12R} - C_{12R}) \quad (187)$$

$$K_{56R} = U_{21R} + V_{21R} + B_I (U_{21I} - C_{21I}) \quad (188)$$

$$K_{56I} = U_{21I} + V_{21I} - B_I (U_{21R} - C_{21R}) \quad (189)$$

Equations (174) - (181) form a system of eight equations with twelve unknowns. However, since it is known that the wake cannot support a pressure difference and that the normal velocities on either side of the wake must be equivalent, i.e.,

$$V_{22RU} = V_{22RL} \equiv V_{22R} \quad (190)$$

$$V_{22IU} = V_{22IL} \equiv V_{22I} \quad (191)$$

$$C_{22RU} = C_{22RL} \equiv C_{22R} \quad (192)$$

$$C_{22IU} = C_{22IL} \equiv C_{22I} \quad (193)$$

we can eliminate four of the unknowns and achieve a determinate system of equations. Equations (174) - (181) become

$$U_{22RU} + C_{22R} - A_I U_{22IU} = K_{12RU} \quad (194)$$

$$U_{22IU} + C_{22I} + A_I U_{22RU} = K_{12IU} \quad (195)$$

$$U_{22RU} + V_{22R} + B_I (C_{22I} - U_{22IU}) = K_{56R} \quad (196)$$

$$U_{22IU} + V_{22I} + B_I (U_{22RU} - C_{22R}) = K_{56I} \quad (197)$$



$$U_{22RL} + C_{22R} - A_I U_{22IL} = K_{12RL} \quad (198)$$

$$U_{22IL} + C_{22I} + A_I U_{22RL} = K_{12IL} \quad (199)$$

$$U_{22RL} - V_{22R} + B_I (C_{22I} - U_{22IL}) = K_{34R} \quad (200)$$

$$U_{22IL} - V_{22I} + B_I (U_{22RL} - C_{22R}) = K_{34I} \quad (201)$$

The pressure distributions along the surfaces of the blades can be determined from equation (11). Dividing both sides of this equation by  $p_\infty$  and using Teipel's amplitude function for  $c$ , the equation can be written,

$$P(x,y) = \gamma M^2 C(x,y) \big|_{y=0^+, y=0^-} \quad (202)$$

where

$$P(x,y) e^{i\omega t} = \frac{p-p_\infty}{p_\infty} \quad (203)$$

Thus the non-dimensional pressure distributions along the upper and lower surfaces of the blades in a cascade can be computed in a point by point calculation of  $U$ ,  $V$ , and  $C$  along lines of  $\xi=\text{constant}$  and  $\eta=\text{constant}$ .

These equations were programmed in Fortran IV. The program description appears in Section IV-B.

#### C. THE LINEARIZED METHOD OF CHARACTERISTICS OF SAUER AND HEINZ

Sauer and Heinz (Ref. 11) developed a linearized method of characteristics for supersonic flow past bodies of revolution at zero angle of attack. This method also is derived from the linearized potential equation for steady supersonic flow, i.e.,

$$(M^2-1)\phi_{xx} - \phi_{rr} - \frac{1}{r}\phi_r = 0 \quad (204)$$





Sauer and Heinz showed that the compatibility relations can be written as

$$\frac{\partial (rv)}{\partial \xi} = -\sqrt{M^2-1} r \frac{\partial u}{\partial \xi} \quad (205)$$

and

$$\frac{\partial (rv)}{\partial \eta} = \sqrt{M^2-1} r \frac{\partial u}{\partial \eta} \quad (206)$$

where

$$u = \frac{\partial \phi}{\partial x} \quad (207)$$

$$v = \frac{\partial \phi}{\partial r} \quad (208)$$

and

$$\xi = x - \sqrt{M^2-1} r \quad (209)$$

$$\eta = x + \sqrt{M^2-1} r \quad (210)$$

are the characteristic coordinates as explained previously.

Writing this equation in finite difference form one obtains for  $u$  and  $v$  at point 4 (Figure 9) using the known values in points 2 and 3,

$$u_4 = \frac{(rv)_3 - (rv)_2 + \sqrt{M^2-1} (r_\eta u_3 + r_\xi u_2)}{\sqrt{M^2-1} (r_\xi + r_\eta)} \quad (211)$$

$$(vr)_4 = \frac{r_\xi (rv)_3 + r_\eta (rv)_2 - \sqrt{M^2-1} r_\xi r_\eta (u_2 - u_3)}{r_\xi + r_\eta} \quad (212)$$

where  $r_\eta$  and  $r_\xi$  are the average  $r$  coordinates between 3 and 4 and between 2 and 4 respectively. Computing the flow properties at the body using the exact flow tangency condition leads to



$$u_5 = \frac{\sqrt{M^2-1} r_\eta u_4 + (rv)_4 - r_5 \left(\frac{dh}{dx}\right)_5}{\sqrt{M^2-1} r_\eta + r_5 \left(\frac{dh}{dx}\right)_5} \quad (213)$$

$$v_5 = \left(\frac{dh}{dx}\right)_5 (1+u_5) \quad (214)$$

where  $r = h(x)$  describes the body contour.

However, in order to apply the Sauer-Heinz procedure to the case of an infinitely long cylinder with a wavy surface between  $0 < x < 1$  a different starting procedure is needed. It is easily seen from Figure 9 that

$$r_2 = \frac{h_0}{2} \left( \frac{1}{\sqrt{M^2-1} \tan \delta_0} + 1 \right) \quad (215)$$

realizing that

$$r_\eta = \frac{R_1 + R_2}{2} \quad (216)$$

where

$$R_1 = R_0 + r_1 \quad (217)$$

and

$$R_2 = R_0 + h_0 \quad (218)$$

one obtains

$$r_\eta = R + \frac{h_0}{4} \left( 3 + \frac{1}{\sqrt{M^2-1} \tan \delta_0} \right) \quad (219)$$

Since there is no disturbance upstream of the leading edge Mach line, one obtains from equation (213)

$$u_2 = \frac{-(R+h_0) \tan \delta_0}{\sqrt{M^2-1} r_\eta + (R+h_0) \tan \delta_0} \quad (220)$$

where the point 2 is the first body point.



Finally, the pressure coefficient is obtained from

$$C_p = 2u - v^2 + u^2 (M^2 - 1) \quad (221)$$

The program listing for these equations is given in Appendix I.

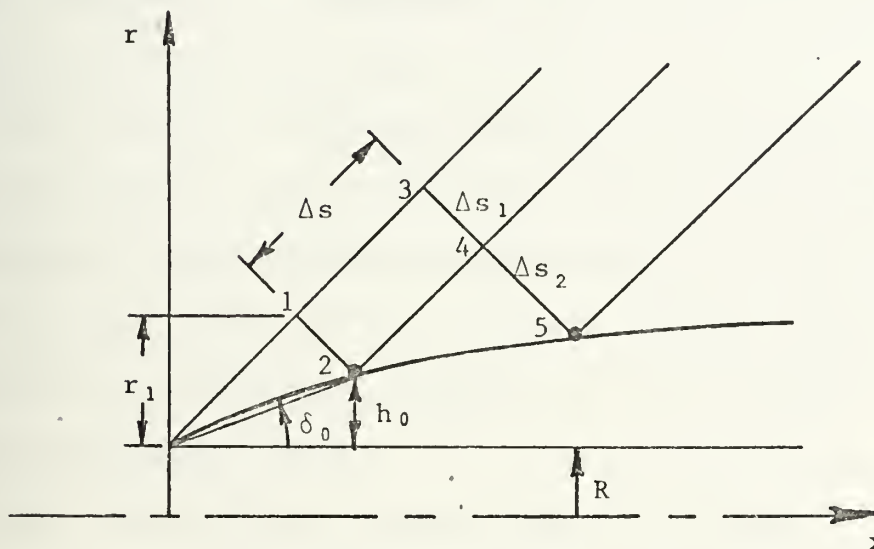


Figure 9. Sauer-Heinz Characteristic Network



#### IV. COMPUTATIONAL PROCEDURE

##### A. CYLINDRICAL SHELL COMPUTER PROGRAM

This program calculates the pressure distribution over a harmonically vibrating cylindrical shell. It is valid only for a cylinder in a supersonic flow field vibrating with small amplitude vibrations.

The program calculates the flow field properties adjacent to the cylinder using the method of characteristics finite difference equations developed previously in Section III. The pressure distribution is then integrated using the trapezoidal rule according to equation (68) to obtain the generalized aerodynamic force.

The computational diagram shown in Figure 3 is used to calculate the flow field quantities at S in the general flow field and on the cylinder surface. The distance  $\Delta s$  shown in the figure is determined by

$$\Delta s = \frac{L \cos \alpha}{v} \quad (222)$$

where  $v$  is the grid fineness ratio. The grid fineness ratio is an arbitrary input variable into the program and is equal to one less than the total number of grid points on the cylinder surface.

Input parameters are entered into the program on two data cards. The first card contains the date, e.g., 11 APR 1973, in the first twelve columns. The second card contains the following input data:





SPACEDATA

1-20	Free-stream Mach number, $M$
21-30	Radius to length ratio, $R$
31-40	Reduced frequency, $k$
41-45	Axial mode number, $m$
46-50	$r$ , as defined in equation (68) for the generalized aero- dynamic force.
51-55	Circumferential mode number, $n$
56-60	Grid fineness ratio, $v$

where the first three quantities are floating point numbers and the rest are integers. The definitions of these parameters are given again in the alphabetical listing of all program variables in Appendix A.

The program has five subroutines. They are as follows:

COMPXR	Computes the $x$ and $r$ position of the given grid point.
MACHLN	Computes the flow quantities along the initial left-running Mach line at the given grid point.
GENFPT	Computes the flow quantities at a general flow field grid point.
PANPNT	Computes the flow quantities on the cylinder surface at the given grid point.
INTEG	Computes the generalized aero- dynamic force.

Flow quantities along the initial left-running Mach line are computed using the equations derived in the method of characteristics for initial conditions. Those quantities on the cylinder surface are computed using the equations derived



for the boundary condition. The values of the velocity potential and its derivatives are derived as a result of the analysis of the flow tangency condition and have been given previously. The procedure starts at the initial Mach line and continues down successive right-running Mach lines. The pressure coefficient is computed when the cylinder surface is met and stored in an array for later use in the integration of the generalized aerodynamic force.

A flow diagram of this program is given in Appendix B.

#### B. OSCILLATING CASCADE PROGRAM

This program calculates the pressure distribution over the upper and lower surfaces of the blades of a subsonic leading edge locus cascade which is oscillating in pitch at arbitrary frequency and interblade phase angle. It is valid only for a cascade in a supersonic flow field vibrating with small amplitude vibrations. The program calculates the flow field quantities within the area governed by the aft-running Mach lines emanating from the leading edge of the first blade and the forward-running Mach lines emanating from the trailing edge of the last blade of the cascade (see Figure 10). These flow field properties are calculated using the method of characteristics finite difference equations developed previously in Section III-B.

The computational molecules shown in Figures 4, 5, 6, 7, and 8 are used to calculate the flow field properties in the general flow field, upper surfaces, lower surfaces, leading edge of a staggered blade, and the wake aft of a blade,



respectively. The distance  $\Delta x$  shown in the figures is determined by

$$\Delta x = \frac{2d}{v} \cot \alpha \quad (223)$$

where  $v$  is the grid fineness ratio. This parameter is an arbitrary input variable into the program and is equal to one less than the total number of grid points on any Mach line that runs from one blade to the next.

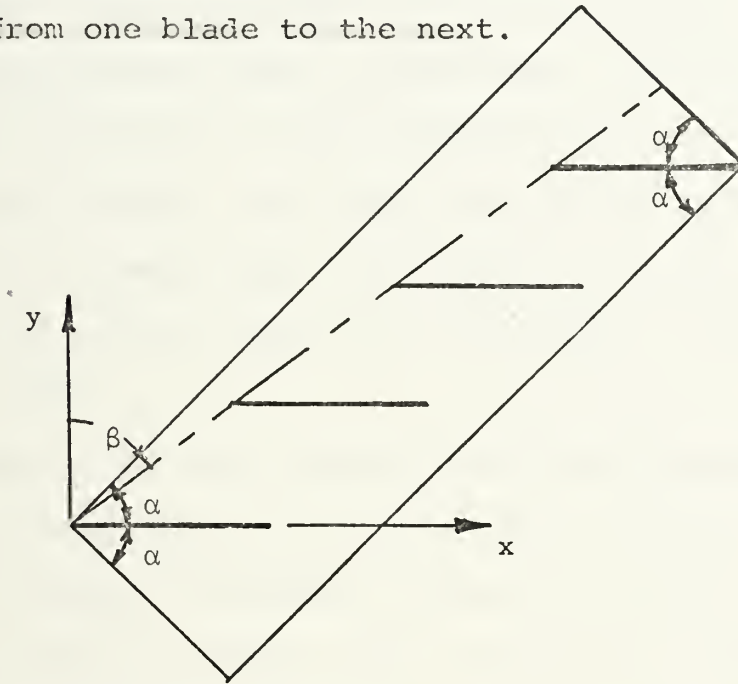


Figure 10. Cascade Computational Area

Input parameters are entered into the program by means of the NAMELIST option of Fortran. In using this option, input parameters are combined in a titled list and then referred to in the program by this title (NAM1). The real advantage of using NAMELIST is that each data card need only contain the value of one input variable while the format of the data card is such that the variable's name is punched on the card as well as its value. In this way, when a different value for an input variable is desired, rather than changing the



entire data deck, only one easily identifiable data card need be changed.

The format for a NAMELIST data deck is as follows: The first column in each card of the data deck is left blank. The first card starts in the second column with the symbol & (ampersand) followed immediately by the title of the NAMELIST (here, NAM1). The next cards list the variables and their input values, one per card, in any order. The format here, starting in the second column and followed by a comma, is: variable name = value. The last card in the data deck and the signal to the computer that the NAMELIST has ended again starts in the second column with the symbol & immediately followed by END.

The value of an input variable may be written in any format as long as integer variables are written without decimal points and real variables are written with a decimal point. Blanks are taken as zeroes, but a comma must appear somewhere between a desired input value and the next data card. The date of the run is entered on a data card in the first twelve spaces. This data card is inserted prior to the NAMELIST dataset.

To illustrate the input procedure, the following example is proposed:

v = 100	d = 0.8
M = $\sqrt{2}$	$\beta = 55^\circ$
k = 0.75	$\delta = 45^\circ$
x <sub>0</sub> = 0.5	
5 blades	





The data cards needed are as follows:

<u>CARD</u>	<u>FORMAT</u>	<u>DESCRIPTION</u>
1	22 JUNE 1973	Date
2	&NAML	NAMELIST title
3	NGRDFN=100,	Grid fineness ratio, must be an even integer, subject to the constraint of equation (227).
4	FSTRMN=1.414214,	Free-stream Mach number
5	REDFRQ=0.80,	Reduced frequency
6	XSUBO=0.50,	Elastic axis position
7	TNWDST=0.80,	Vertical distance between blades.
8	STGANG=55.0,	Complimentary stagger angle, $\tan \beta > \cot \alpha$ .
9	FAZE=45.0,	Interblade phase angle
10	NUMBLD=5,	Number of blades
11	&END	End of NAMELIST

The definitions of these parameters are given again in the alphabetical listing of all program variables in Appendix C.

The program has nine subroutines. They are as follows:

INPUT	Reads in all input data and sets up the finite difference grid.
INITIAL	Initializes all the flow quantities at the leading edge of the first blade and initializes most of the logic variables.
MACHLN	Computes the flow quantities along the initial left and right-running Mach lines at the given grid point.
TOP	Computes the flow quantities on the upper surface of a blade at the given grid point.



GENFPT	Computes the flow quantities at the given general flow field point.
BOTTOM	Computes the flow quantities on the lower surface of a blade at the given grid point.
NEWBLD	Computes the flow quantities at the leading edge of all staggered blades.
WAKE	Computes the flow quantities in the wake aft of each blade at the given grid point. This subroutine uses IBM subroutine SIMQ for the solution of its simultaneous equations.
COMPXY	Computes the x and y position of the given grid point.

In INPUT the grid is determined using the grid fineness ratio, blade spacing, number of blades, and the free-stream Mach number. The value of  $\Delta x$  as shown in equation (223) is obtained. The stagger angle is then adjusted such that the distance the upper blades are staggered back is the nearest multiple number of  $\Delta x$  increments. The "compatible stagger angle" is then printed out. The blades may be staggered such that the first staggered blade is at least one  $\Delta x$  increment aft of the initial left-running Mach line, but no further forward, or,

$$d \cdot (\tan \beta - \cot \alpha) \geq \Delta x \quad (224)$$

Flow quantities along the initial left and right-running Mach lines are computed using the equations derived in the method of characteristics, Section B, for initial conditions. Those flow quantities along the blades' surfaces are computed using the equations derived for the appropriate boundary condition. The equations for the normal velocities are derived as a result of the analysis of the flow tangency condition and have been given previously. The flow quantities



in the wake aft of each blade are computed using the set of simultaneous equations derived as a result of the assumptions made about the flow quantities on either side of the wake and are given in the Method of Characteristics, Section III-B.

The procedure starts at the leading edge of the first blade and computes the flow quantities at grid points along the initial right-running Mach line. It then jumps back to the initial left-running Mach line and computes the flow quantities along the next right-running Mach line, using the applicable subroutines at the appropriate grid points. Only flow quantities on the Mach line presently being computed and the Mach line which preceded it are kept in storage at any one time. Flow quantities at successive grid points are computed in like manner until the trailing edge of the last blade of the cascade is met.

A flow diagram of this program is given in Appendix D.

#### C. SAUER-HEINZ COMPUTER PROGRAM

This program computes the pressure distribution over a cylindrical shell or body of revolution. It is written so that the shape of the body or cylindrical surface may be easily changed. It is valid only for non-oscillating bodies or shells in a supersonic flow field at zero angle of attack. The following discussion applies to the cylindrical shell.

The program calculates the flow field adjacent the cylinder using the method of characteristics finite difference equations developed previously in Section III-C.



The computational diagram shown in Figure 9 is used to compute the flow field properties at 4 in the general flow field and at 5 on the cylinder surface. The distance  $\Delta s$  shown in the figure is determined by,

$$\Delta s = \frac{\cos \alpha}{v} \quad (225)$$

where  $v$  is the grid fineness ratio. The grid fineness ratio is an arbitrary input variable into the program and is equal to one less than the number of grid points on the initial Mach line. The length  $\Delta s_n$ ,  $n=1,2,3\dots$  is determined by the intersection of the right-running Mach lines with the surface.

Input parameters are entered into the program on one data card. This card contains the following input data:

<u>SPACES</u>	<u>DATA</u>
1-10	Free-stream Mach number, $M$
11-20	Maximum amplitude of the axial mode, $h_0$
21-30	Cylinder radius to length ratio, $R$ .
31-40	Axial mode number, $m$
41-50	Grid fineness ratio, $v$

where the first three quantities are floating point numbers and the last two are integers. The definitions of these quantities are given again in the alphabetical listing of all program variables in Appendix E.

The program has three subroutines. They are as follows:

COMPXR	Computes the $x$ and $r$ position of the grid point and determines the position of the intersection of the current right-running Mach line with the body.
GENFPT	Computes the flow quantities at a general flow field grid point.





SURFAC

Computes the flow quantities at the given surface point.

Flow quantities on the initial left-running Mach line are assumed to be zero. Those quantities on the surface are computed using the appropriate equations developed in Section III-C, for surface grid points.

The procedure starts at the initial Mach line and continues down successive right-running Mach lines. The pressure coefficient is computed when the surface is met.

A flow diagram of this program is given in Appendix F.



## V. RESULTS AND COMPARISONS

### A. CYLINDRICAL SHELL

Pressure distributions and generalized aerodynamic forces were computed for sinusoidal deflection modes, i.e.,

$$\psi_m(x) = \sin(m\pi x) \quad m=1,2,\dots \quad (226)$$

Figures 11 through 16 show results for the generalized aerodynamic forces  $Q_{11}$  and  $Q_{12}$  as a function of circumferential mode number for two radius to length ratios,  $r=0.5$  and  $r=1.0$ , at a Mach number of  $\sqrt{2}$  and reduced frequencies of zero and one. Also shown is the comparison with two previous solutions by Dowell and Widnall (Ref. 2) and by Matsuzaki and Kobayashi (Ref. 5). The Dowell and Widnall solution is also based on the complete linearized unsteady potential equation, but uses Laplace transform techniques for its solution. As can be seen, agreement between this solution and the method of characteristics solution is excellent. For the sake of interest, a recent approximate solution by Matsuzaki and Kobayashi, valid only for large values of the circumferential mode number is also shown.

Figures 17 through 24 show the generalized aerodynamic forces  $Q_{11R}$  and  $Q_{12R}$  as a function of radius to length ratio again for a Mach number of  $\sqrt{2}$ , zero reduced frequency, and circumferential mode numbers  $n=0,1,2$ , and 3. The main purpose of these figures is to show that the infinite cylinder theory is a poor approximation for small radius to length ratios, but approaches the exact theory for large values of  $R$ .



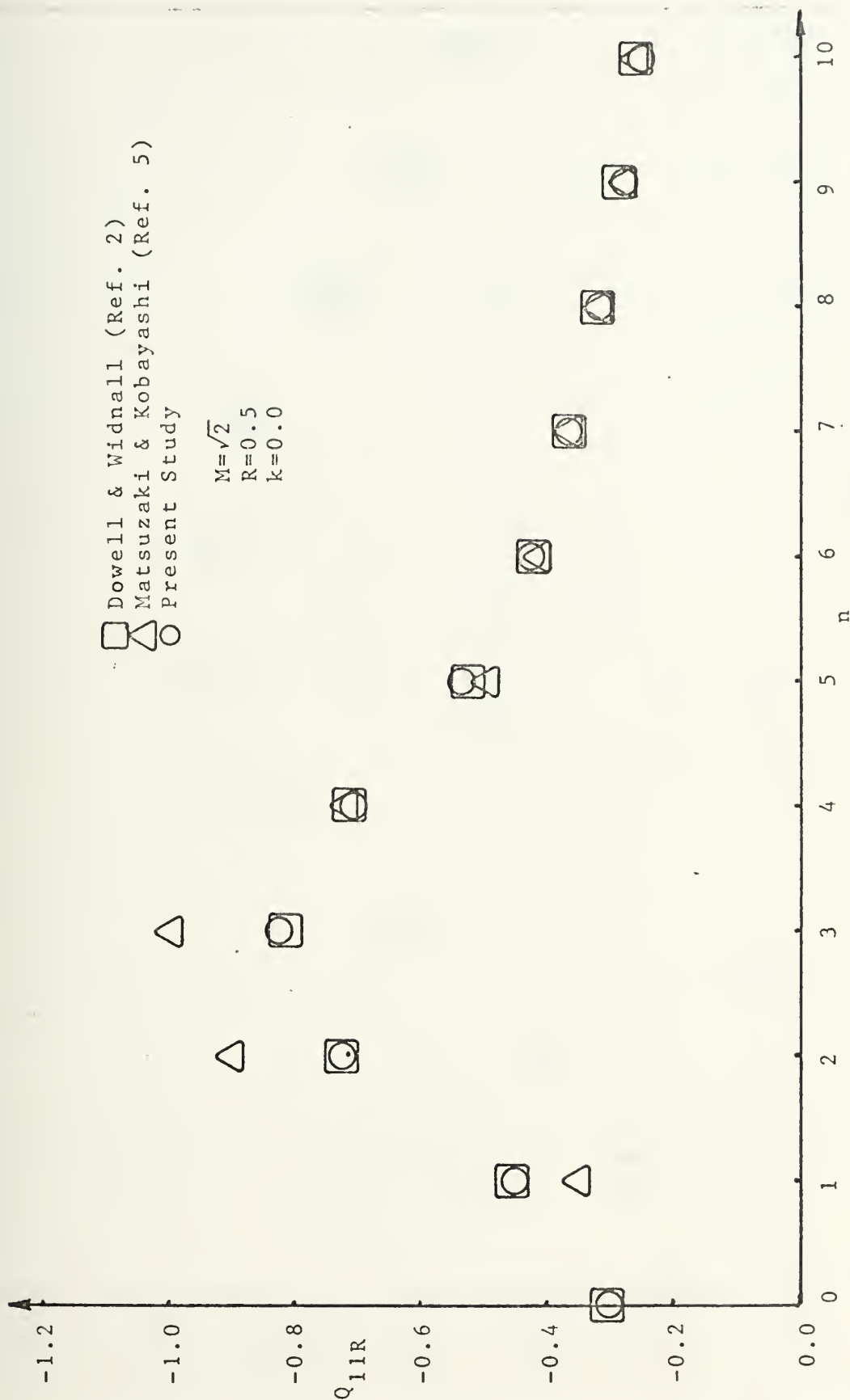


Figure 11. Generalized Aerodynamic Force vs. Circumferential Mode Number



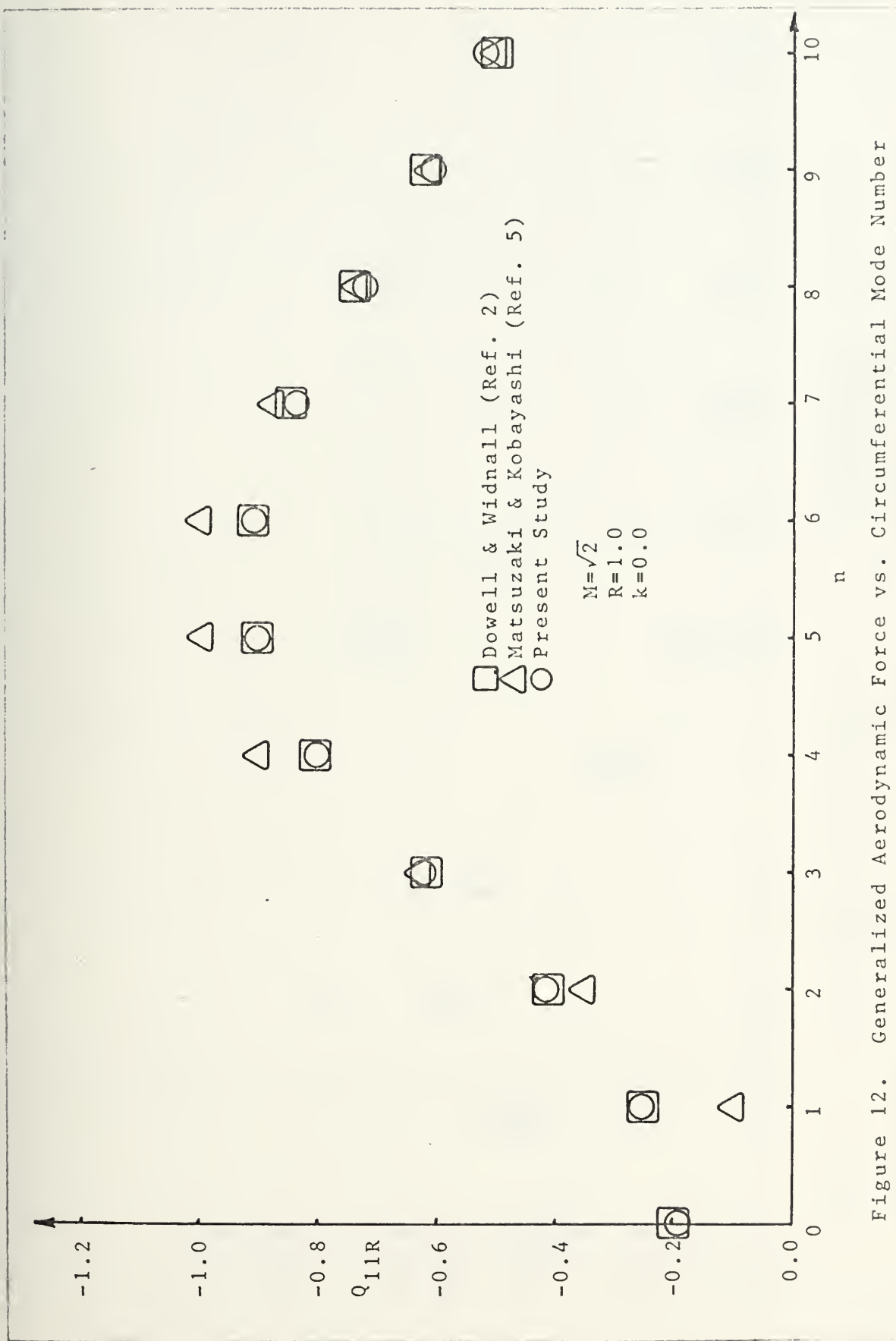


Figure 12. Generalized Aerodynamic Force vs. Circumferential Mode Number





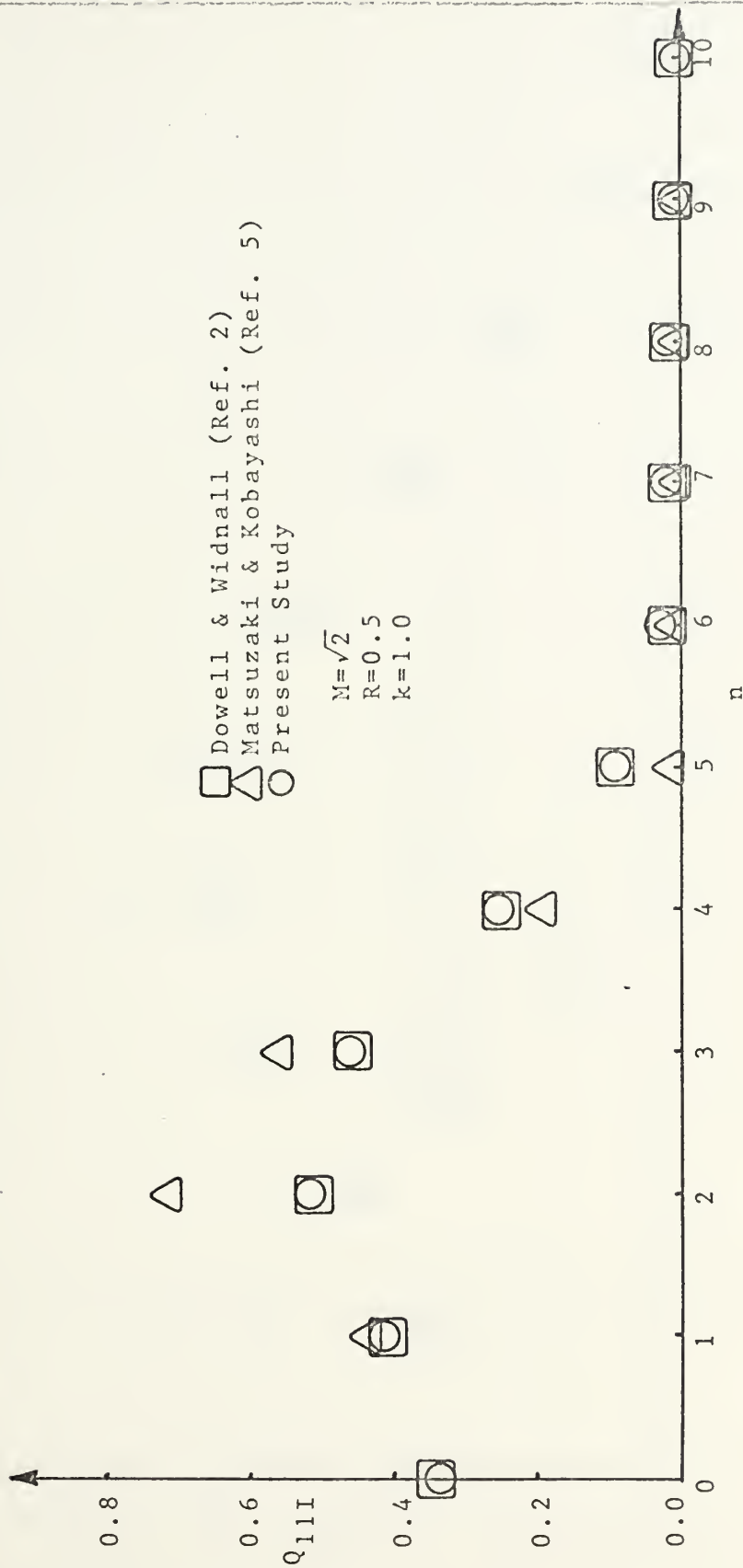


Figure 13. Generalized Aerodynamic Force vs. Circumferential Mode Number



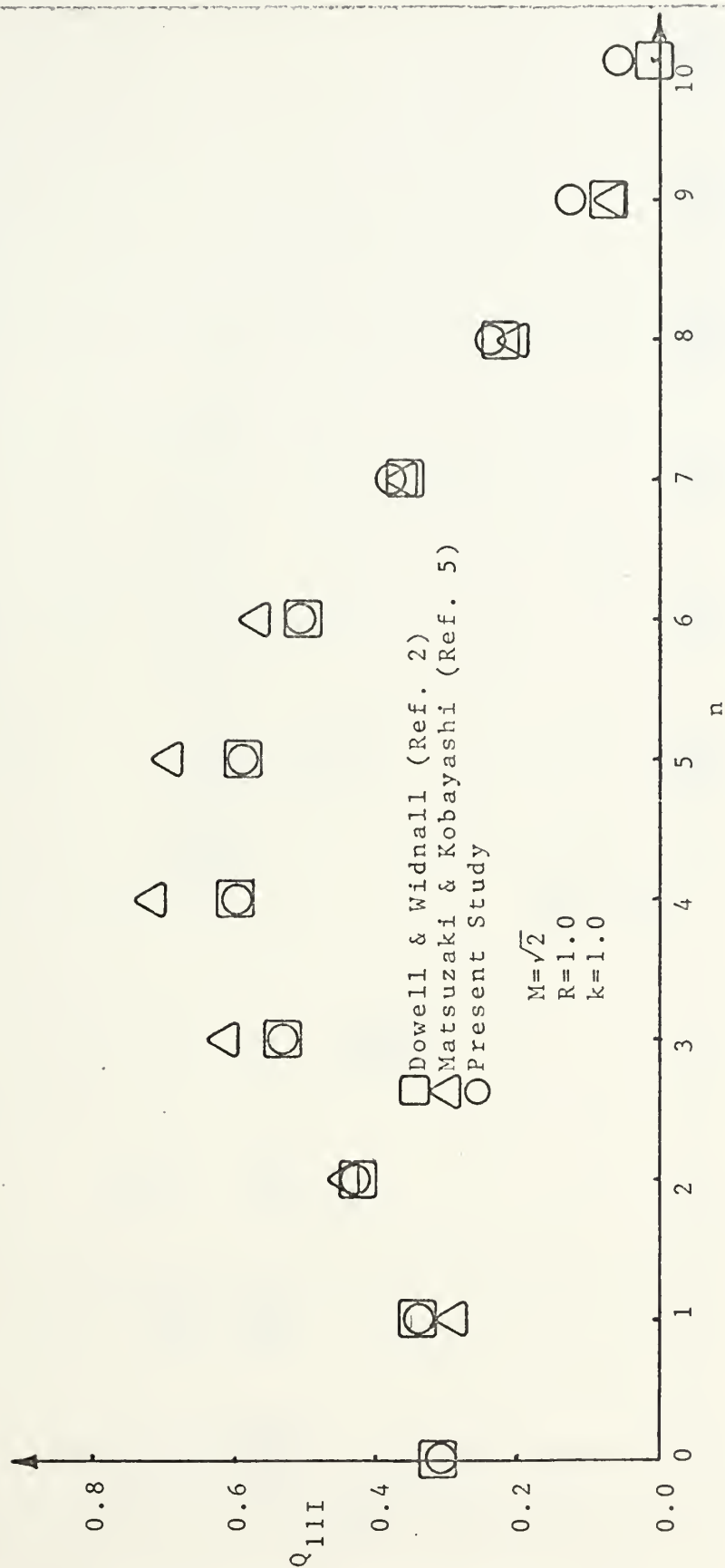


Figure 14. Generalized Aerodynamic Force vs. Circumferential Mode Number



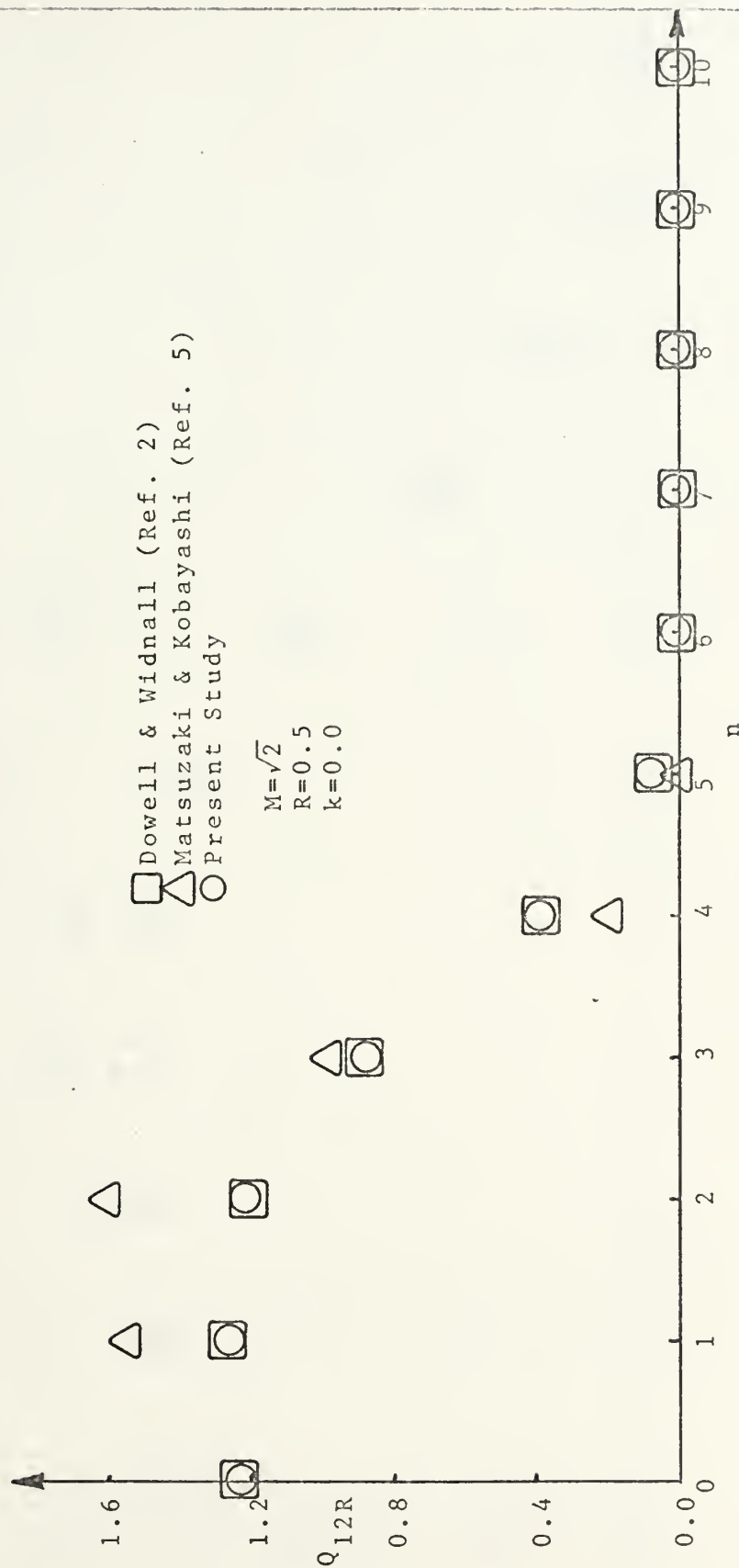


Figure 15. Generalized Aerodynamic Force vs. Circumferential Mode Number



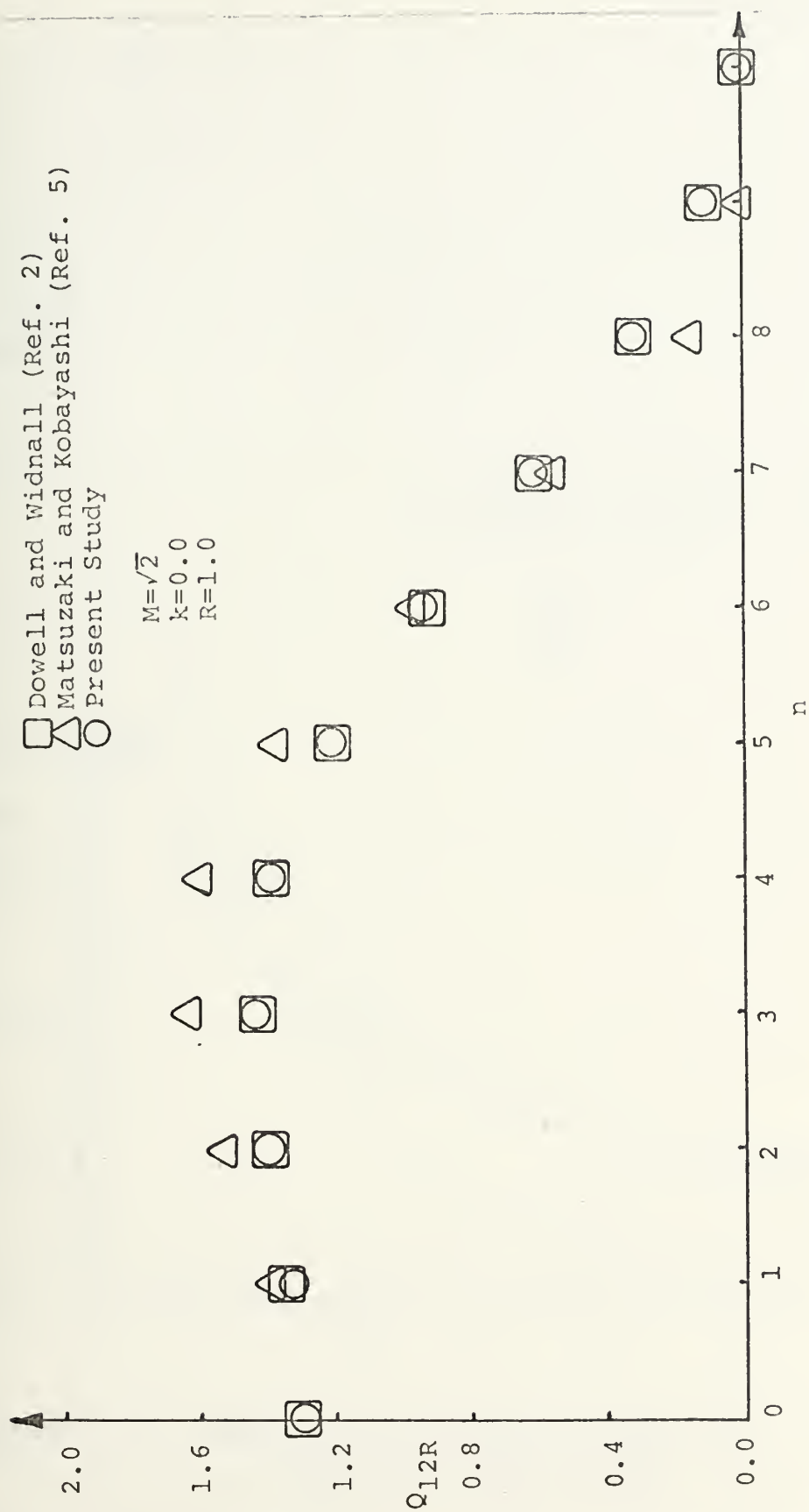


Figure 16. Generalized Aerodynamic Force vs. Circumferential Mode Number





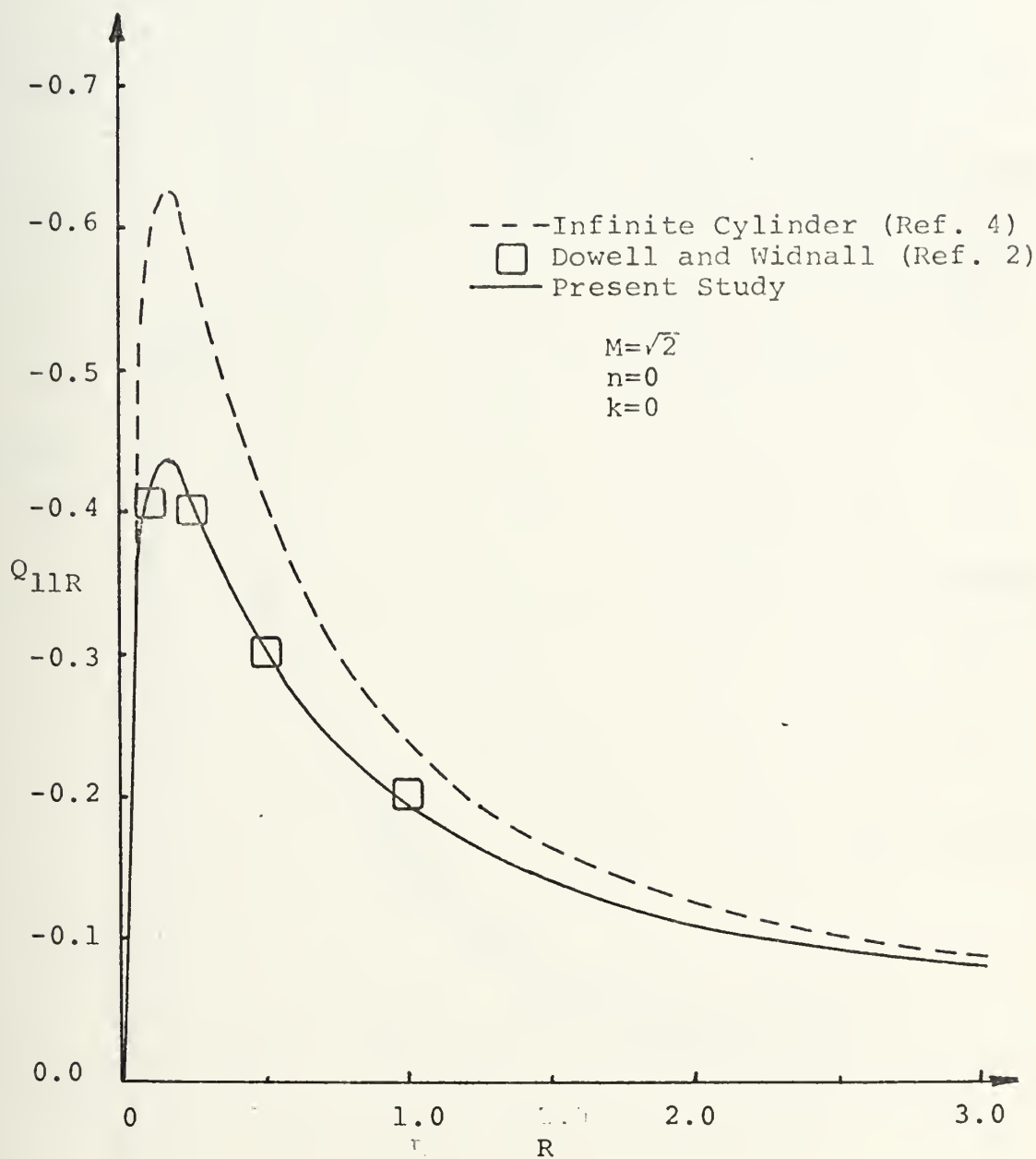


Figure 17. Generalized Aerodynamic Force vs.  
Radius to Length Ratio



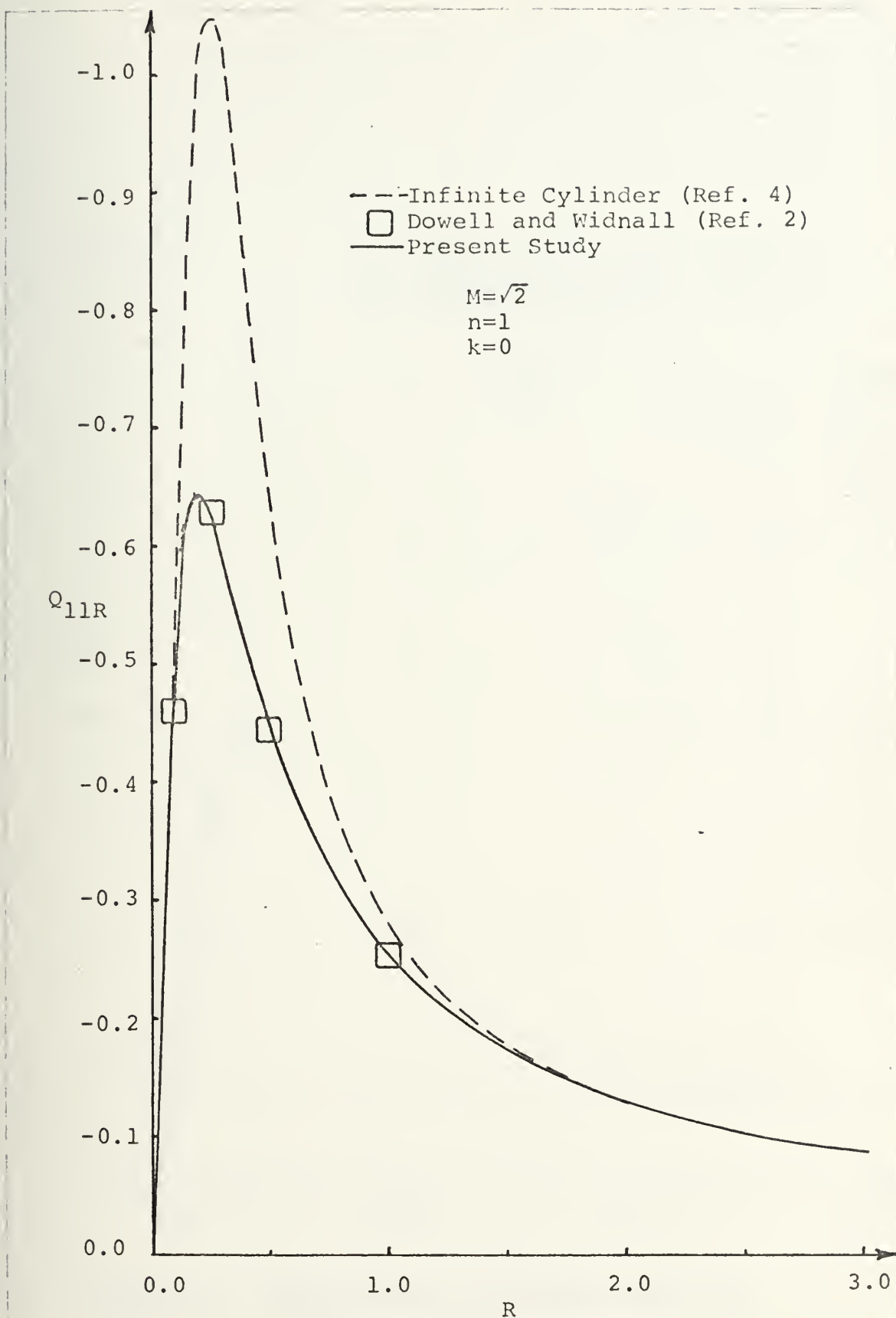


Figure 18. Generalized Aerodynamic Force vs.

Radius to Length Ratio



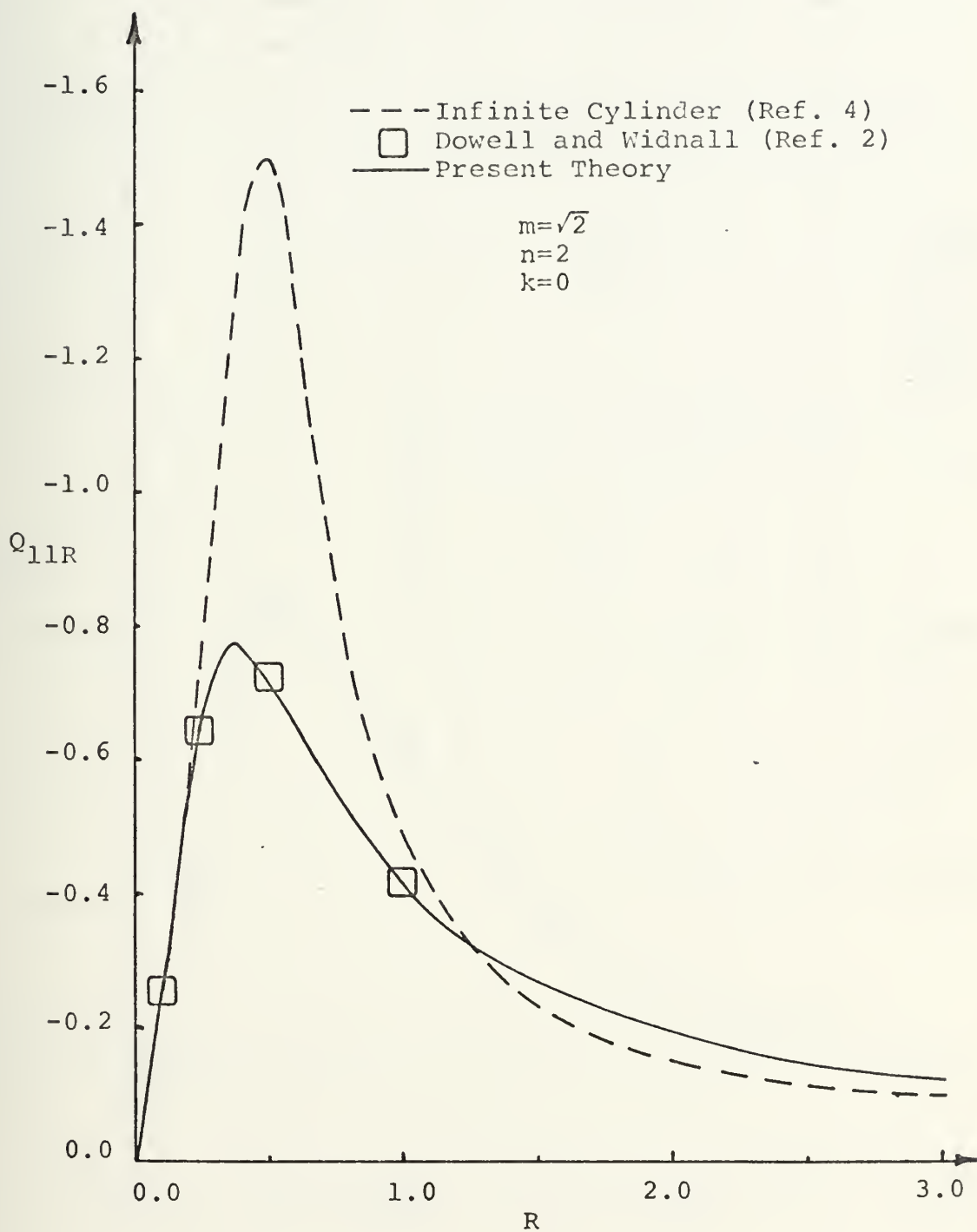


Figure 19. Generalized Aerodynamic Force vs.  
Radius to Length Ratio



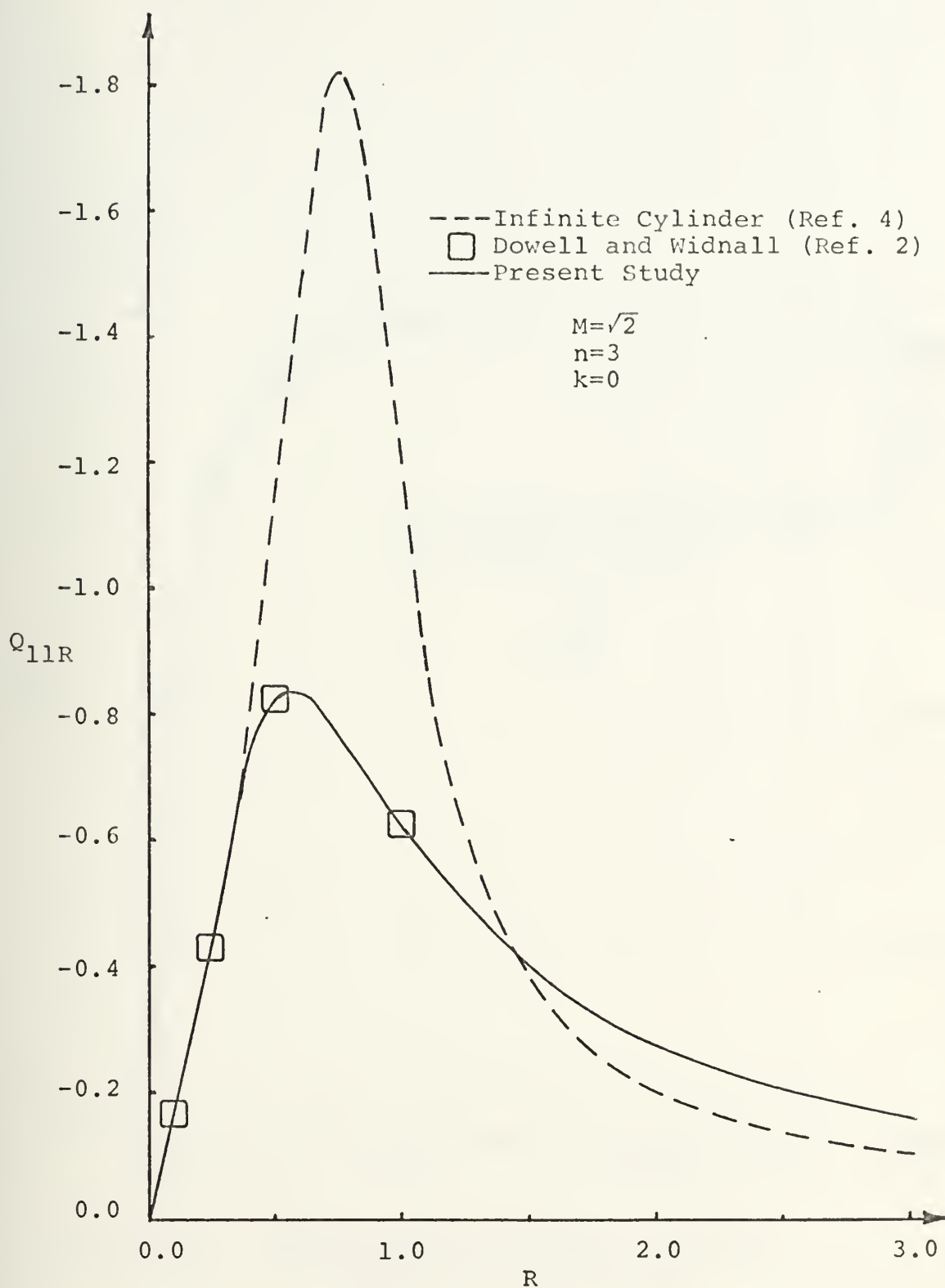


Figure 20. Generalized Aerodynamic Force vs.  
Radius to Length Ratio





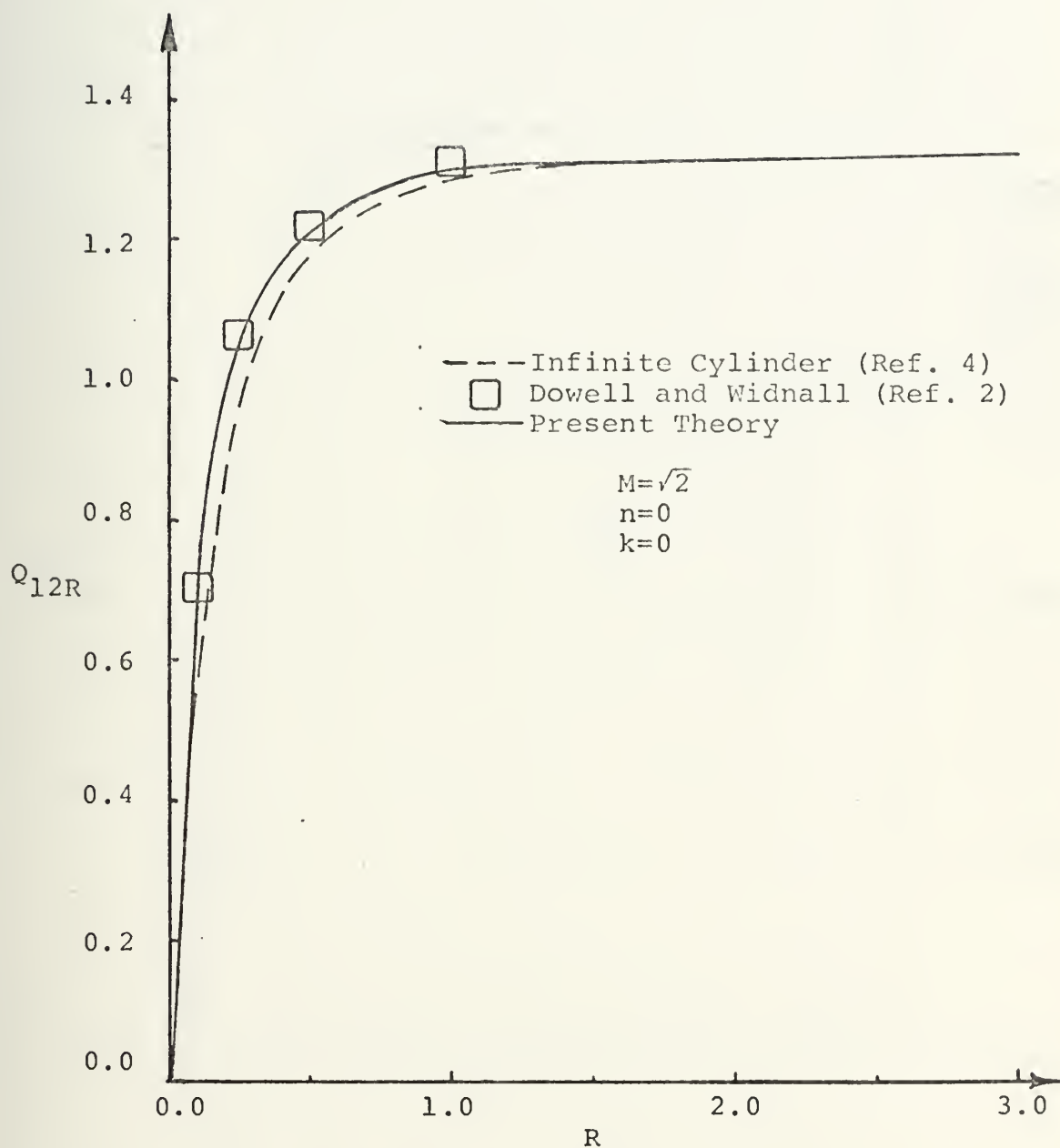


Figure 21. Generalized Aerodynamic Force vs.  
Radius to Length Ratio



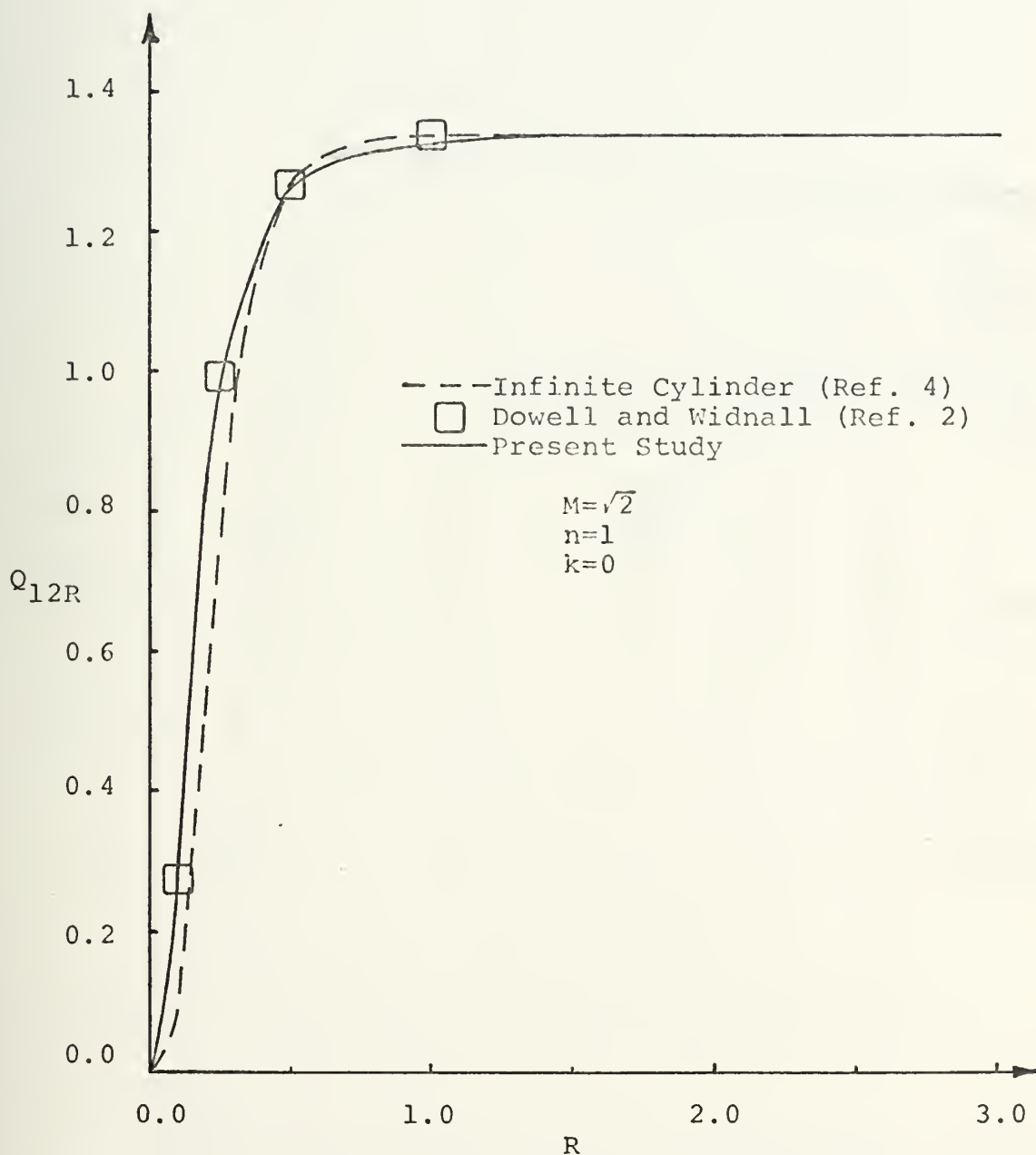


Figure 22. Generalized Aerodynamic Force vs.  
Radius to Length Ratio



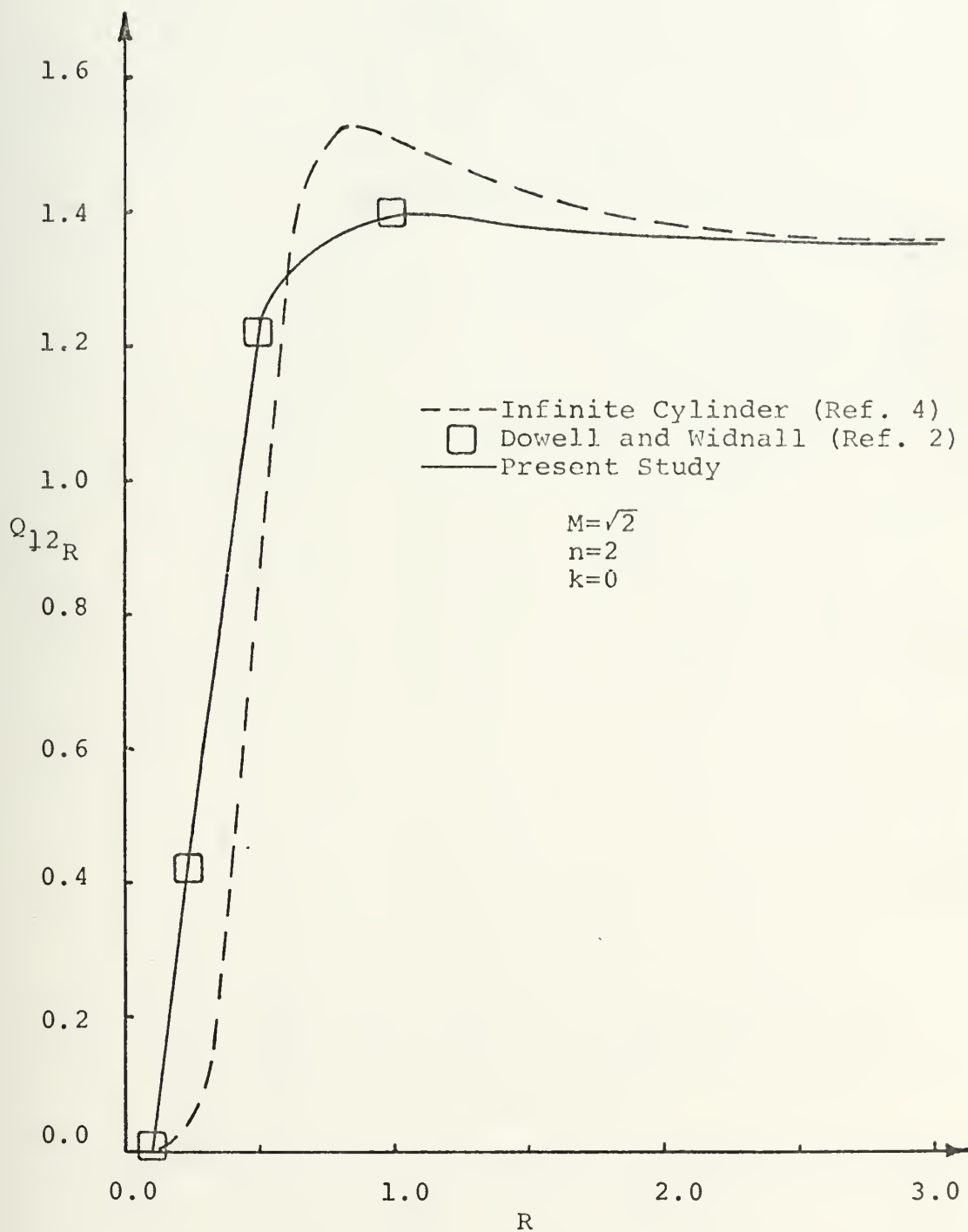


Figure 23. Generalized Aerodynamic Force vs.  
Radius to Length Ratio



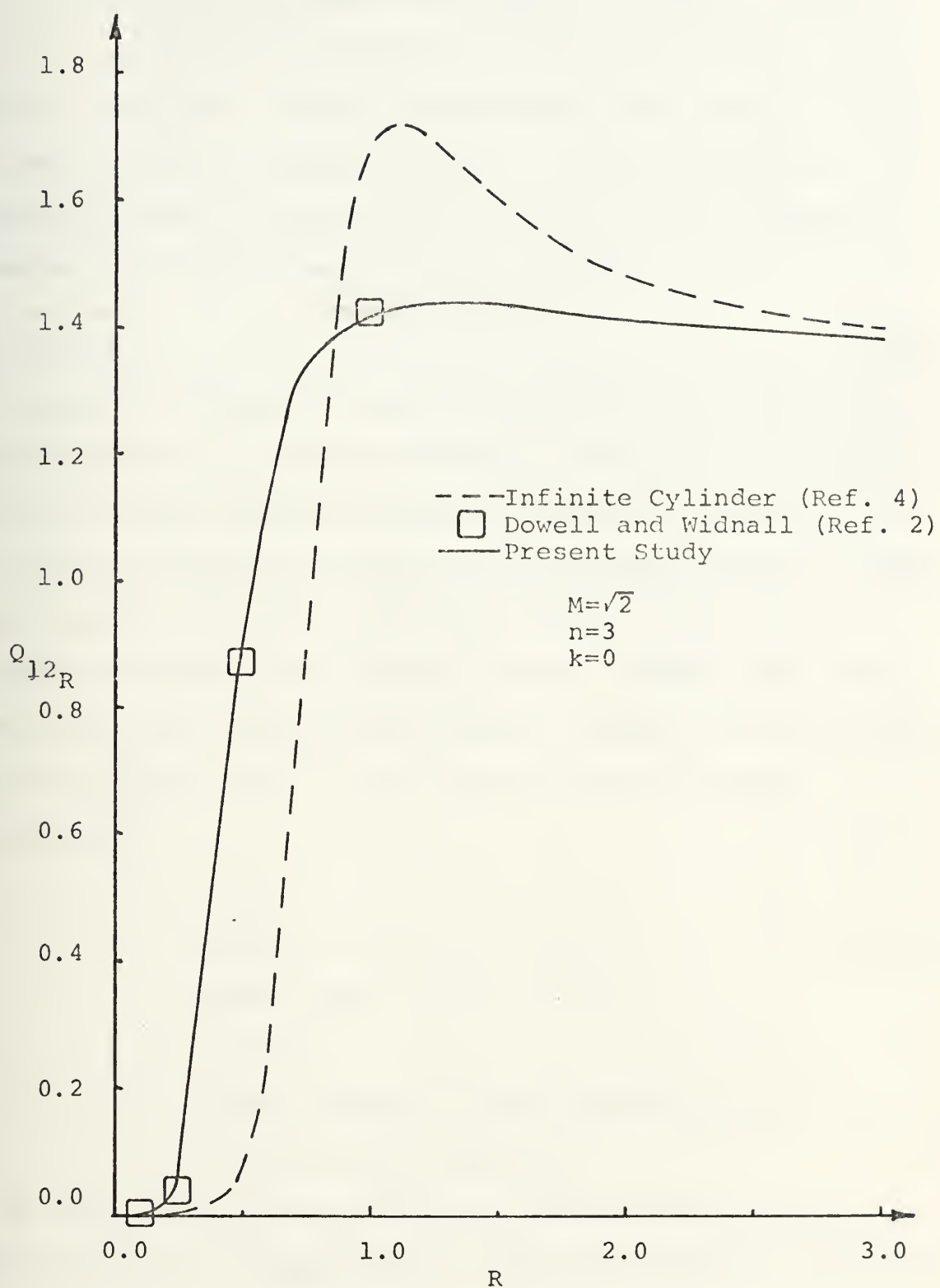


Figure 24. Generalized Aerodynamic Force vs.  
Radius to Length Ratio





Finally, Figure 25 shows the change in pressure distribution as a function of radius to length ratio for the case  $M=\sqrt{2}$ ,  $m=1$ ,  $n=0$ ,  $k=0$ . These distributions were computed using the characteristics method outlined in Section III-A and the Sauer-Heinz theory as described in Section III-C. Complete agreement was found between the two methods.

## B. CASCADE

Figures 26 through 29 show the instantaneous pressure distributions on the first and second blades of a finite cascade for four different values of reduced frequencies. The pressure difference between lower and upper blade surface is plotted for the instant when the airfoil is at its mean horizontal position and pitching nose up. Results for these cases were given very recently by L. E. Snyder, of Pratt and Whitney Aircraft (Ref. 8), for the following parameter combinations:

$$M = 1.5$$

$$\text{Solidity} = 1.33 \quad (d = 0.317)$$

$$\text{Stagger angle} = 25^\circ \quad (\beta = 65^\circ)$$

$$x_0 = 0.5$$

$$S = 40^\circ \quad (\text{Blade 2 leads blade 1})$$

$$k = 0.04, 0.332, 0.832, 1.25$$

It can be seen that appreciable differences exist in a number of cases, in particular in the wave reflection regions. These differences are not fully understood at this time.



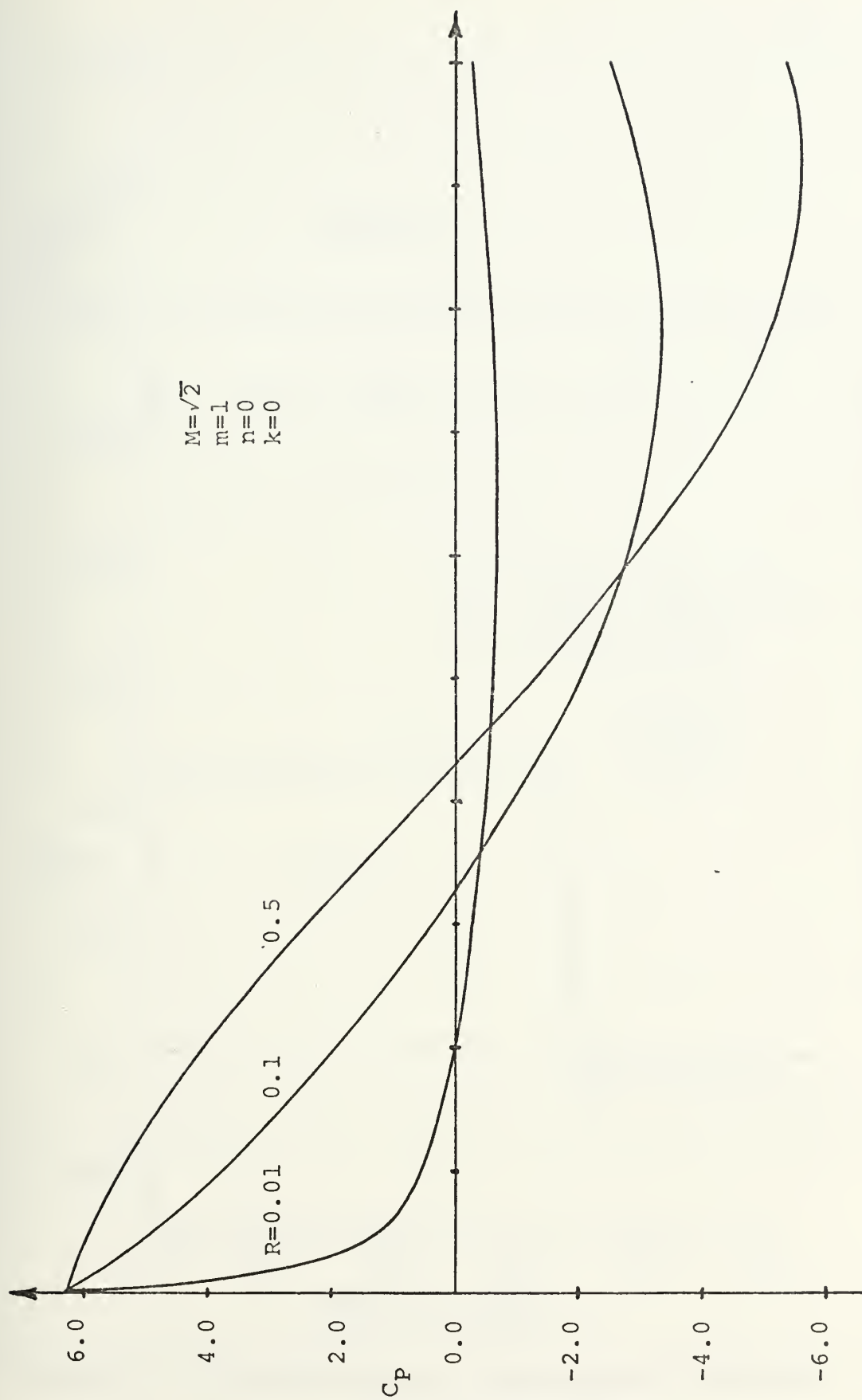


Figure 25. Pressure Distribution Over Wavy-Walled Cylinder



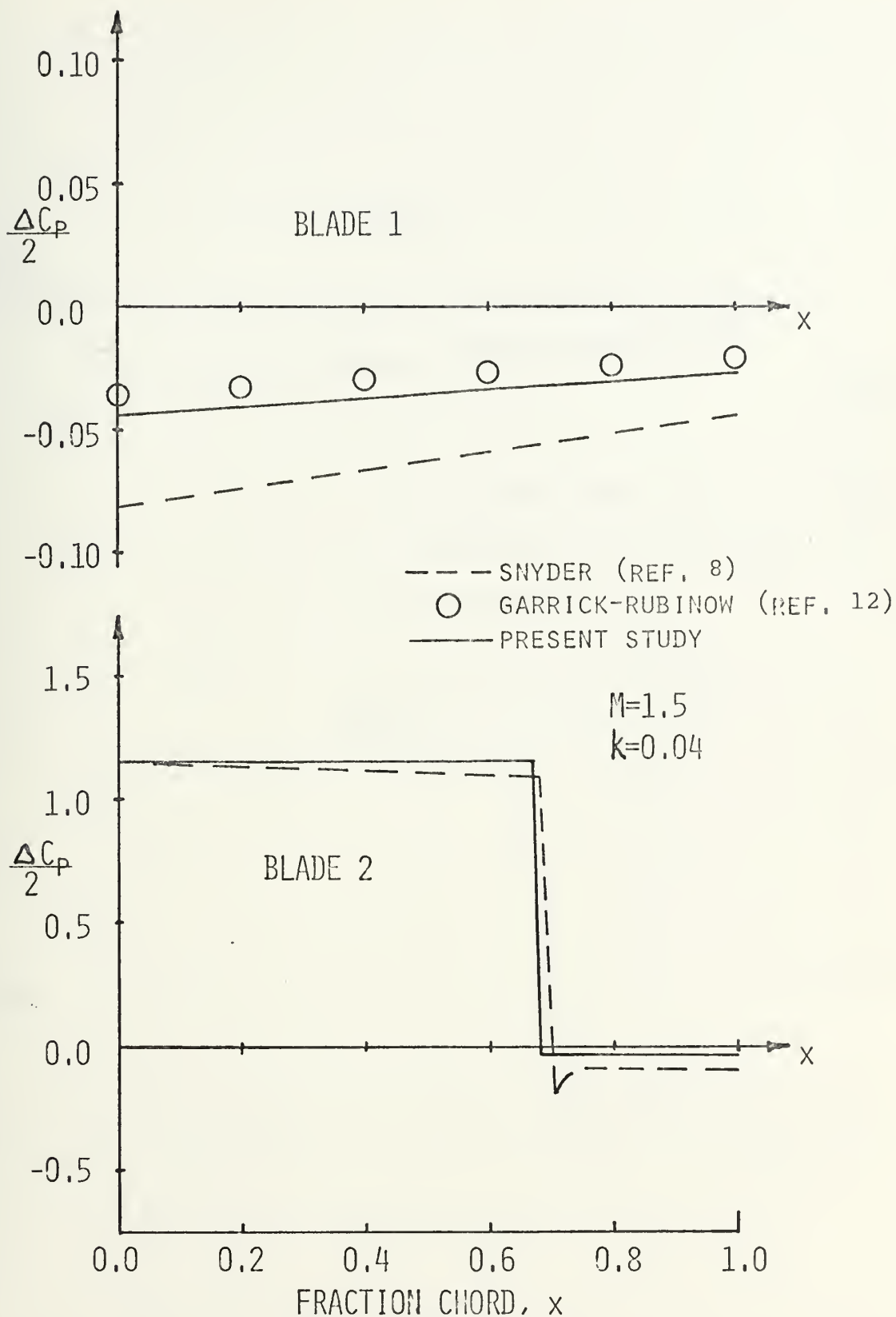


Figure 26. Cascade Pressure Coefficient Difference vs. Fraction Chord



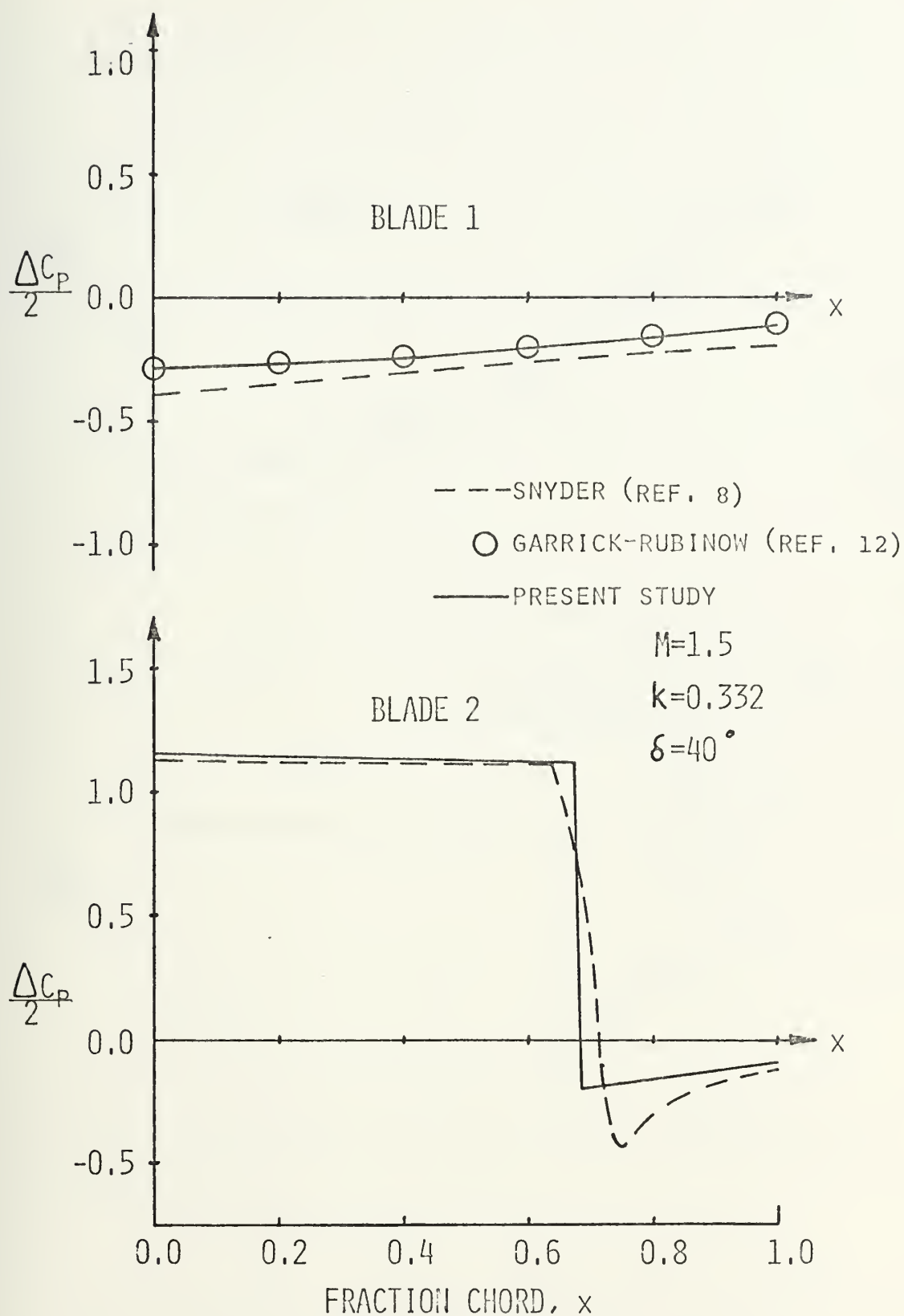


Figure 27. Cascade Pressure Coefficient Difference vs. Fraction Chord





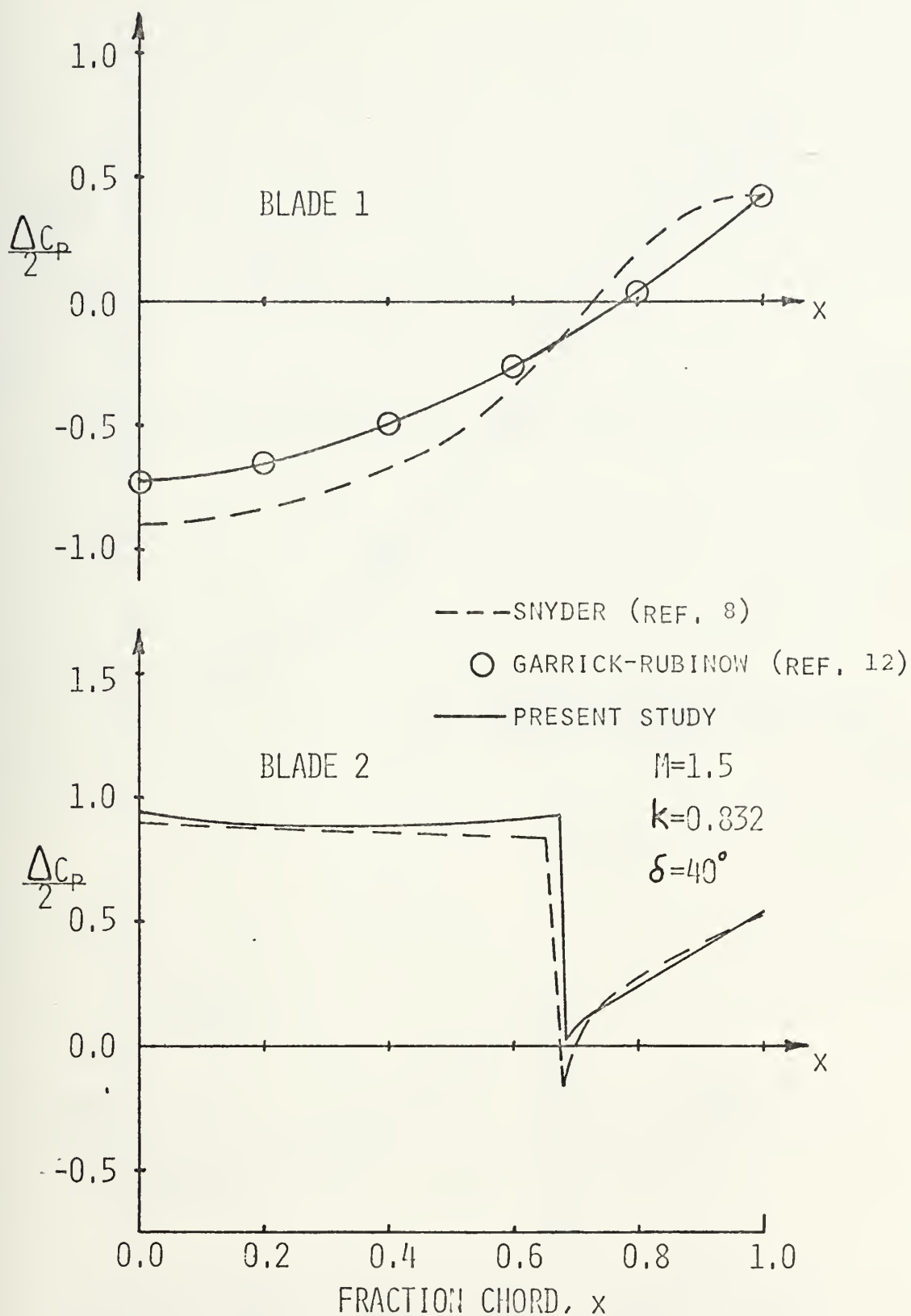


Figure 28. Cascade Pressure Coefficient Difference vs. Fraction Chord



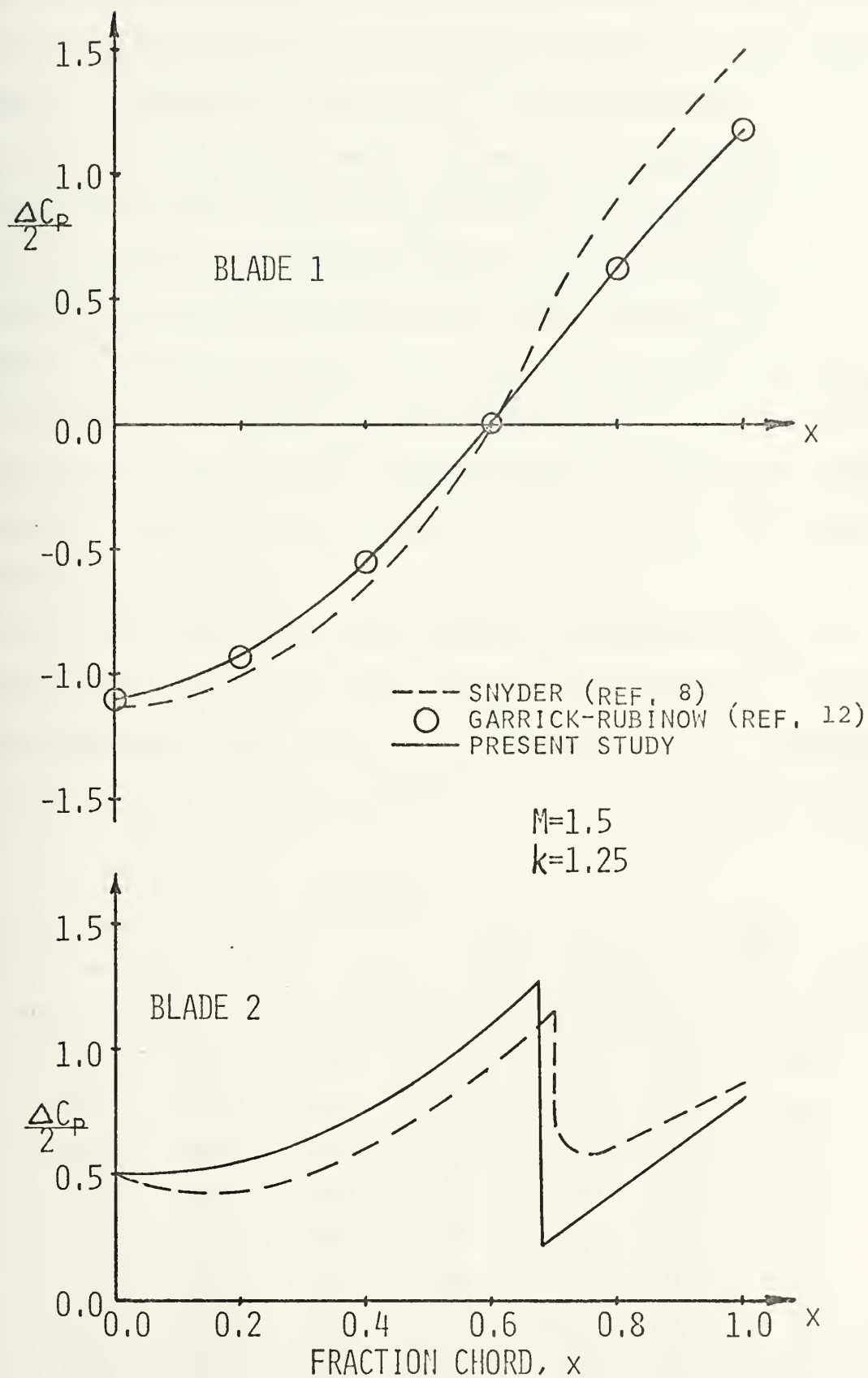


Figure 29. Cascade Pressure Coefficient Difference  
vs. Fraction Chord



Snyder uses a finite difference procedure and further work is required to evaluate the validity and accuracy of this procedure is compared to the method of characteristics procedure developed in the present work. However, a check could be made for the first blade solutions for which the method of singularities of Garrick and Rubinow (Ref. 12) is available. This solution was programmed according to the equations given in Appendix H and the results are shown in Figures 26 through 29. The method of characteristics solution is in complete agreement with the Garrick-Rubinow prediction whereas considerable deviations are seen to exist for the finite difference predictions.

A further check using the method of singularities was developed for two blades oscillating with zero phase difference. This approach is also described in Appendix H and a comparison with the method of characteristics is given in Table 1 below:

TABLE 1

k	0.1				0.5			
M	$\sqrt{2}$		1.8		$\sqrt{2}$		1.8	
x	M.O.C.	M.O.S.	M.O.C.	M.O.S.	M.O.C.	M.O.S.	M.O.C.	M.O.S.
0.1	.979	.979	.667	.660	.693	.694	.640	.486
0.2	.977	.977	.666	.661	.686	.687	.638	.511
0.3	.974	.974	.666	.662	.680	.681	.635	.536
0.4	.972	.972	.666	.663	.676	.677	.631	.562
0.5	.969	.969	.666	.664	.674	.675	.627	.588
0.6	.966	.966	.665	.666	.675	.676	.623	.614
0.7	.963	.963	.665	.667	.678	.679	.618	.641
0.8	.959	.959	.665	.668	.682	.683	.614	.668
0.9	.956	.956	.664	.669	.689	.690	.607	.694



Further method of characteristics results for a finite subsonic leading edge cascade are shown in Figures 30 through 32 for the following parameter combinations:

$$\begin{array}{ll} M=\sqrt{2} & x_0=0.5 \\ d=1.0 & k=0.5 \\ \beta=59.8^\circ & \delta=120^\circ \end{array}$$

As mentioned previously, the computer program is written sufficiently general so that the pressure distribution can be computed and printed out for arbitrary specified Mach number, reduced frequency, stagger angle, blade spacing, and number of blades subject to the following constraint:

$$v \tan \alpha [(N-1) (\tan \beta - \cot \alpha) + \frac{1}{d}] < 800 \quad (227)$$

Equation (227) is the expression which governs the maximum grid fineness that may be used with a given set of input parameters. This constraint is necessary because the program is dimensioned such that the maximum number of grid points allowed on any one right-running Mach line is 400.





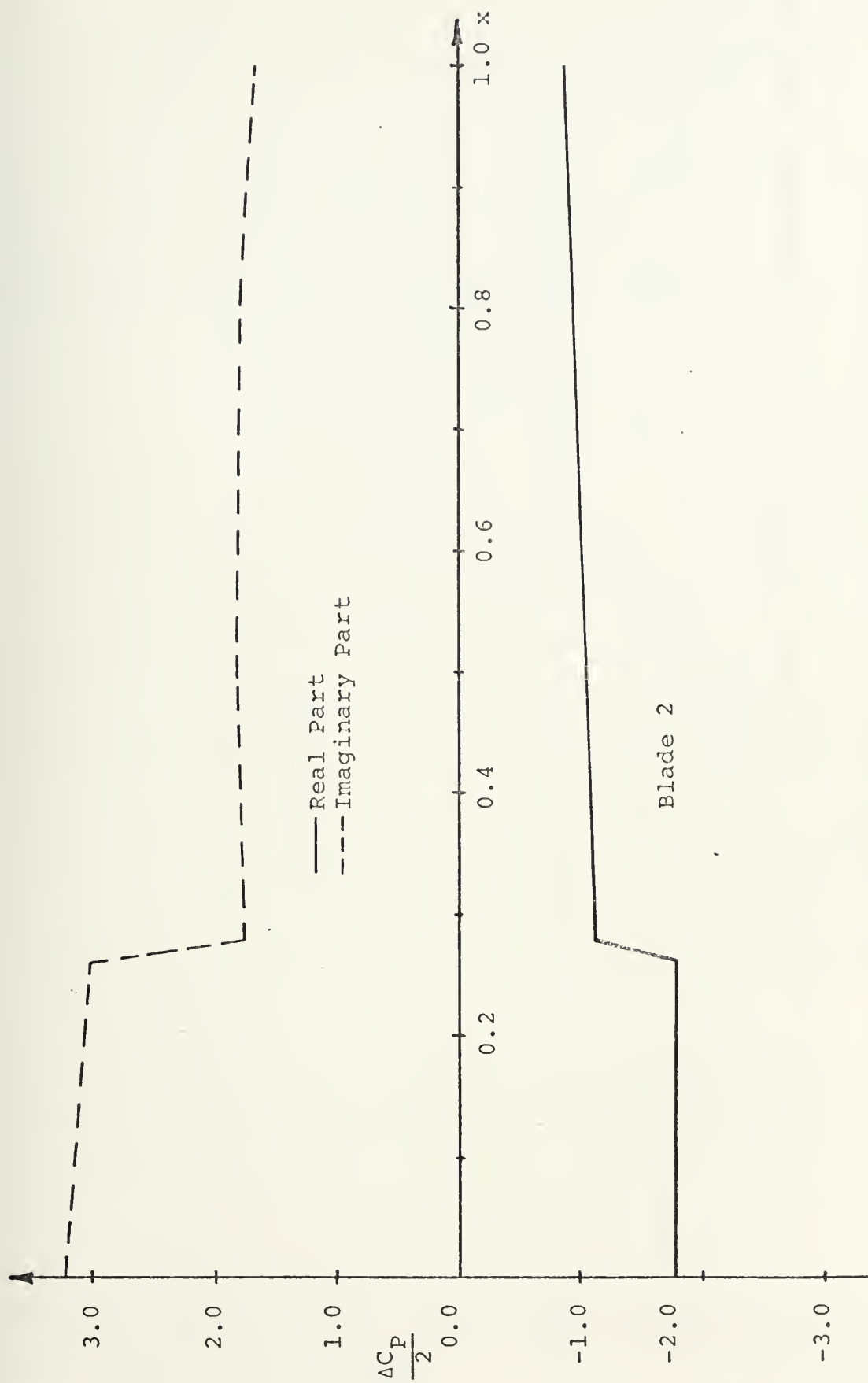


Figure 30. Pressure Coefficient Difference vs. Fraction Chord



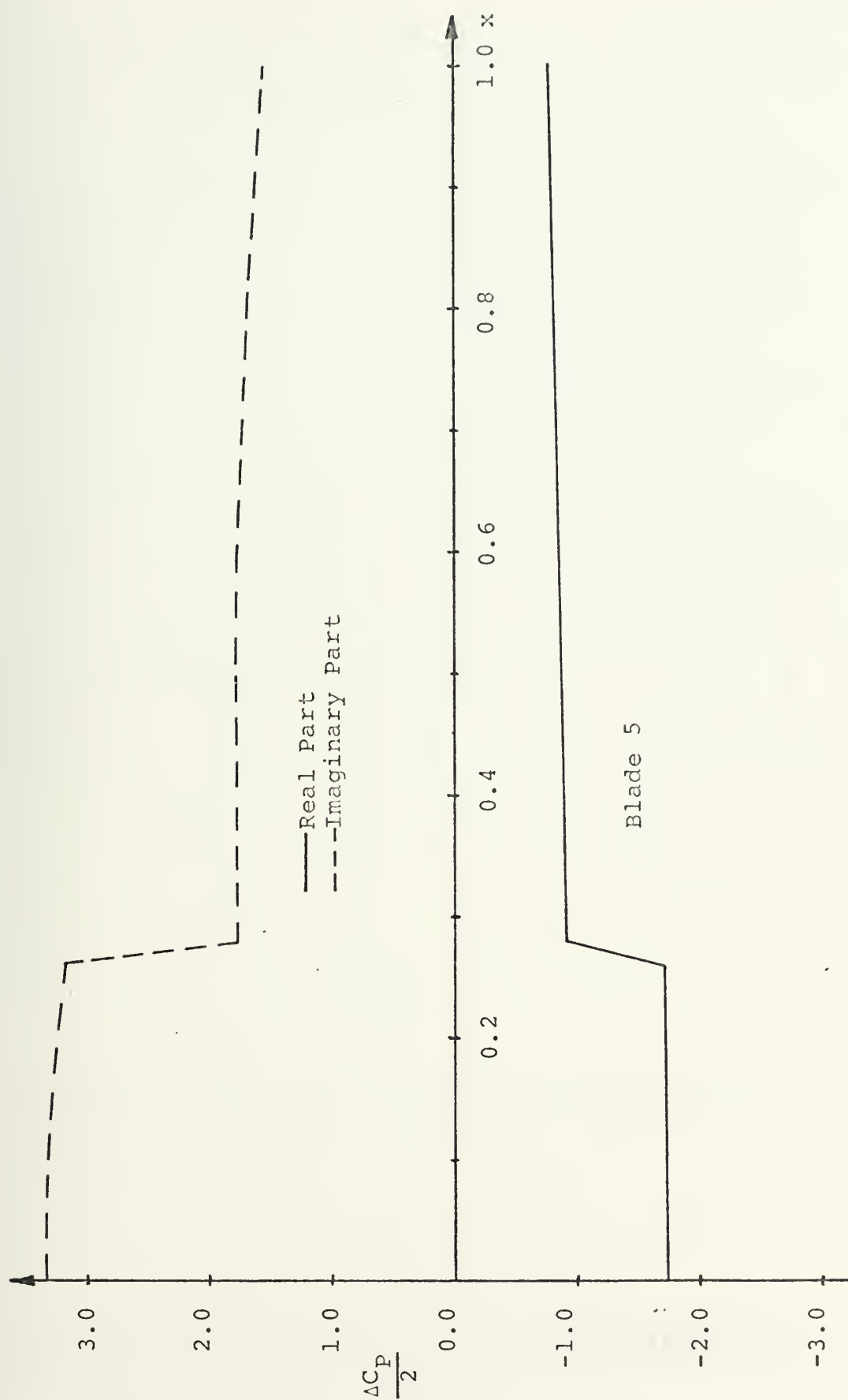


Figure 31. Pressure Coefficient Difference vs. Fraction Chord



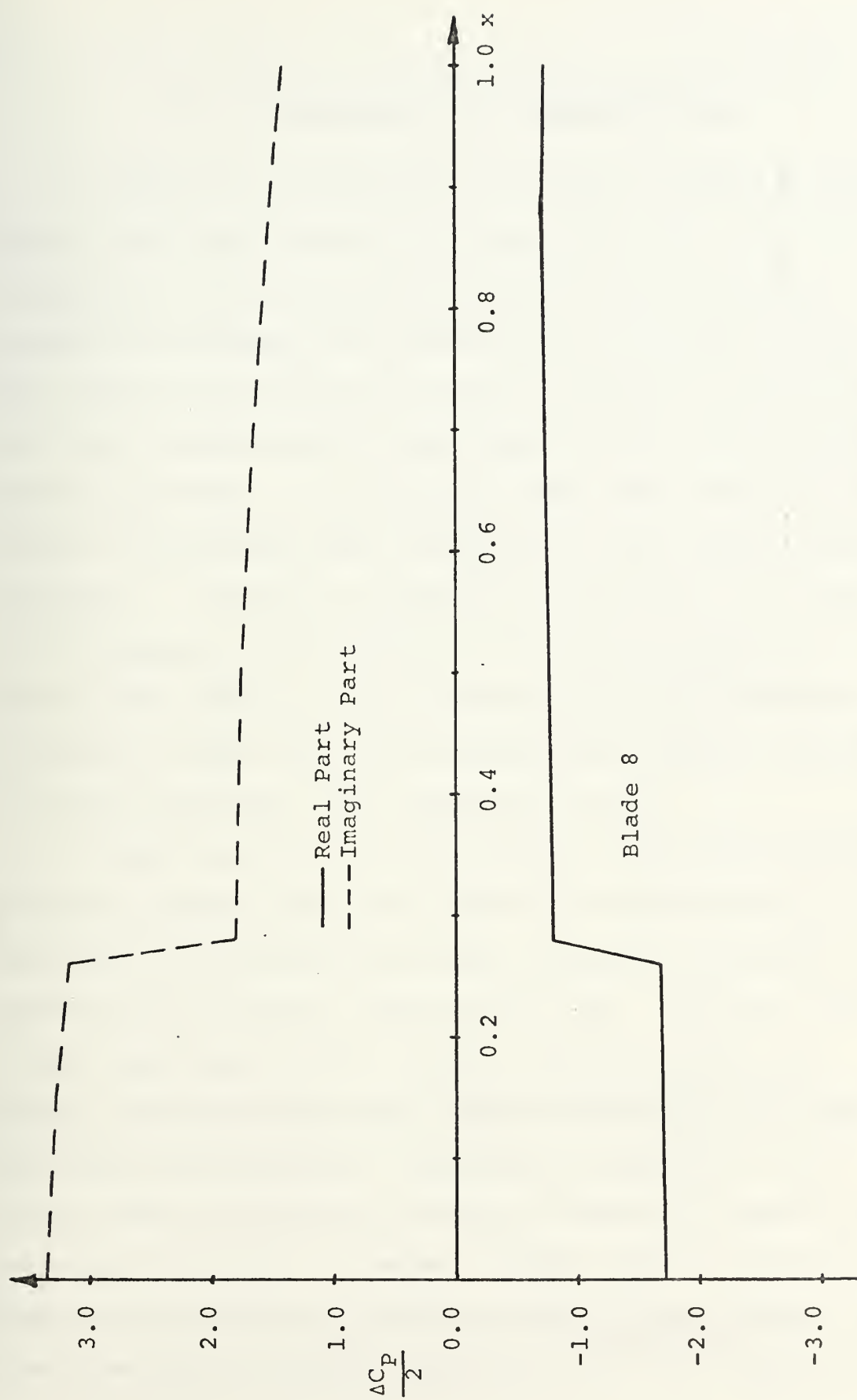


Figure 32. Pressure Coefficient Difference vs. Fraction Chord



## VI. CONCLUSIONS AND RECOMMENDATIONS

A solution of the complete linearized unsteady potential equation has been developed for supersonic flow past vibrating cylindrical shells using the method of characteristics. Pressure distributions and generalized aerodynamic forces were computed for shells of arbitrary radius-to-length ratios, axial and circumferential wave numbers, Mach number, and reduced frequencies. A solution for this same problem was previously obtained by Dowell and Widnall using Laplace transform techniques. Excellent agreement was obtained in all cases. It is believed that the present method can be applied more easily than methods requiring complex variable techniques. It should be noted that the procedure can easily be modified to include arbitrary axial deflection modes.

A further solution of the complete linearized unsteady potential equation using the method of characteristics was developed for supersonic flow past vibrating flat plate cascades with subsonic leading edge locus. Pressure distributions were computed for finite cascades of arbitrary stagger and interblade phase angles performing small amplitude pitch oscillations. Preliminary comparisons with a recent finite difference solution by Verdon and Snyder showed reasonable agreement. However, further work is necessary to assess the validity and accuracy of the present method. This should be done by further comparisons with the Verdon and





Snyder procedure and Fourier and Laplace transform methods currently under development at Stevens Institute of Technology, General Motors Corporation (Detroit Diesel, Allison Division), and General Electric. Also, flutter calculations should be carried out using the method of characteristics predictions of the oscillatory aerodynamic forces which would allow comparisons with the Pratt and Whitney cascade flutter tests.



## APPENDIX A

### CYLINDRICAL SHELL COMPUTER PROGRAM VARIABLES

#### A. LOGIC VARIABLES

The following variables appear in the logic statements of the program:

IHAVEP	The number of the computation along any right-running Mach line. IHAVEP is used as the first subscript for a grid point.
ISWTCH	Switch variable used to designate the right-running Mach line being calculated, alternately set equal to "1" or "2" and used as a second subscript.
JSWTCH	Switch variable used to designate the previously computed right-running Mach line, always the opposite of ISWTCH and used as a second subscript.
KOUNT	The value of IHAVEP at the cylinder surface.
ML	The number of grid points along the initial Mach line and along the cylinder surface.

#### B. QUANTITY VARIABLES

The following variables in the program take on the values defined below. All are floating point quantities unless otherwise stated. The dimensioned variables are listed first.

AMAGCP(400)	The imaginary part of the pressure coefficient.
CP(400)	The complex pressure coefficient.
PHI(400,2)	The derivative of the velocity potential along the right-running Mach line.
PHK(400,2)	The derivative of the velocity potential along the left-running Mach line.
QPHI(400,2)	The velocity potential.

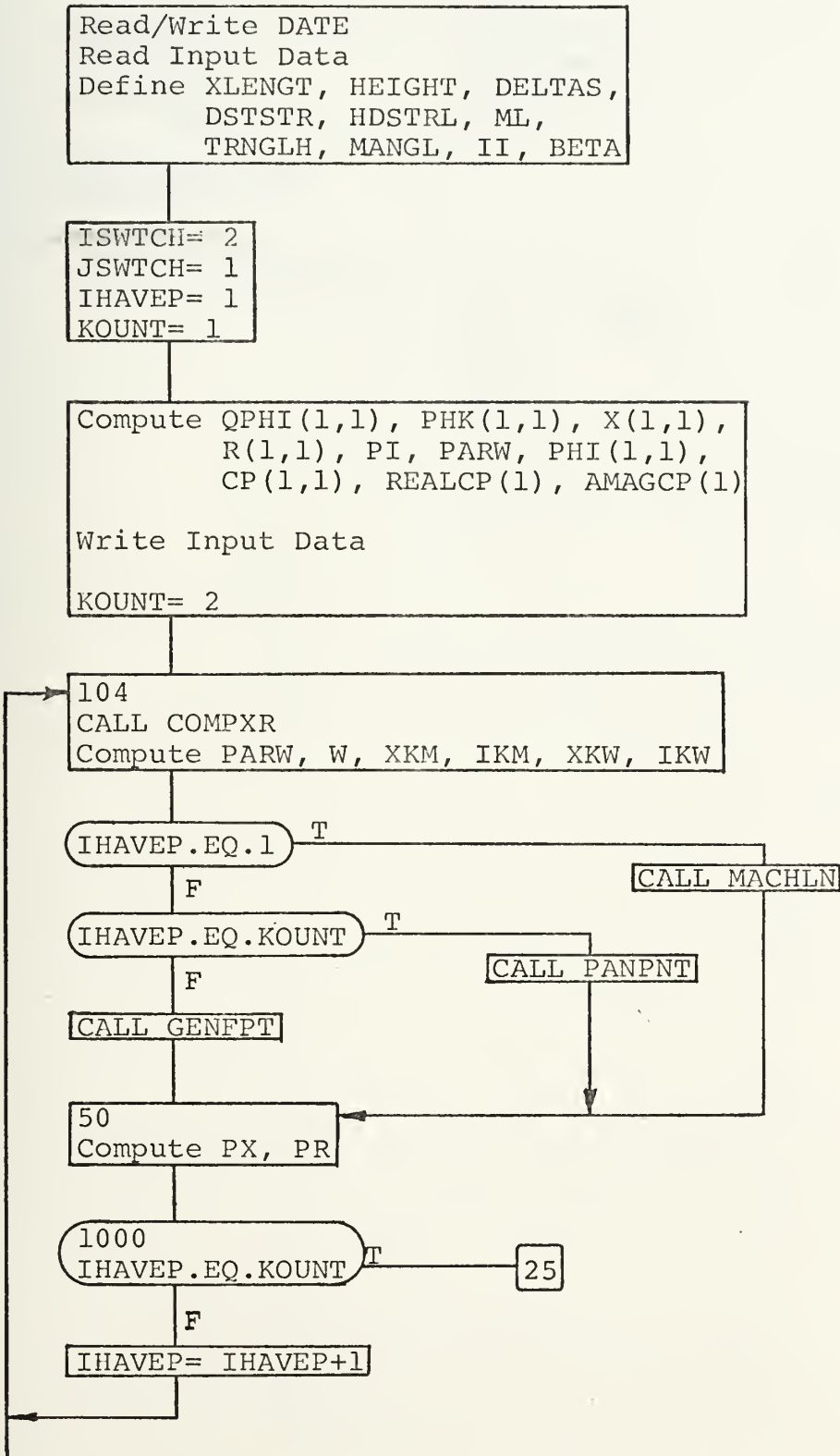


REALCP(400,2)	The real part of the pressure coefficient.
X,R(400,2)	The x and r coordinates of a grid point.
A,B,C,D,E,F	See equations (57) - (62)
BETA	The square root of the quantity Mach number squared minus one.
DELTAS	The step size along the characteristics.
DSTSTR	The horizontal distance between grid points.
FINGRD	The grid fineness ratio. An even integer less than 400.
HDSTRL	One-half DSTSTR.
HEIGHT	The increment $HDSTRL \frac{1}{2} \tan \alpha$ .
II	The square root of minus one.
IKM	The factor, $ik \frac{M}{M^2-1}$
IKW	The quantity, $ik \sin m\pi x$
IPHI1, IPHI2	The velocity potential as described in equations (51) and (54).
K	The reduced frequency.
MACH	The free-stream Mach number
MANGL	The Mach angle, $\alpha$ .
MFREQ	The axial mode number. An integer.
NFREQ	The circumferential mode number. An integer.
NR	r, as defined in equation (68). An integer.
PARW	The partial derivative of the deflection taken with respect to x.
PI	3.141593
PX	The partial derivative of the velocity potential taken with respect to x.
RADIUS	The radius to length ratio.
W	The cylinder deflection.



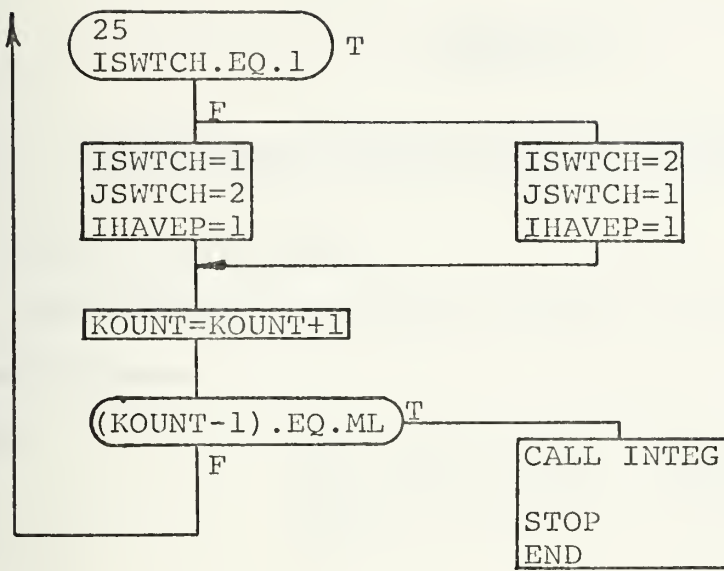
# APPENDIX B

## CYLINDRICAL SHELL FLOW DIAGRAM











## APPENDIX C

### OSCILLATING CASCADE COMPUTER PROGRAM VARIABLES

#### A. LOGICAL VARIABLES

The following variables appear in the logic statements of the program:

ICO	Set equal to "1" when a blade or wake computation is made. Set equal to "0" after the next general flow field computation occurs.
IHAVEP	The number of the computation along any right-running Mach line starting with zero at the initial left-running Mach line. The value IHAVEP+1 is the first subscript for a flow quantity.
ISWTCH	Switch variable used to designate the right-running Mach line being calculated, alternately set equal to "1" or "2" and used as a second subscript.
JLINE	The Mach line counter incremented each time a right-running Mach line is completed. Reset equal to the value of IHAVEP at the leading edge of a new blade.
JSWTCH	Switch variable used to designate the previously computed right-running Mach line, always the opposite of ISWTCH and used as a second subscript.
LCOUNT	The value of IHAVEP at a surface or wake grid point.
LIMIT	The maximum value of IHAVEP.
LIMW	The value of LCOUNT at the trailing edge of a blade.
MAXI	The value of JLINE on a right-running Mach line which intersects a blade's leading edge.
NEW DST	The number of $\Delta x$ increments in a blade chord.



NSTPTS	The number of $\Delta x$ increments between the initial Mach line and the leading edge of the first blade.
NUM	Set equal to one less than the number of the blade encountered on a Mach line.
NUMBLD	The number of blades in the cascade.
NUMOLD	Preserves the maximum value of NUM.
NUMPI	NUMOLD plus one.
OLDL	Preserves the value of LCOUNT at the highest blade or wake yet encountered.

## B. QUANTITY VARIABLES

The following variables in the program take on the values defined below. All are floating point quantities unless otherwise stated. The dimensioned variables are listed first.

A(8,8)	Matrix of coefficients in wake computation.
B(8)	Right-hand side of equations (194) - (201)
U22R,U22I,V22R,V22I,C22R,C22I(400,2).	The velocities, real and imaginary of general flow field, upper blade, and upper wake points. Equivalent to the respective Teipel amplitude functions, $U_{22R}$ through $C_{22I}$ .
U33R,U33I,V33R,V33I,C33R,C33I(400,2).	Same as above, but used only at lower blade and lower wake points.
X,Y(400,2)	The x and y coordinates based on chord length.
AI	$A_I$ as defined in equation (122).
ARG	The argument $k \frac{M^2}{M^2-1} x$
BI	$B_I$ as defined in equation (123).
DELTA	The interblade phase angle in radians.
DELTAS	Incremental distance between grid points along Mach line.
DSTSTR	The increment $\Delta x$ .



FAZE	The interblade phase angle in degrees.
FMANGL	Mach angle, $\alpha$ .
FNGDPT	Floating point NGRDFN.
FSTRMN	The free-stream Mach number.
G1,...,G9	Intermediate factors used in velocity computations in GENFPT, TOP, BOTTOM, and NEWBLD.
HDSTRL	The increment $\Delta x/2$ .
K12R,...,K56I	$K_{12R}, \dots, K_{56I}$ as defined in equations (116) - (121).
KS	Dummy variable used in SIMQ. An integer.
NGRDFN	The grid fineness ratio. An even integer, less than 400.
REDFRQ	The reduced frequency.
STAG	The distance the second blade is staggered back from the y-axis.
STGR	The distance from the initial Mach line to the second blade's leading edge.
STGANG	The stagger angle in degrees.
S	The factor $\sqrt{M^2-1}$ .
TNWDST	The vertical distance between adjacent blades.
TRNGLH	The increment $\frac{1}{2}\Delta x \cos \alpha$ .
U	The factor $\cos(k \frac{M^2}{M^2-1} x)$ .
V	The factor $\sin(k \frac{M^2}{M^2-1} x)$ .
VIPANL	The imaginary part of the normal flow velocity at the first blade's leading edge.
VRPANL	The real part of the normal flow velocity at the first blade's leading edge.
W	The factor $\frac{M^2}{\sqrt{M^2-1}}$ .



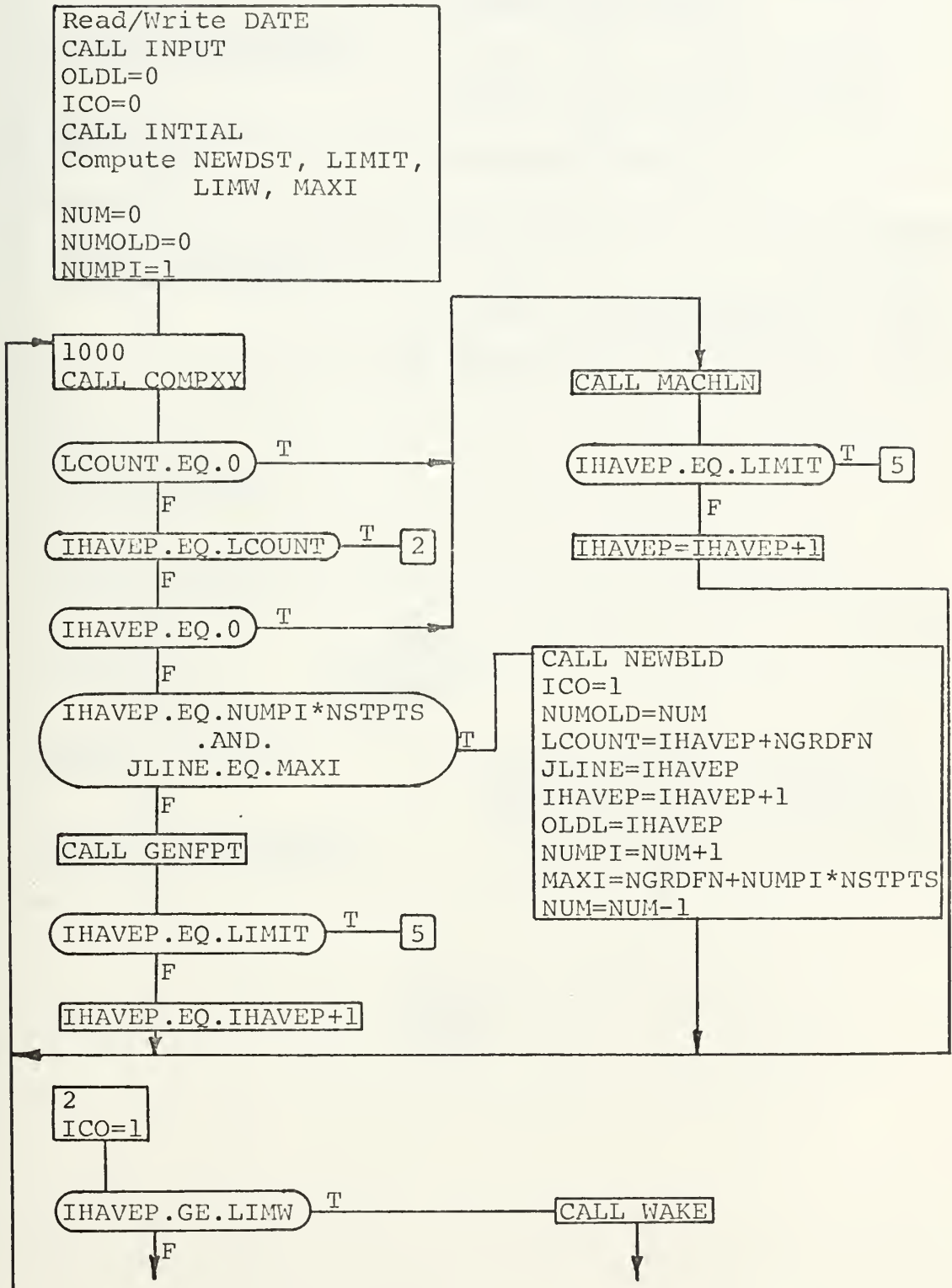


XSUBO	The elastic axis position based on chord length.
XLNGTH	The length of the initial Mach line between the planes of adjacent blades.
XN	Floating point NUM.
XNEW	The x-coordinate on a blade based on the blade's leading edge.

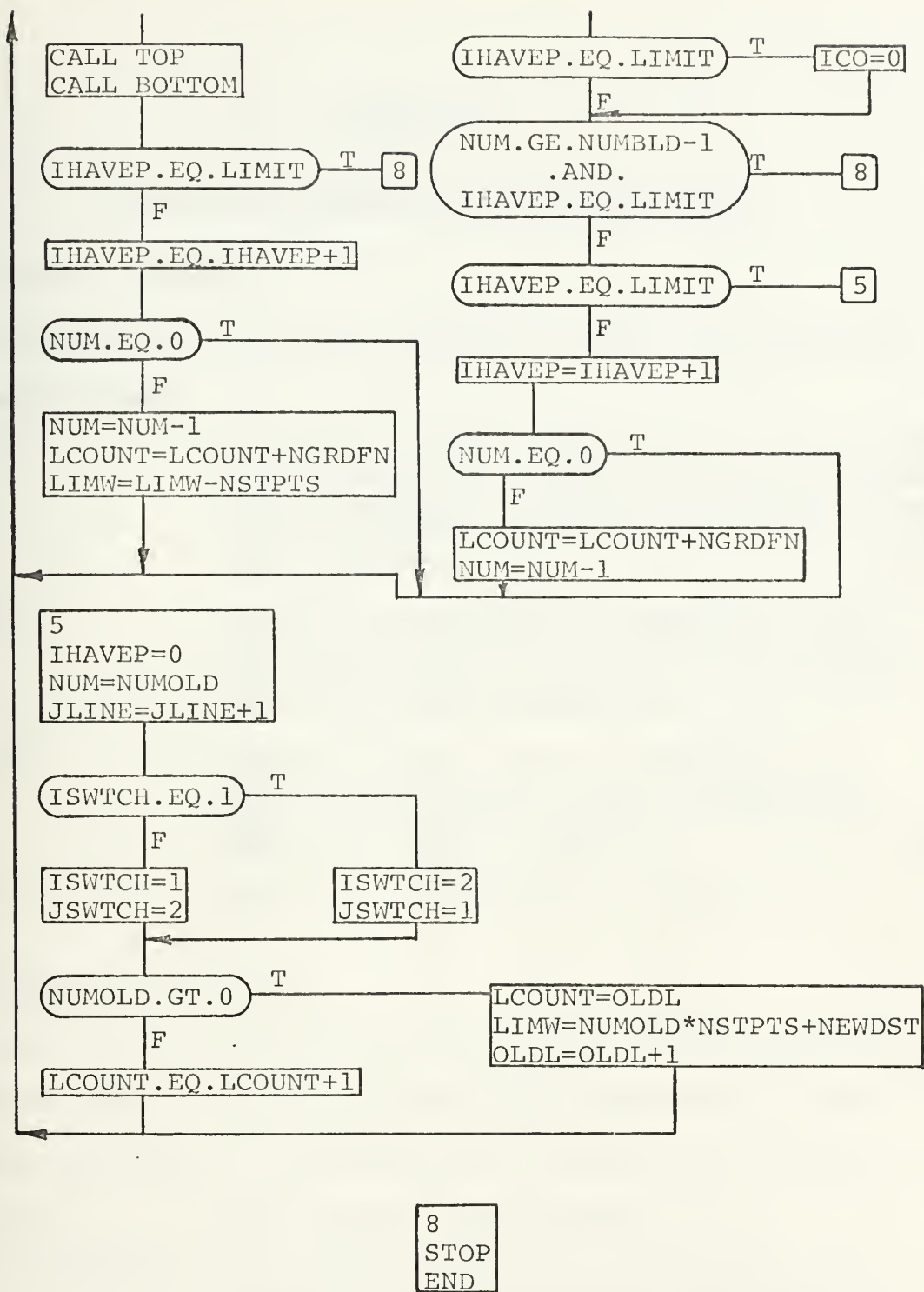


# APPENDIX D

## CASCADE FLOW DIAGRAM









## APPENDIX E

### SAUER-HEINZ COMPUTER PROGRAM VARIABLES

#### A. LOGIC VARIABLES

The following variables appear in the logic statements of the program:

IHAVEP	The number of the computation along any right-running Mach line starting with zero at the initial left-running Mach line. The value IHAVEP+1 is the first subscript for a flow quantity.
ISWTCH	Switch variable used to designate the right-running Mach line being calculated, alternately set equal to "1" or "2" and used as a second subscript.
JSWTCH	Switch variable used to designate the previously computed right-running Mach line, always the opposite of ISWTCH and used as a second subscript.
KOUNT	The value of IHAVEP at the surface.

#### B. QUANTITY VARIABLES

The following variables in the program take on the values defined below. All are floating point quantities unless otherwise stated. The dimensioned variables are listed first.

CP(200)	The pressure coefficient.
DELX,DELR(200)	The incremental distances between grid points on a right-running characteristic.
U(200,2)	The streamwise velocity perturbation.
V(200,2)	The product $vr$ .
X,R(200,2)	The $x$ and $r$ coordinates of the grid point.
A,B	Used as factors in the equations for $u$ and $v$ .



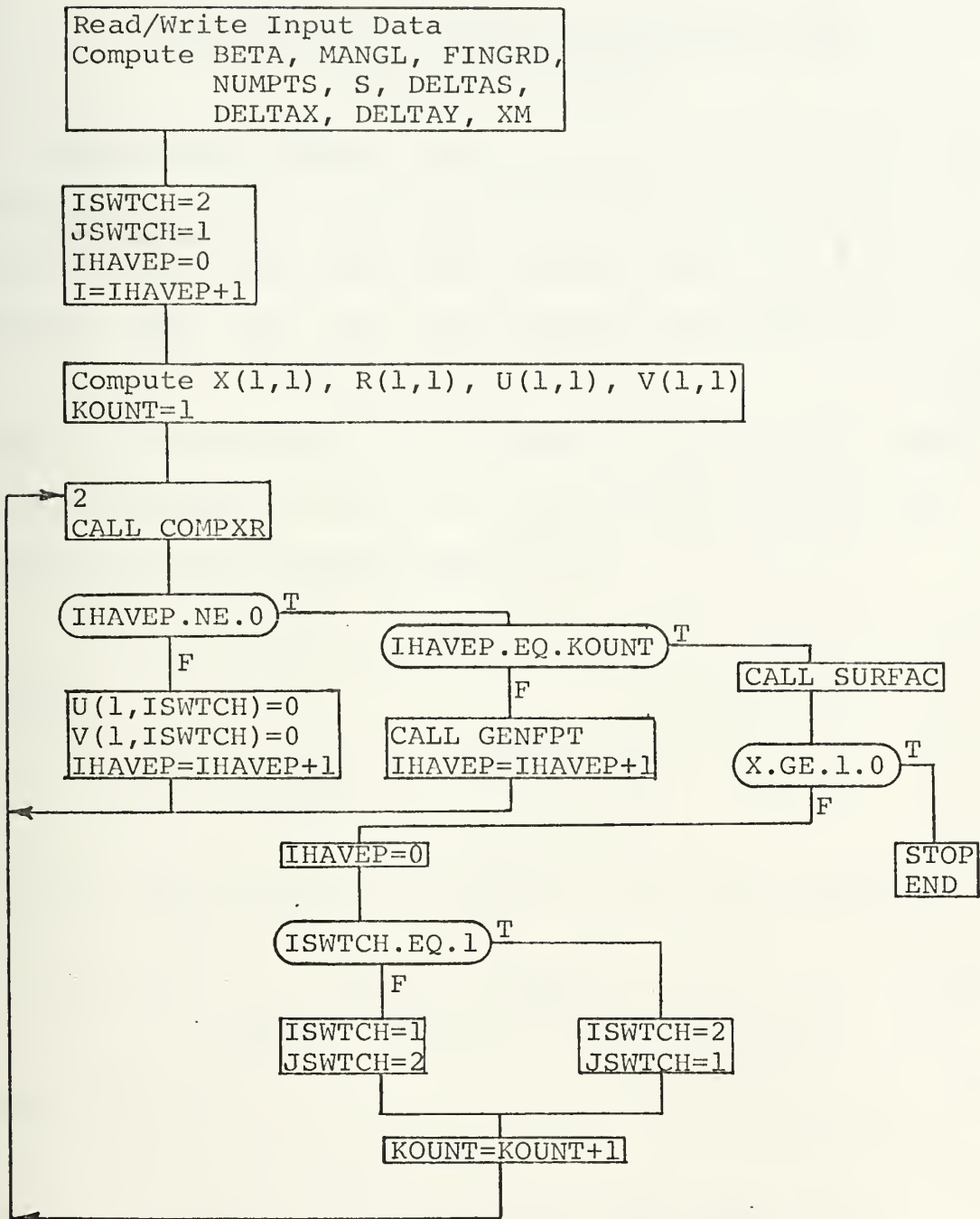


BETA	The square root of the quantity $M^2-1$ .
DELTAS	The incremental distance between adjacent grid points along the initial Mach line.
DELTAX	The change in $x$ from one point to the next on the initial Mach line.
DELTAY	The change in $r$ from one point to the next on the initial Mach line.
FINGRD	Floating point NGFN.
HO	The maximum amplitude of the deflection.
MACH	Free-stream Mach number.
MANGL	The Mach angle, $\alpha$ .
MFREQ	The axial mode number, an integer.
NGFN	The grid fineness ratio, an even integer, less than 200.
NUMPTS	The number of grid points on the initial Mach line.
PI	3.141593
RETA	$r_\eta$
RO	The radius to length ratio.
RZETA	$r_\xi$
S	The length of the initial Mach line.
SLP	Slope of the surface at a surface grid point.
XM	Floating point MFREQ.
XMAX	The value of $x$ at a surface grid point.
YO	The intercept of a right-running Mach line with the $r$ -axis.



# APPENDIX F

## SAUER-HEINZ FLOW DIAGRAM





## APPENDIX G

### SUPERSONIC FLOW PAST AN INFINITELY LONG WAVY WALL CYLINDER

Leonard and Hedgepeth (Ref. 4) gave a solution for supersonic flow past an infinitely long wavy wall cylinder. Detailed computations using this solution were carried out by Anderson (Ref. 14). For the cylinder wall deflection

$$h = h_0 \sin m\pi x \cos n\theta \quad (G-1)$$

where  $m$  is the number of half-waves per unit axial length and  $n$  indicates the number of circumferential waves, one obtains for the pressure distribution.

$$C_p = 2h_0 \frac{m\pi}{M} A_1 \sin(m\pi x + \psi_1) \quad (G-2)$$

where

$$A_1 e^{i\psi_1} = \frac{\frac{M}{\sqrt{M^2-1}} H_n^2 [m\pi R (M^2-1)^{\frac{1}{2}}]}{H_n^2 [m\pi R (M^2-1)^{\frac{1}{2}}]} \quad (G-3)$$

For the actual computation equation (G-3) was rewritten as

$$A_1 e^{i\psi_1} = \frac{J_n(\gamma) - i Y_n(\gamma)}{[J_{n-1}(\gamma) - J_{n+1}(\gamma)] - i [Y_{n-1}(\gamma) - Y_{n+1}(\gamma)]} \cdot \frac{2M}{\sqrt{M^2-1}} \quad (G-4)$$

where

$$\gamma = m\pi R \sqrt{M^2-1} \quad (G-5)$$

For the case  $n = 0$  the equation was rewritten as

$$A_1 e^{i\psi_1} = \frac{J_0(\gamma) - i Y_0(\gamma)}{-J_1(\gamma) + i Y_1(\gamma)} \cdot \frac{M}{\sqrt{M^2-1}} \quad (G-6)$$



and

$$A_1 = |A_1 e^{i\psi_1}| \quad (G-7)$$

$$\psi_1 = \tan^{-1} \left[ \frac{\text{Im}(A_1 e^{i\psi_1})}{\text{Re}(A_1 e^{i\psi_1})} \right] \quad (G-8)$$

The program listing appears in Appendix I.





## APPENDIX H

### TWO BLADE SOLUTION USING THE METHOD OF SINGULARITIES

As shown by Garrick and Rubinow (Ref. 12), the velocity potential of a single blade oscillating in supersonic flow is

$$\phi(x, y) = \frac{-1}{\sqrt{M^2-1}} \int_0^{x-y\sqrt{M^2-1}} v(\xi) e^{-ik \frac{M^2}{M^2-1}(x-\xi)} J_0 \left[ \frac{kM}{M^2-1} \sqrt{(x-\xi)^2 - (M^2-1)y^2} \right] d\xi \quad (H-1)$$

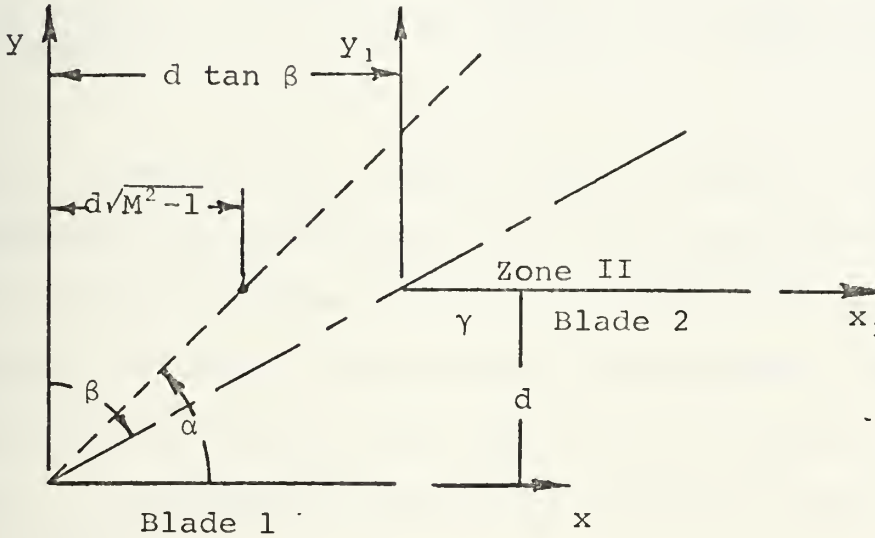


Figure H-1. Method of Singularities Configuration

The solution for supersonic flow past two oscillating blades in Zone II, (Figure H-1), can be obtained by superposition of single blade solutions. For this purpose the disturbed flow field in Zone II is written as the linear superposition of the single blade solutions for blades 1 and 2. However, in order to satisfy the flow tangency condition on the upper surface



of blade 2, a third single blade solution with unknown normal velocity must be added. Hence, one can write

$$\phi_T = \phi_1 + \phi_2 + \phi_{IP} \quad (H-2)$$

where

$$\phi_1 = \frac{-1}{\sqrt{M^2-1}} \int_0^{x-y\sqrt{M^2-1}} v(\xi) e^{-ik \frac{M^2}{M^2-1} (x-\xi)} J_0 \left[ \frac{kM}{M^2-1} \sqrt{(x-\xi)^2 - (M^2-1)y^2} \right] d\xi \quad (H-3)$$

$$\phi_2 = \frac{-1}{\sqrt{M^2-1}} \int_0^{x_1-y_1\sqrt{M^2-1}} v(\xi) e^{-i \frac{kM^2}{M^2-1} (x_1-\xi)} J_0 \left[ \frac{kM}{M^2-1} \sqrt{(x_1-\xi)^2 - (M^2-1)y_1^2} \right] d\xi \quad (H-4)$$

$$\phi_{IP} = \frac{-1}{\sqrt{M^2-1}} \int_0^{x_1-y_1\sqrt{M^2-1}} v_\sigma(\xi) e^{-i \frac{kM^2}{M^2-1} (x_1-\xi)} J_0 \left[ \frac{kM}{M^2-1} \sqrt{(x_1-\xi)^2 - (M^2-1)y_1^2} \right] d\xi \quad (H-5)$$

where  $v_\sigma$  denotes the unknown normal velocity. Equation (H-3) represents the disturbance due to the first blade, equation (H-4) the disturbance due to the second blade alone, and equation (H-5) the interference disturbance. Note that the blade 2 and interference potentials are expressed in terms of an  $x_1, y_1$  coordinate system with origin at the leading edge of blade 2.

Satisfying the boundary condition on the upper surface of blade 2 gives an equation for the unknown velocity,  $v_\sigma$ , i.e.,

$$v_\sigma(x, y) = \frac{1}{\sqrt{M^2-1}} \frac{\partial}{\partial y} \int_0^{x-y\sqrt{M^2-1}} v(\xi) e^{-i \frac{kM^2}{M^2-1} (x-\xi)} \cdot J_0 \left[ \frac{kM}{M^2-1} \sqrt{(x-\xi)^2 - (M^2-1)y^2} \right] d\xi \quad (H-6)$$

at  $y = d$ .



Now setting

$$v(\xi) = ik Z(\xi) + Z'(\xi) \quad (H-7)$$

and assuming the blades to pitch about their leading edges, i.e.,

$$Z(\xi) = \xi \quad (H-8)$$

and then performing the differentiation, one obtains

$$\begin{aligned} v_{\sigma}(x, y) = & \frac{1}{\sqrt{M^2-1}} \left\{ \int_0^{x-y\sqrt{M^2-1}} [ikZ(\xi) + Z'(\xi)] e^{-i\frac{kM^2}{M^2-1}(x-\xi)} \right. \\ & \cdot \frac{kMy}{\sqrt{(x-\xi)^2 - (M^2-1)y^2}} \cdot J_1\left[\frac{kM}{M^2-1} \sqrt{(x-\xi)^2 - (M^2-1)y^2}\right] d\xi \\ & \left. - [ikZ(x-y\sqrt{M^2-1}) + Z'(x-y\sqrt{M^2-1})] \cdot e^{-i\frac{kM^2}{M^2-1}y} \right\} \\ & \text{at } y = d \end{aligned} \quad (H-9)$$

Since, in general

$$C_P = ik\phi + \phi_x \quad (H-10)$$

the total pressure coefficient can be written as

$$C_P = C_{P1} + C_{P2} - C_{PIP} \quad (H-11)$$

where  $C_{P1}$  is obtained from the single blade solution for blade 1 at  $y = d$ ,

$$\begin{aligned} C_{P1} = & \frac{k^2}{\sqrt{M^2-1}} \left( \int_0^{x-d\sqrt{M^2-1}} [-Z(\xi) + \frac{i}{k}Z'(\xi)] e^{-i\frac{kM^2}{M^2-1}(x-\xi)} \right. \\ & \cdot J_0\left[\frac{kM}{M^2-1} \sqrt{(x-\xi)^2 - (M^2-1)d^2}\right] d\xi - \frac{i}{k} \left\{ \int_0^{x-d\sqrt{M^2-1}} [-Z'(\xi) + \frac{i}{k}Z''(\xi)] \right. \\ & \cdot e^{-i\frac{kM^2}{M^2-1}(x-\xi)} \cdot J_0\left[\frac{kM}{M^2-1} \sqrt{(x-\xi)^2 - (M^2-1)d^2}\right] d\xi \\ & \left. \left. + \frac{i}{k} e^{-i\frac{kM^2}{M^2-1}x} \cdot J_0\left[\frac{kM}{M^2-1} \sqrt{x^2 - (M^2-1)d^2}\right] \right\} \right) \end{aligned} \quad (H-12)$$



$C_{P2}$  from the single blade solution for blade 2 at  $y_1 = 0$ ,

$$C_{P2} = \frac{k^2}{\sqrt{M^2-1}} \int_0^{x_1} [-Z(\xi) + \frac{i}{k} Z'(\xi)] e^{-i \frac{kM^2}{M^2-1} (x_1 - \xi)} \cdot J_0 \left[ \frac{kM}{M^2-1} (x_1 - \xi) \right] d\xi - \frac{i}{k} \left\{ \int_0^{x_1} [-Z'(\xi) + \frac{i}{k} Z''(\xi)] e^{-i \frac{kM^2}{M^2-1} (x_1 - \xi)} \cdot J_0 \left[ \frac{kM}{M^2-1} (x_1 - \xi) \right] d\xi + \frac{i}{k} e^{-i \frac{kM^2}{M^2-1} x_1} J_0 \left[ \frac{kM}{M^2-1} x_1 \right] \right\} \quad (H-13)$$

and

$$C_{P_{IP}} = ik \phi_{IP} + \phi_{IP} \quad (H-14)$$

where

$$\phi_{IP} = \frac{-1}{\sqrt{M^2-1}} \int_0^{x_1} v_\sigma(\gamma) e^{-i \frac{kM^2}{M^2-1} (x_1 - \gamma)} J_0 \left[ \frac{kM}{M^2-1} (x_1 - \gamma) \right] d\gamma \quad (H-15)$$

and

$$\phi_{IPx} = \frac{-1}{\sqrt{M^2-1}} \left\{ \int_0^{x_1} v_\sigma(\gamma) \left[ -i \frac{kM^2}{M^2-1} e^{-i \frac{kM^2}{M^2-1} (x_1 - \gamma)} \cdot J_0 \left[ \frac{kM}{M^2-1} (x_1 - \gamma) \right] d\gamma - \int_0^{x_1} v_\sigma(\gamma) e^{-i \frac{kM^2}{M^2-1} (x_1 - \gamma)} \cdot \frac{kM}{M^2-1} \cdot J_1 \left[ \frac{kM}{M^2-1} (x_1 - \gamma) \right] d\gamma \right\} \quad (H-16)$$

where

$$v_\sigma(x) = \frac{1}{\sqrt{M^2-1}} \left\{ \int_0^{x-d\sqrt{M^2-1}} [ikZ(\xi) + Z'(\xi)] e^{-i \frac{kM^2}{M^2-1} (x - \xi)} \cdot \frac{kMd}{\sqrt{(x-\xi)^2 - (M^2-1)d^2}} \cdot J_1 \left[ \frac{kM}{M^2-1} \sqrt{(x-\xi)^2 - (M^2-1)d^2} \right] d\xi - [ikZ(x-d\sqrt{M^2-1}) + Z'(x-d\sqrt{M^2-1})] e^{-i \frac{kM^2}{M^2-1} d} \right\} \quad (H-17)$$

Note that the substitution of  $v_\sigma(x)$  into equations (H-15) and (H-16) for  $\phi_{IP}$  and  $\phi_{IPx}$  requires one to relate  $x$  and  $\gamma$  by





$$x = \gamma + d \tan \beta$$

(H-18)

(see Figure H-1)

These integrals were computed using the Trapexoidal Rule and IBM subroutine BESJ. A listing of the program follows in Appendix I.



## PROGRAM LISTINGS

100



```

C      COMPUTE INITIAL VALUES
C      I=IHAVEP
      QPHI(I,JSWITCH)=(0.,0.)
      PHK(I,JSWITCH)=(0.,0.)
      X(IHAVEP,JSWITCH)=0.0
      R(IHAVEP,JSWITCH)=RADIUS
      PI=3.141593
      PARW=MFREQ*PI*COS(MFREQ*PI*X(IHAVEP,JSWITCH))
      QR=PARW
      PHI(I,JSWITCH)=-2.0*QR/MACH
      PX=(MACH/(2.0*BETA))*(PHK(I,JSWITCH)+PHI(I,JSWITCH))
      CP(KOUNT)=-2.0*(II*K*QPHI(I,JSWITCH)+PX)
      REALCP(KOUNT)=REAL(CP(KOUNT))
      AMAGCP(KOUNT)=AIMAG(CP(KOUNT))

C      WRITE OUT INPUT
C      WRITE (6,12) MACH,K,NFREQ,FINGRD,RADIUS,MFREQ
      FORMAT (1H0,20X,'FREESTREAM MACH NUMBER =',F9.6//20X,'REDUCED FREQ
1 1=',F9.5//20X,'RAD MODE NO. N=',I2//20X,'GRID FINENESS IS =',
2 13 //20X,'CYLINDER RADIUS IS =',F9.2//20X,'AXIAL MODE NO. M
3,12)
      KCUNT=2

C      COMPRX COMPUTES THE VALUE FOR X AND R GIVEN IHAVEP,ISWITCH
C      104
      CALL COMPRX
      PARW=MFREQ*PI*COS(MFREQ*PI*X(IHAVEP,ISWITCH))
      W=SIN(MFREQ*PI*X(IHAVEP,ISWITCH))
      XKM=(K*MACH)/BETA
      IKM=II*XKM
      XKW=K*W
      IKW=II*XKW

C      THE PROGRAM NOW GOES TO 30 IF POINT IS ON INITIAL MACH LINE.
C      1001 IF (IHAVEP.EQ.1) GO TO 30
C      TEST WHETHER THIS IS A SURFACE POINT.
C      IF (IHAVEP.EQ.KOUNT) GO TO 40
C      GO TO 60
C      30
      CALL MACHLN
      GO TO 50
C      40
      CALL PANPNT

```



00000970  
00000980  
00000990  
00001000  
00001010  
00001020  
00001030  
00001040  
00001050  
00001060  
00001070  
00001080  
00001090  
00001100  
00001110  
00001120  
00001130  
00001140  
00001150  
00001160  
00001170  
00001180  
00001190  
00001200  
00001210  
00001220  
00001230  
00001240  
00001250  
00001260  
00001270  
00001280  
00001290  
00001300

00001310  
00001320  
00001330  
00001340  
00001350  
00001360  
00001370  
00001380  
00001390  
00001400  
00001410  
00001420

```

C      GO TO 50
C      CALL GENFPT
C      A=IHAVEP
C      B=ISWITCH
C      PX=(MACH/(2.0*BETA))*(PHK(A,B)+ PHI(A,B))
C      PR=(MACH/2.0)*(PHK(A,B)-PHI(A,B))
C      IF (IHAVEP.EQ.KOUNT) GO TO 25
C      GO TO 35
C      INCREMENT FOR NEXT LINES
C      IF (ISWITCH.EQ.1.) GO TO 103
C      ISWITCH=1
C      JSWITCH=2
C      IHAVEP=1
C      GO TO 108
C      ISWITCH=2
C      JSWITCH=1
C      IHAVEP=1
C      GO TO 108
C      AT 35 INCREMENT ALONG PRESENT LINE
C      IHAVEP=IHAVEP+1
C      GO TO 104
C      KOUNT=KOUNT+1
C      IF ((KOUNT-1).EQ.ML) GO TO 101
C      GO TO 104
C      CONTINUE
C      CALL INTEG-REALCP,MFREQ,NR,DSTSTR,ML)
C      STOP
C      END
C      SUBROUTINE COMPR
C      REAL MACH,MANGL,K,KW
C      COMPUTES THE X AND R COORDINATES
C      COMMON DPHII,DPHIK,PHI(400,2),PHK(400,2),QPHI(400,2),IPHI1,IPHI2,
C      4 IKM,IKW,PARW,W,II,REALCP(400),CP(400),AMAGCP(400),
C      1 MACH,K,MANGL,RADIUS,DELTAS,XLENGT,BETA,DSTSTR,HDSTRL,TRNGLH,
C      2 X(400,2),R(400,2),NFREQ,FINGRD,ISWITCH,JSWICH,ILINE,MLINE,JLINE,
C      3 MFREQ,IHAVEP,KOUNT
C      COMPLEX DPHII,DPHIK,PHI,IKM,CP,PX ,IPHI1,IPHI2,IKW,PHK,II,QPHI,PR

```





00001430  
00001440  
00001450  
00001460  
00001470  
00001480  
00001490  
00001500  
00001510  
00001520  
00001530  
00001540  
00001550  
00001560  
00001570

```

INTEGER FINGRD
TEST FOR POINT ON MACH LINE
IF (IHAVEP.EQ.1) GO TO 10
I=IHAVEP
J=IHAVEP-1
X(I,ISWITCH)=X(J
R(I,ISWITCH)=R(J
RETURN
I=IHAVEP
X(I,ISWITCH)=X(I
R(I,ISWITCH)=R(I
RETURN
END

```

10

00001580  
00001590  
00001600  
00001610  
00001620  
00001630  
00001640  
00001650  
00001660  
00001670  
00001680  
00001690  
00001700  
00001710  
00001720  
00001730  
00001740  
00001750  
00001760

```

SUBROUTINE MACHLN
COMMON DPHII,DPHIK,PHI(400,2),PHK(400,2),QPHI(400,2),IPHI1,IPHI2,
4 IKM,IKW,PARW,W,II,REALCP(400),CP(400),AMAGCP(400),
1 MACH,K,MANGL,RADIUS,DELTAS,XLENGT,BETA,DSTSTR,HDSTRL,TRNGLH,
2 X(400,2),R(400,2),NFREQ,FINGRD,ISWITCH,JSWITCH,ILINE,MLINE,JLINE,
3 MFREQ,IHAVEP,KOUNT
REAL MACH,MANGL,K,KW
COMPLEX AA2
1A,B,C,D,DPHII,DPHIK,PHI,IKM,CP,PX,IPHI1,IPHI2,IKW,PHK,II,QPHI
2 ,PR
INTEGER FINGRD
I=IHAVEP
PHK(I,ISWITCH)=(0.,0.)
A=1.+DELTAS/(4.*R(I,ISWITCH)*MACH)+0.5*IKM*DELTAS
AA2=1.-DELTAS/(4.*R(I,JSWITCH)*MACH)-0.5*IKM*DELTAS
PHI(I,ISWITCH)=PHI(I,JSWITCH)*(AA2/A)
QPHI(I,ISWITCH)=(0.,0.)
RETURN
END

```

10

00001770  
00001780  
00001790  
00001800  
00001810  
00001820  
00001830  
00001840  
00001850  
00001860

```

SUBROUTINE GENFPT
GENFPT COMPUTES THE VELOCITY POTENTIAL AND ITS DERIVATIVES AT A
GENERAL FLOW FIELD POINT.
COMMON DPHII,DPHIK,PHI(400,2),PHK(400,2),QPHI(400,2),IPHI1,IPHI2,
4 IKM,IKW,PARW,W,II,REALCP(400),CP(400),AMAGCP(400),
1 MACH,K,MANGL,RADIUS,DELTAS,XLENGT,BETA,DSTSTR,HDSTRL,TRNGLH,
2 X(400,2),R(400,2),NFREQ,FINGRD,ISWITCH,JSWITCH,ILINE,MLINE,JLINE,
3 MFREQ,IHAVEP,KOUNT

```

10



```

REAL MACH,MANGL,K,KW,N
CCOMPLEX AA1,AA2,AA3,
1A,B,C,D,DPHI1,DPHIK,PHI,IKM,CP,PX',IPHI1,IPHI2,IKW,PHK,I,I,QPHI
2,PR,E,F
INTEGER FINGRD
C
I=IHAVEP
J=IHAVEP -1
N=FLOAT(NFREQ)
C
A=1.-DELTA/(4.*R(I,ISWCH)*MACH)+0.5*IKM*DELTA
C
AA1=1.+DELTA/(4.*R(J,ISWCH)*MACH)-0.5*IKM*DELTA
C
AA3=-1.+DELTA/(4.*R(I,JSWCH)*MACH)+0.5*IKM*DELTA
C
B=DELTA/(4.*R(I,ISWCH)*MACH)+0.5*IKM*DELTA-0.25*DELTA**2*
1 (K**2-(N**2/(R(I,ISWCH)**2*MACH**2)))
C
C=PHK(J,ISWCH)*AA1+PHI(J,ISWCH)*(-DELTA/(4.*R(J,ISWCH)*MACH)
1 -0.5*IKM*DELTA+0.25*DELTA**2*(K**2-(N**2/(R(I,ISWCH)**2*MACH**
2 2)))+ QPHI(J,ISWCH)*DELTA*0.5*(K**2-N**2/(R(J,ISWCH)**2*MACH
3 **2))+ QPHI(J,ISWCH)*DELTA*0.5*(K**2-N**2/(R(I,ISWCH)**2*
4 MACH**2))
C
D=DELTA/(4.0 *R(I,ISWCH)*MACH)-0.5 *IKM*DELTA+0.25 *DELTA**
12*(K**2-(N**2/(R(I,ISWCH)**2*MACH**2)))
C
F=PHI(I,JSWCH)*AA3+PHK(I,JSWCH)*(-DELTA/(4.*R(I,JSWCH)*MACH)
1 +0.5*IKM*DELTA-0.25*DELTA**2*(K**2-(N**2/(R(I,ISWCH)**2*MACH**
2 2)))- QPHI(I,JSWCH)*DELTA*0.5*(K**2-N**2/(R(I,JSWCH)**2*MACH
3 **2))- QPHI(I,JSWCH)*DELTA*0.5*(K**2-N**2/(R(I,ISWCH)**2*
4 MACH**2))
C
E=-1.-DELTA/(4.*R(I,ISWCH)*MACH)-0.5*IKM*DELTA
C
CRAMER'S RULE
C
PHK(I,ISWCH)=(C*E-B*F)/(A*E -B*D)
PHI(I,ISWCH)=(F*A-C*D)/(A*E -B*D)
C
TRAPAZOIDAL RULE TO INTEGRATE.
C
IPHI1=QPHI(I,JSWCH)+0.5*(PHK(I,JSWCH)+PHK(I,ISWCH))*DELTA
IPHI2=QPHI(J,ISWCH)+0.5*(PHI(J,ISWCH)+PHI(I,ISWCH))*DELTA
00001870
00001880
00001890
00001900
00001910
00001920
00001930
00001940
00001950
00001960
00001970
00001980
00001990
00002000
00002010
00002020
00002030
00002040
00002050
00002060
00002070
00002080
00002090
00002100
00002110
00002120
00002130
00002140
00002150
00002160
00002170
00002180
00002190
00002200
00002210
00002220
00002230
00002240
00002250
00002260
00002270
00002280
00002290
00002300
00002310
00002320
00002330
00002340

```



00002350  
00002360  
00002370  
00002380  
00002390  
00002400

AVERAGE THE TWO

QPHI(I, ISWITCH)=0.5\*(IPHI1+IPHI2)  
RETURN  
END

15

00002410  
00002420  
00002430  
00002440  
00002450  
00002460  
00002470  
00002480  
00002490  
00002500  
00002510  
00002520  
00002530  
00002540  
00002550  
00002560  
00002570  
00002580  
00002590  
00002600  
00002610  
00002620  
00002630  
00002640  
00002650  
00002660  
00002670  
00002680  
00002690  
00002700  
00002710  
00002720  
00002730  
00002740  
00002750  
00002760  
00002770  
00002780  
00002790

SUBROUTINE PANPNT

PANPNT COMPUTES THE VALUES OF PHI'S AND QPHI AT A SURFACE POINT

COMMON DPHI1,DPHIK,PHI(400,2),PHK(400,2),QPHI(400,2),IPHI1,IPHI2,  
4 IKM,IKW,PARW,W,II,REALCP(400),CP(400),AMAGCP(400),  
1 MACH,K,MANGL,RADIUS,DELTAS,XLENGT,BETA,DSTSTR,HDSTRL,TRNGLH,  
2 X(400,2),R(400,2),NFREQ,FINGRD,ISWITCH,JSWITCH,ILINE,MLINE,JLINE,  
3 MFREQ,IHAVEP,KOUNT  
REAL MACH,MANGL,K,KW,N  
COMPLEX AA1,AA2

1A,B,C,D,DPHI1,DPHIK,PHI,IKM,CP,PX,IPHI1,IPHI2,IKW,PHK,II,QPHI

2,PR

INTEGER FINGRD

N=FLOAT(NFREQ)

I=IHAVEP

J=IHAVEP-1

A=1.-DELTAS/(4.\*R(I,ISWITCH)\*MACH)+0.5\*IKM\*DELTAS

AA1=1.+DELTAS/(4.\*R(J,ISWITCH)\*MACH)-0.5\*IKM\*DELTAS

B=DELTAS/(4.\*R(I,ISWITCH)\*MACH)+0.5\*IKM\*DELTAS\*\*2\*

1 (K\*\*2-(N\*\*2/(R(I,ISWITCH)\*\*2\*MACH\*\*2)))

1 C=PHK(J,ISWITCH)\*AA1+PHI(J,ISWITCH)\*(-DELTAS/(4.\*R(J,ISWITCH)\*MACH)

1 -0.5\*IKM\*DELTAS+0.25\*DELTAS\*\*2\*(K\*\*2-(N\*\*2/(R(I,ISWITCH)\*\*2\*MACH

22))) + QPHI(J,ISWITCH)\*DELTAS\*0.5\*(K\*\*2-N\*\*2/(R(I,ISWITCH)\*\*2\*

3\*\*2)) + QPHI(J,ISWITCH)\*DELTAS\*0.5\*(K\*\*2-N\*\*2/(R(I,ISWITCH)\*\*2\*

4 MACH\*\*2))

PHK(I, ISWITCH)= (C+B\*(2.0/MACH)\*(PARW+IKW))/(A+B)

PHI(I, ISWITCH)= (-A\*(2.0/MACH)\*(PARW+IKW)+C)/(A+B)

QPHI(I, ISWITCH)=QPHI(J,ISWITCH)+0.5\*(PHI(J,ISWITCH)+PHI(I

1 ISWITCH))\*DELTAS

PX=(MACH/(2.0\*BETA))\*(PHK(I,ISWITCH)+PHI(I,ISWITCH))

CP(KOUNT)=-2.0\*(I\*K\*QPHI(I,ISWITCH)+PX)

REALCP(KOUNT)=REAL(CP(KOUNT))

AMAGCP(KOUNT)=AIMAG(CP(KOUNT))

RETURN

END

10



```

00002800
00002810
00002820
00002830
00002840
00002850
00002860
00002870
00002880
00002890
00002900
00002910
00002920
00002930
00002940
00002950
00002960
00002970
00002980
00002990
00003000

```

```

SUBROUTINE INTEG(Y,M,NR,DX,ML)
DIMENSION Y(ML)
Q=0.0
X1=0.0
RN=FLOAT(NR)
PSI1=0.0
PRD1=0.0
DO 1 I=2,ML
X2=X1+DX
PSI2=SIN(RN*3.141593*X2)
PRD2=PSI2*Y(I)
Q=Q+(PRD2+PRD1)*DX/2.0
PRD1=PRD2
X1=X2
1 CCNTINUE
Q=Q/2.0
WRITE(6,100)M,NR,Q
FORMAT(' ',10X,'Q(',I2,' ',I2,' ')R= ',E13.7,'//')
FORMAT('0 ',GENERALIZED AERODYNAMIC FORCE:',//)
100 RETURN
101 END

```





```

C C C
      ONE DEGREE OF FREEDOM CASCADE
      DIMENSION DATE(3)
      DIMENSION U22R(400,2),U22I(400,2),V22R(400,2),V22I(400,2),C22R(400,2),C22I(400,2),X(400,2),Y(400,2)
      DIMENSION U33R(400,2),U33I(400,2),V33R(400,2),V33I(400,2),C33R(400,2),C33I(400,2)
      COMMON/BLK1/NGRDFN,FSTRMN,REDFRC,XSUBO,INWDST,FMANGL,XLNGTH,DELTA
      1,DSTSTR,HDSRRL,TRNGLH,U22R,U22I,V22R,V22I,C22R,C22I,X,Y,S,DELTA,
      2,SWTCH,JSWTCH,JLINE,IHAVEP,AI,BI,K12R,K12I,K34R,K34I,K56R,K56I,
      3VRPANL,VIPANL,STGANG,NSTPTS,LCOUNT,STAG
      COMMON/BLK5/U33R,U33I,V33R,V33I,C33R,C33I
      COMMON/PCOR/ICO
      COMMON/STG/STGR
      COMMON/BLADE/NUM,NUMBLD
      COMMON/BLK6/W
      REAL K12R,K12I,K34R,K34I,K56R,K56I
      INTEGER OLDL
      PRINT NAME OF PROGRAM/DATE OF RUN.
      READ(5,100)DATE
      100 FORMAT(3A4)
      WRITE(6,101)DATE
      101 FORMAT(1H1,14(/),14(/),37X,51H OSCILLATING CASCADE PROGRAM
      1 ---RUN OF---,3A4,/,1H1)
      PRINT OUT ALL INPUT INFORMATION VIA INPUT.
      CALL INPUT
      OLDL=0
      ICC=0
      INITIALIZE FLOW QUANTITIES AND LOGIC VARIABLES.
      CALL INTIAL
      FAC=1.0/DSTSTR
      NEWDST=FAC
      XX=FAC-NEWDST
      IF(XX.GE.0.5)NEWDST=NEWDST+1
      LIMIT=(NUMBLD-1)*NSTPTS+NEWDST
      LIMW=NEWDST
      MAXI=NGRDFN+NSTPTS
      NUM=0
      NUMOLD=0
      NUMPI=1
      1000 CCNTINUE

```



C	CALL COMPLY	00000490
C	IF POINT IS ON THE INITIAL RIGHT-RUNNING MACH LINE, CALL MACHLN.	00000500
C	IF(LCOUNT.EQ.0)GO TO 1	00000510
C	IF POINT IS ON A BLADE OR IN A WAKE, GO TC 2.	00000520
C	IF(IHAVEP.EQ.LCOUNT)GO TO 2	00000530
C	IF POINT IS ON INITIAL LEFT-RUNNING MACH LINE, CALL MACHLN.	00000540
C	IF(IHAVEP.EQ.0)GO TO 1	00000550
C	CONDITION FOR FIRST ENCOUNTER WITH A BLADE.	00000560
C	IF((IHAVEP.EQ.NUMPI*NSTPTS).AND.(JLINE.EQ.MAXI))GO TO 7	00000570
C	CALL GENFPT	00000580
C	IF(IHAVEP.EQ.LIMIT)GO TO 5	00000590
C	IFAVEP=IHAVEP+1	00000600
C	GO TO 1000	00000610
C	1 CALL MACHLN	00000620
C	IF(IHAVEP.EQ.LIMIT)GO TO 5	00000630
C	IFAVEP=IHAVEP+1	00000640
	GO TO 1000	00000650
	2 ICC=1	00000660
	IF POINT IS IN A WAKE, CALL WAKE.	00000670
	IF(IHAVEP.GE.LIMW)GO TO 4	00000680
	CALL TOP	00000690
	CALL BOTTCM	00000700
	IF(IHAVEP.EQ.LIMIT)GO TO 8	00000710
	IFAVEP=IHAVEP+1	00000720
	IF(NUM.EQ.0)GO TO 1000	00000730
	NCM=NUM-1	00C00740
	LCOUNT=LCOUNT+NGRDFN	00000750
	LIMW=LIMW-NSTPTS	00000760
	GO TO 1000	00000770
	4 CALL WAKE	00000780
	IF(IHAVEP.EQ.LIMIT)ICO=0	00000790
	IF THIS IS THE LAST POINT TO BE COMPUTED IN THE ENTIRE FLOW	00C00800
	FIELD AREA, TERMINATE PROGRAM.	00000810
	IF((NUM.GE.NUMBLD-1).AND.(IHAVEP.EQ.LIMIT))GO TO 8	00000820
	IF(IHAVEP.EQ.LIMIT)GO TO 5	00G00830
	IFAVEP=IHAVEP+1	00000840
		00000850
		00C00860
		00000870
		00000880
		00000890
		00000900
		00000910
		0C000920
		00000930
		00000940
		00000950
		00000960



```

C
C
C
5
IF(NUM.EQ.0)GO TO 1000
LCOUNT=LCOUNT+NGRDFN
NUM=NUM-1
GO TO 1000
CCNTINUE

SWITCH LOGIC VARIABLES TO START THE COMPUTATION BACK AT THE
INITIAL LEFT-RUNNING MACH LINE.

IHAVEP=0
NUM=NUMOLD
JLINE=JLINE+1
IF((ISWITCH.EQ.1)GO TO 9
ISWITCH=1
JSWITCH=2
GO TO 10
ISWITCH=2
JSWITCH=1
CCNTINUE
10
IF(NUMOLD.GT.0)GO TO 6
LCOUNT=LCOUNT+1
GO TO 1000
6
LCOUNT=OLDL
LIMW=NUMOLD*NSTPTS+NEW DST
OLDL=OLDL+1
GO TO 1000
7
CALL NEWBLD
ICO=1
NUMOLD=NUM
LCOUNT=IHAVEP+NGRDFN
JLINE=IHAVEP
IHAVEP=IHAVEP+1
OLDL=IHAVEP
NUMPI=NUM+1
MAXI=NGRDFN+NUMPI*NSTPTS
NUM=NUM-1
GO TO 1000
8
CCNTINUE
STOP
END

```

```

C
C
C
SUBROUTINE INPUT
SUBROUTINE INPUT READS ALL INPUT.
DIMENSION U22R(400,2),U22I(400,2),V22R(400,2),V22I(400,2),C22R(400
1,2),C22I(400,2),X(400,2),Y(400,2)

```



```

COMMON/BLK1/NGRDFN,FSTRMN,REDFRQ,XSUBO,TNWDST,FMANGL,XLNGTH,DELTA,
1,DSTSTR,HDSTRL,TRNGLH,U22I,V22R,V22I,C22R,C22I,X,Y,S,DELTA,
21SWITCH,JSWITCH,JLINE,IHAVEP,A1,B1,K12R,K12I,K34R,K34I,K56R,K56I,
3VRPANL,VIPANL,STGANG,NSTPTS,LCOUNT,STAG
COMMON/STG/STGR
COMMON/BLADE/NUM,NUMBLD
COMMON/BLK6/W
REAL K12R,K12I,K34R,K34I,K56R,K56I
NAMELIST/NAME1/NGRDFN,FSTRMN,REDFRQ,XSUBO,TNWDST,STGANG,FAZE,NUMBLD
READ(5,NAME1)
WRITE(6,NAME1)
FMANGL=ARSIN(1.0/FSTRMN)
XLNGTH=TNWDST/SIN(FMANGL)
FNGDPT=FLOAT(NGRDFN)
DELTAS=XLNGTH/FNGDPT
TRNGLH=TNWDST/FNGDPT
HDSTRL=DELTAS*COS(FMANGL)
DSTSTR=HDSTRL*2.0
STAG=TNWDST*TAN(STGANG*0.1745329E-01)
STGR=STAG-(TNWDST/TAN(FMANGL))
NSTPTS=STGR/DSTSTR
IF(NSTPTS.LT.1)NSTPTS=1
STGR=NSTPTS*DSTSTR
STGANG=ATAN((STGR+(TNWDST/TAN(FMANGL)))/(TNWDST*57.29578)
STAG=STGR+(TNWDST/TAN(FMANGL))
S=SQRT((FSTRMN*FSTRMN-1.0)
W=FSTRMN*FSTRMN/(FSTRMN*FSTRMN-1.0)
DELTAFAZE*0.1745329E-01
WRITE(6,5)NGRDFN,FSTRMN,REDFRQ,TNWDST,XSUBO,STGANG,DSTSTR,FAZE,NUM
1BLD
5FORMAT(///,28H GRID FINENESS INPUT NUMBER=,I10,///,24H FREESTREAM,
1MACH NUMBER=,F20.7,///,34H REDUCED(DIMENSIONLESS) FREQUENCY=,F20.00001730
27,///,27H DISTANCE BETWEEN AIRFOILS=,F20.7,///,52H HORIZONTAL POSI
3TION(DIMENSIONLESS) OF ELASTIC AXIS=,F20.7,///,26H COMPATIBLE STAG
4GER ANGLE=,F20.7,///,9H DELTA X=,F20.7,///,25H UPPER AIRFOIL PHASE
5LAG=,F20.7,///,1X,12,' BLADES:',/)
WRITE(6,6)
6FORMAT(1,'10X,'VALUES OF TEIPEL COMPLEX PERTURBATION AMPLITUDES',
1///,1X,'BLD',T10,'X',T21,'UR',T42,'UI',T58,'VR',T73,'VI',T90,'CR',
2T107,'CI',/)
RETURN
END

```





```

C
C
C
SUBROUTINE INITIAL
INITIAL INITIALIZES ALL FLOW FIELD QUANTITIES.
DIMENSION U22R(400,2), U22I(400,2), V22R(400,2), V22I(400,2), C22R(400,2), C22I(400,2), X(400,2), Y(400,2)
DIMENSION U33R(400,2), U33I(400,2), V33R(400,2), V33I(400,2), C33R(400,2), C33I(400,2)
COMMON/BLK1/NGRDN, FSTRMN, REDFRQ, XSUBO, TNWCST, FMANGL, XLNGTH, DELTAS
1, DSTSTR, HDSTRL, TRNGLH, U22R, U22I, V22R, V22I, C22R, C22I, X, Y, S, DELTA,
2, SWITCH, JSWTCH, JLINE, IHAVEP, AI, BI, K12R, K12I, K34R, K34I, K56R, K56I,
3, VRPANL, VIPANL, STGANG, NSTPTS, LCOUNT, STAG
COMMON/BLK5/U33R, U33I, V33R, V33I, C33R, C33I
COMMON/BLK6/W
COMMON/BLADE/NUM, NUMBLD
REAL K12R, K12I, K34R, K34I, K56R, K56I
AI=.5*REDFRQ*DSTSTR
BI=AI*W/2.0
SET UP INITIAL VALUES FOR U,V,AND C AT (0,0).
50 VRPANL=-1.0/S
VIPANL=REDFRQ*XSUBO/S
U22R(1,1)=-VRPANL
U22I(1,1)=-VIPANL
V22R(1,1)=-U22R(1,1)
V22I(1,1)=-U22I(1,1)
C22R(1,1)=-U22R(1,1)
C22I(1,1)=-U22I(1,1)
X(1,1)=0.0
Y(1,1)=0.0
U33R(1,1)=VRPANL
U33I(1,1)=VIPANL
V33R(1,1)=VRPANL
V33I(1,1)=VIPANL
C33R(1,1)=-VRPANL
C33I(1,1)=-VIPANL
ISWTCH=1
JSWTCH=2
JLINE=0
IHAVEP=1
LCOUNT=0
WRITE(6,100) X(1,1), U22R(1,1), U22I(1,1), V22R(1,1), V22I(1,1), C22R(1,1), C22I(1,1)
100 WRITE(6,100) X(1,1), U33R(1,1), U33I(1,1), V33R(1,1), V33I(1,1), C33R(1,1), C33I(1,1)
FORMAT(2H I,7E16.7,/)
RETURN
00001850
00001860
00001870
00001880
00001890
00001900
00001910
00001920
00001930
00001940
00001950
00001960
00001970
00001980
00001990
00002000
00002010
00002020
00002030
00002040
00002050
00002060
00002070
00002080
00002090
00002100
00002110
00002120
00002130
00002140
00002150
00002160
00002170
00002180
00002190
00002200
00002210
00002220
00002230
00002240
00002250
00002260
00002270
00002280
00002290
00002300
00002310
00002320

```







```

1,2),C33I(400,2)
CCMON/BLK1/NGRDFN,FSTRMN,REDFRQ,XSUBO,TNWCST,FMANGL,XLNGTH,DELTA
1,DSTSTR,HDSTRL,TRNGLH,U22R,U22I,V22R,V22I,C22R,C22I,X,Y,S,DELTA,
2ISWITCH,JSWITCH,ALINE,IHAVEP,AI,BI,K12R,K12I,K34R,K34I,K56R,K56I,
3VRPANL,VIPANL,STGANG,NSTPTS,LCOUNT,STAG
CCMON/PCOR/ICO
COMMON/BLK5/U33R,U33I,V33R,V33I,C33R,C33I
REAL K12R,K12I,K34R,K34I,K56R,K56I
I=IHAVEP+1

'ICO' INSURES PROPER SELECTION OF FLOW QUANTITIES AT P21 IF GRID
PCINT IS THE FIRST GRID POINT AFTER A BLADE GRID POINT.

IF(ICO.EQ.1)GO TO 1.
GO TO 2
1 A=U33R(IHAVEP,ISWITCH)
B=U33I(IHAVEP,ISWITCH)
C=U33R(IHAVEP,ISWITCH)
D=U33I(IHAVEP,ISWITCH)
ICO=0
GO TO 10
2 A=U22R(IHAVEP,ISWITCH)
B=U22I(IHAVEP,ISWITCH)
C=U22R(IHAVEP,ISWITCH)
D=U22I(IHAVEP,ISWITCH)
K12R=U22R(IHAVEP,JSWITCH)+C22R(IHAVEP,JSWITCH)+AI*U22I(IHAVEP,JSWITCH)
K12I=-AI*U22R(IHAVEP,JSWITCH)+U22I(IHAVEP,JSWITCH)+C22I(IHAVEP,JSWITCH)
K34R=U22R(IHAVEP+1,JSWITCH)-V22R(IHAVEP+1,JSWITCH)+BI*(U22I(IHAVEP+1,JSWITCH)-C22I(IHAVEP+1,JSWITCH))
K34I=U22I(IHAVEP+1,JSWITCH)-V22I(IHAVEP+1,JSWITCH)+BI*(U22R(IHAVEP+1,JSWITCH)-C22R(IHAVEP+1,JSWITCH))
K56I=B+V22I(IHAVEP,ISWITCH)+BI*(B-D)
K56R=A+V22R(IHAVEP,ISWITCH)-BI*(A-C)
G1=.5*(K34R+K56R)
G2=BI*K12I
G3=1.0-AI*BI
G4=.5*(K34I+K56I)
G5=BI*K12R
G6=2.0*BI
G7=G3*G3+G6*G6
G8=G1-G2
G9=G4+G5
U22R(I,ISWITCH)=(G8*G3+G9*G6)/G7
U22I(I,ISWITCH)=(-G8*G6+G9*G3)/G7
V22R(I,ISWITCH)=.5*(K56R-K34R)
V22I(I,ISWITCH)=.5*(K56I-K34I)

```

CC  
CC  
CC





```

C22R(I, ISWITCH)=K12R-U22R(I, ISWITCH)+U22I(I, ISWITCH)*AI
C22I(I, ISWITCH)=K12I-U22I(I, ISWITCH)-U22R(I, ISWITCH)*AI
RETURN
END

```

```

00003250
00003260
00003270
00003280

```

```

SUBROUTINE TOP

```

```

00003290
00003300
00003310
00003320
00003330
00003340
00003350
00003360
00003370
00003380
00003390
00003400
00003410
00003420
00003430
00003440
00003450
00003460
00003470
00003480
00003490
00003500
00003510
00003520
00003530
00003540
00003550
00003560
00003570
00003580
00003590
00003600
00003610
00003620
00003630
00003640
00003650
00003660
00003670
00003680
00003690
00003700

```

```

TCP COMPUTES U,V, AND C AT AN UPPER SURFACE POINT.

```

```

DIMENSION U22R(400,2),U22I(400,2),V22R(400,2),V22I(400,2),C22R(400,2),C22I(400,2),X(400,2),Y(400,2)
COMMON/BLK1/NGRDFN,FSTRMN,REDFRQ,XSUBO,TNWDST,FMANGL,XLNGTH,DELTAS
1,DSTSTR,HDSRTR,TRNGHL,U22R,U22I,V22R,V22I,C22R,C22I,X,Y,S,DELTA,
2,ISWITCH,JSWITCH,JLINE,IHAVEP,AI,BI,K12R,K12I,K34R,K34I,K56R,K56I,
3VRPANL,VIPANL,STGANG,NSTPTS,LCOUNT,STAG
COMMON/BLADE/NUM,NUMBLD
REAL K12R,K12I,K34R,K34I,K56R,K56I
XN=FLOAT(NUM)
J=IHAVEP
I=IHAVEP+1
XNEW=X(I,ISWITCH)-STAG*XN

```

```

XNEW=X(I,ISWITCH)-STAG*XN

```

```

IF THIS IS THE FIRST BLADE OR IF THE INTERBLADE PHASE ANGLE IS
ZERO, SIMPLIFY THE NORMAL VELOCITY COMPUTATION.

```

```

C
C
C
C

```

```

IF((DELTA.LE.1.0E-05).OR.(NUM.EQ.0))GO TO 999

```

```

ARG=DELTA*XN
V22I(I,ISWITCH)=-((COS(ARG)-{(XNEW-XSUBO)*REDFRQ*SIN(ARG)})/S
V22I(I,ISWITCH)=-((SIN(ARG)+{(XNEW-XSUBO)*REDFRQ*COS(ARG)})/S
GO TO 90

```

```

999

```

```

V22R(I,ISWITCH)=-1.0/S
V22I(I,ISWITCH)={(-REDFRQ*(XNEW-XSUBO))/S
K34R=V22R(I,ISWITCH)
K34I=V22I(I,ISWITCH)

```

```

90

```

```

1 K12R=U22R(J,JSWITCH)+C22R(J,JSWITCH)+AI*U22I(J,JSWITCH)
K12I=U22I(J,JSWITCH)+C22I(J,JSWITCH)-AI*U22R(J,JSWITCH)
K56R=U22R(J,ISWITCH)+V22R(J,ISWITCH)+BI*(U22I(J,ISWITCH)-
K22I(J,ISWITCH))
K56I=U22I(J,ISWITCH)+V22I(J,ISWITCH)-BI*(U22R(J,ISWITCH)-
K22R(J,ISWITCH))
G1=1.0-AI*BI
G2=2.0*BI
G3=G1*G1+G2*G2
G4=K56R-K34R-BI*K12I
G5=K56I-K34I+BI*K12R
U22R(I,ISWITCH)=(G4*G1+G5*G2)/G3
U22I(I,ISWITCH)=(-G4*G2+G5*G1)/G3

```

```

,JSWITCH)
,ISWITCH)-
,ISWITCH)-

```





```

C22R(I      ,ISWITCH)=K12R-U22R(I      ,ISWITCH)+AI*U22I(I,I,ISWITCH)
C22I(I      ,ISWITCH)=K12I-U22I(I      ,ISWITCH)-AI*U22R(I,I,ISWITCH)
147 WRITE(6,145)NUM,XNEW,U22R(I,I,ISWITCH),U22I(I,I,ISWITCH),V22R(I,I,ISWITCH),
145 V22I(I,I,ISWITCH),C22R(I,I,ISWITCH),C22I(I,I,ISWITCH)
145 FORMAT(2H T,I2,7E16.7,/)
RETURN
END
00003710
00003720
00003730
00003740
00003750
00003760
00003770

```

```

SUBROUTINE COMPHY
COMPHY COMPUTES THE GRID POINT'S X,Y POSITION.
DIMENSION U22R(400,2),U22I(400,2),V22R(400,2),V22I(400,2),C22R(400,2),C22I(400,2),X(400,2),Y(400,2)
COMMON/BLK1/NGRDFN,FSTRMN,REDFRC,XSUBO,TNW CST,FMANGL,XLNGTH,DELTA
1,DSSTR,HDSSTR,TRNGLH,U22I,V22I,V22R,C22R,C22I,X,Y,S,DELTA,
2,ISWITCH,JSWITCH,JLINE,IHAVEP,AI,BI,K12R,K34R,K34I,K56R,K56I,
3VRPANL,VIPANL,STGANG,NSTPTS,LCOUNT,STAG
REAL K12R,K12I,K34R,K34I,K56R,K56I
I=IHAVEP+1
00003780
00003790
00003800
00003810
00003820
00003830
00003840
00003850
00003860
00003870
00003880
00003890
00003900
00003910
00003920
00003930
00003940
00003950
00003960
00003970
00003980
00003990
00004000
00004010
00004020

```

```

CHECK WHETHER GRID POINT IS ON THE INITIAL LEFT-RUNNING MACH LINE.
IF((IHAVEP.EQ.0).AND.(LCOUNT.NE.0))GO TO 1
X(I,ISWITCH)=X(IHAVEP,ISWITCH)+HDSSTR
Y(I,ISWITCH)=Y(IHAVEP,ISWITCH)-TRNGLH
RETURN
00003920
00003930
00003940
00003950
00003960
00003970
00003980
00003990
00004000
00004010
00004020

```

```

1 X(I,ISWITCH)=X(I,JSWITCH)+HDSSTR
Y(I,ISWITCH)=Y(I,JSWITCH)+TRNGLH
RETURN
END
00004030
00004040
00004050
00004060
00004070
00004080
00004090
00004100
00004110
00004120
00004130
00004140

```

```

SUBROUTINE NEWBLD
NEWBLD COMPUTES U,V, AND C AT THE FIRST POSITION ON A BLADE
ENCOUNTERED FOR THE FIRST TIME.
DIMENSION U22R(400,2),U22I(400,2),V22R(400,2),V22I(400,2),C22R(400,2),C22I(400,2),X(400,2),Y(400,2)
1,DSSTR,HDSSTR,TRNGLH,U22I,V22I,V22R,C22R,C22I,X,Y,S,DELTA,
2,ISWITCH,JSWITCH,JLINE,IHAVEP,AI,BI,K12R,K34R,K34I,K56R,K56I,
3VRPANL,VIPANL,STGANG,NSTPTS,LCOUNT,STAG
COMMON/BLK1/NGRDFN,FSTRMN,REDFRC,XSUBO,TNW CST,FMANGL,XLNGTH,DELTA
1,DSSTR,HDSSTR,TRNGLH,U22I,V22I,V22R,C22R,C22I,X,Y,S,DELTA,
2,ISWITCH,JSWITCH,JLINE,IHAVEP,AI,BI,K12R,K34R,K34I,K56R,K56I,
3VRPANL,VIPANL,STGANG,NSTPTS,LCOUNT,STAG
00004030
00004040
00004050
00004060
00004070
00004080
00004090
00004100
00004110
00004120
00004130
00004140

```



```

3VRPANL,VIPANL,STGANG,NSTPTS,LCOUNT,STAG
CCMMON/BLK5/U33R,U33I,V33R,V33I,C33R,C33I
CCMMON/BLADE/NUM,NUMBLD
REAL K12R,K12I,K34R,K34I,K56R,K56I
NUM=NUM+1
XN=FLOAT(NUM)
I=IHAVEP+1
K12R=U22R(IHAVEP,JSWTC)+C22R(IHAVEP,JSWTC)+AI*U22I(IHAVEP,JSWTC)
1)
K12I=-AI*U22R(IHAVEP,JSWTC)+U22I(IHAVEP,JSWTC)+C22I(IHAVEP,JSWTC)
1H)
K56R=U22R(IHAVEP,ISWTC)+V22R(IHAVEP,ISWTC)+BI*(U22I(IHAVEP,ISWTC)
1H)-C22I(IHAVEP,ISWTC))
K56I=U22I(IHAVEP,ISWTC)+V22I(IHAVEP,ISWTC)-BI*(U22R(IHAVEP,ISWTC)
1H)-C22R(IHAVEP,ISWTC))
IF THE INTERBLADE PHASE ANGLE IS ZERO, SIMPLIFY THE NORMAL
VELOCITY COMPUTATION.
IF(DELTA.LT.1.OE-05)GO TO 1
V22R(I,ISWTC)=-COS(DELTA*XN)+XSUBO*REDFRQ*SIN(DELTA*XN))/S
V22I(I,ISWTC)=-SIN(DELTA*XN)-XSUBO*REDFRQ*COS(DELTA*XN))/S
GC TO 2
1 V22R(I,ISWTC)=-1.O/S
2 K34R=V22R(I,ISWTC)
K34I=V22I(I,ISWTC)
G1=1.O-AI*BI
G2=2.O*BI
G3=G1*G1+G2*G2
G4=K56R-K34R-BI*K12I
G5=K56I-K34I+BI*K12R
U22R(I,ISWTC)=(G4*G1+G5*G2)/G3
U22I(I,ISWTC)=(-G4*G2+G5*G1)/G3
C22R(I,ISWTC)=K12R-U22R(I,ISWTC)+AI*U22I(I,ISWTC)
C22I(I,ISWTC)=K12I-U22I(I,ISWTC)-AI*U22R(I,ISWTC)
K34R=U22R(I,JSWTC)-V22R(I,JSWTC)-C22I(I,JSWTC)
1H))
K34I=U22I(I,JSWTC)-V22I(I,JSWTC)-C22R(I,JSWTC)
1H))
V33R(I,ISWTC)=V22R(I,ISWTC)
V33I(I,ISWTC)=V22I(I,ISWTC)
K56R=V33R(I,ISWTC)
K56I=V33I(I,ISWTC)
G4=K56R+K34R-BI*K12I
G5=K56I+K34I+BI*K12R
U33R(I,ISWTC)=(G4*G1+G5*G2)/G3
U33I(I,ISWTC)={-G4*G2+G5*G1}/G3
00004150
00004160
00004170
00004180
00004190
00004200
00004210
00004220
00004230
00004240
00004250
00004260
00004270
00004280
00004290
00004300
00004310
00004320
00004330
00004340
00004350
00004360
00004370
00004380
00004390
00004400
00004410
00004420
00004430
00004440
00004450
00004460
00004470
00004480
00004490
00004500
00004510
00004520
00004530
00004540
00004550
00004560
00004570
00004580
00004590
00004600
00004610
00004620

```



```

C33R(I,ISWTCR)=K12R-U33R(I,ISWTCR)+AI*U33I(I,ISWTCR)
C33I(I,ISWTCR)=K12I-U33I(I,ISWTCR)-AI*U33R(I,ISWTCR)
NUM=NUM+1
WRITE(6,100)NUM
NUM=NUM-1
100 FORMAT('O',I0X,'BLADE #',I2,/)
147 WRITE(6,145)X(I,ISWTCR),U22R(I,ISWTCR),U22I(I,ISWTCR),
1V22R(I,ISWTCR),V22I(I,ISWTCR),C22R(I,ISWTCR),C22I(I,ISWTCR),
2,ISWTCR)
WRITE(6,145)X(I,ISWTCR),U33R(I,ISWTCR),U33I(I,ISWTCR),
1V33R(I,ISWTCR),V33I(I,ISWTCR),C33R(I,ISWTCR),C33I(I,ISWTCR),
2,ISWTCR)
145 FORMAT(2H N,7E16.7,/)
RETURN
END

```

```

SUBROUTINE WAKE
WAKE COMPUTES U,V, AND C ABOVE AND BELOW THE SLIP PLANE AFT OF A
BLADE.
DIMENSION A(8,8),B(8)
DIMENSION U22R(400,2),U22I(400,2),V22R(400,2),C22R(400,2),C22I(400,2)
1,2),C22I(400,2),X(400,2),Y(400,2)
DIMENSION U33R(400,2),U33I(400,2),V33R(400,2),C33R(400,2),C33I(400,2)
1,2),C33I(400,2)
COMMON/BLK1/NGRDFN,FSTRMN,REDFRQ,XSUBO,TNWCST,FMANGL,XLNGTH,DELTAS
1,DSTSTR,HDSTRL,TRNGLH,U22R,U22I,V22R,V22I,C22R,C22I,X,Y,S,DELTA,
2,ISWTCR,JSWTCR,JLINE,IHAVEP,AI,BI,K12R,K12I,K34R,K34I,K56R,K56I,
3VRPANL,VIPANL,STGANL,STGANG,NSTPTS,LCCOUNT,STAG
CCMMON/BLK5/U33R,U33I,V33R,V33I,C33R,C33I
REAL K12R,K12I,K34R,K34I,K56R,K56I
I=IHAVEP
II=IHAVEP+1
J=ISWTCR
JJ=JSWTCR

```

```

CCMPUTE RIGHT HAND SIDE OF EQUATIONS.
B(1)=U22R(I,JJ)+C22R(I,JJ)+AI*U22I(I,JJ)
B(2)=U22I(I,JJ)+C22I(I,JJ)-AI*U22R(I,JJ)
B(3)=U22R(I,JJ)+V22R(I,JJ)+BI*(U22I(I,JJ)-C22I(I,JJ))
B(4)=U22I(I,JJ)+V22I(I,JJ)-BI*(U22R(I,JJ)-C22R(I,JJ))
B(5)=U33R(I,JJ)+C33R(I,JJ)+AI*U33I(I,JJ)
B(6)=U33I(I,JJ)+C33I(I,JJ)-AI*U33R(I,JJ)
B(7)=U22R(I,JJ)+V22R(I,JJ)+BI*(U22I(I,JJ)-C22I(I,JJ))
B(8)=U22I(I,JJ)+V22I(I,JJ)-BI*(U22R(I,JJ)-C22R(I,JJ))

```



C  
C  
C

SET UP MATRIX OF COEFFICIENTS.

```
DO 1 K=1,8
DC 1 L=1,8
A(K,L)=0.0
1 CONTINUE
A(1,1)=1.0
A(2,2)=1.0
A(3,3)=1.0
A(4,4)=1.0
A(5,5)=1.0
A(6,6)=1.0
A(7,7)=1.0
A(8,8)=1.0
A(1,2)=-AI
A(2,1)=-AI
A(3,1)=AI
A(4,1)=-BI
A(5,2)=-BI
A(6,3)=BI
A(7,4)=-BI
A(8,5)=BI
A(1,3)=BI
A(2,4)=BI
A(3,5)=BI
A(4,6)=BI
A(5,7)=BI
A(6,8)=BI
A(7,8)=-1.0
A(8,6)=1.0
CALL SI(MQ,A,B,8,KS)
U22R(I,I,J,J)=B(1)
U33R(I,I,I,J)=B(2)
U33R(I,I,I,I)=B(3)
V22R(I,I,I,J)=B(4)
V22R(I,I,I,I)=B(5)
C22R(I,I,I,I)=B(6)
V33R(I,I,I,I)=B(7)
C33R(I,I,I,I)=B(8)
```

00005090  
00005100  
00005110  
00005120  
00005130  
00005140  
00005150  
00005160  
00005170  
00005180  
00005190  
00005200  
00005210  
00005220  
00005230  
00005240  
00005250  
00005260  
00005270  
00005280  
00005290  
00005300  
00005310  
00005320  
00005330  
00005340  
00005350  
00005360  
00005370  
00005380  
00005390  
00005400  
00005410  
00005420  
00005430  
00005440  
00005450  
00005460  
00005470  
00005480  
00005490  
00005500  
00005510  
00005520  
00005530  
00005540  
00005550  
00005560







```

C
C
C
RETURN
END
00005570
00005580

SUBROUTINE BOTTOM
00005590
BOTTOM COMPUTES U,V, AND C AT A LOWER SURFACE POINT.
00005600
00005610
00005620
00005630
00005640
00005650
00005660
00005670
00005680
00005690
00005700
00005710
00005720
00005730
00005740
00005750
00005760
00005770
00005780
00005790
00005800
00005810
00005820
00005830
00005840
00005850
00005860
00005870
00005880
00005890
00005900
00005910
00005920
00005930
00005940
00005950
00005960
00005970

DIMENSION U22R(400,2),U22I(400,2),V22R(400,2),V22I(400,2),C22R(400,2),C22I(400,2),X(400,2),Y(400,2)
DIMENSION U33R(400,2),U33I(400,2),V33R(400,2),V33I(400,2),C33R(400,2),C33I(400,2)
COMMON/BLK1/NGRDFN,FSTRMN,REDFRG,XSUBO,TNWCST,FMANGL,XLNGTH,DELTA
1,DSSTSTR,HDSSTRL,TRNGLH,U22R,U22I,V22R,V22I,C22R,C22I,X,Y,S,DELTA,
2,ISWITCH,JSWITCH,JLINE,IHAVEP,AI,BI,K12R,K12I,K34R,K34I,K56R,K56I,
3VRPANL,VIPANL,STGANG,NSIPT,LCOUNT,STAG
COMMON/BLK5/U33R,U33I,V33R,V33I,C33R,C33I
REAL K12R,K12I,K34R,K34I,K56R,K56I
I=IHAVEP
J=JSWITCH
II=IHAVEP+1
JJ=ISWITCH
K12R=U33R(I,J)+C33R(I,J)+AI*U33I(I,J)+AI*U33I(I,J)
K12I=U33I(I,J)+C33I(I,J)-AI*U33R(I,J)-AI*U33R(I,J)
K34R=U22R(II,J)-V22R(II,J)+BI*(U22I(II,J)-C22I(II,J))
K34I=U22I(II,J)-V22I(II,J)-BI*(U22R(II,J)-C22R(II,J))
V33R(II,JJ)=V22R(II,JJ)
V33I(II,JJ)=V22I(II,JJ)
K56R=V33R(II,JJ)
K56I=V33I(II,JJ)
G1=L.0-AI*BI
G2=2.0*BI
G3=G1+G2*G2
G4=K56R+K34R-BI*K12I
G5=K56I+K34I+BI*K12R
U33R(II,JJ)=(G4*G1+G5*G2)/G3
U33I(II,JJ)=(-G4*G2+G5*G1)/G3
C33R(II,JJ)=K12R-U33R(II,JJ)-AI*U33I(II,JJ)
C33I(II,JJ)=K12I-U33I(II,JJ)-AI*U33R(II,JJ)
WRITE(6,100)X(II,ISWITCH),U33R(II,ISWITCH),U33I(II,ISWITCH),V33R(II,ISWITCH),V33I(II,ISWITCH)
100 FORMAT(2H B,7E16.7,/)
RETURN

```



# THE SAUER-HEINZ PROCEDURE

```

REAL MACH, MANGL
DIMENSION X(200,2), R(200,2), U(200,2), V(200,2), CP(200)
COMMON/BLK1/X,R,U,V,ISWITCH,JSWITCH,IHAVEP,CP
COMMON/BLK3/BETA,PI,HO,XM,RO
COMMON/BLK4/KOUNT,DELTA,X,DELTA,Y
COMMON/BLK5/MANGL
COMMON/BLK6/RO,MREQ,NGFN
READ(5,100)MACH,RO,MREQ,NGFN
WRITE(6,101)NGFN,MACH,MREQ,HO,RO

```

# SET UP GRID AND LOGIC

```
PI=3.141593
BETA=SQRT(MACH**2-1.0)
MANGL=ARCSIN(1.0/MACH)
FINGRD=FLOAT(NGFN)
NUMPTS=NGFN+1
S=0.5/COS(MANGL)
DELTAS=S/FINGRD
DELTAY=DELTAS*COS(MANG)
DELTAX=DELTAS*SIN(MANG)
XN=FLOAT(MFREQ)
ISWICH=2
JSWICH=1
IHAVEP=0
I=IHAVEP+1
```

## INITIALIZE FLOW QUANTITIES

```
X(I,J,SWTCH)=0.0  
R(I,J,SWTCH)=R0  
U(I,J,SWTCH)=0.0  
V(I,J,SWTCH)=0.0  
KCUNT=1
```

2 CALL COMPR

IF POINT IS NOT ON THE INITIAL MACH LINE, GO TO 3.

```

9 IF (IHAVEP.NE.0)GO TO 3
  U(1,ISWITCH)=0.0
  V(1,ISWITCH)=0.0
  IHAVEP=IHAVEP+1
  GO TO 2

```

IF POINT IS ON THE SURFACE, CALL SURFAC.

3 IF(IHAVP.EQ.KOUNT)GO TO 4

00000020
00000030
00000040
00000050
00000060
00000070
00000080
00000090
00000100
00000110
00000120
00000130
00000140
00000150
00000160
00000170
00000180
00000190
00000200
00000210
00000220
00000230
00000240
00000250
00000260
00000270
00000280
00000290
00000300
00000310
00000320
00000330
00000340
00000350
00000360
00000370
00000380
00000390
00000400
00000410
00000420
00000430
00000440
00000450
00000460
00000470
00000480
00000490



```

CALL GENFPT
IHAVEP=IHAVEP+1
GO TO 2
4 CALL SURFAC
IF THIS IS THE LAST SURFACE POINT, TERMINATE THE PROGRAM.
IF(X(IHAVEP+1,ISWITCH).GE.1.0)GO TO 7
AFTER MEETING SURFACE, SWITCH LOGIC VARIABLES TO GO BACK
TO THE INITIAL MACH LINE.
IHAVEP=0
IF(ISWITCH.EQ.1)GO TO 5
ISWITCH=1
JSWITCH=2
GO TO 6
5 ISWITCH=2
JSWITCH=1
6 KCOUNT=KOUNT+1
GO TO 2
7 CONTINUE
100 FFORMAT(3,F10.5,2I10)
101 FFORMAT(1,10X,'SUPERSONIC FLOW OVER A CYLINDRICAL SHELL: THE SAUE
1R-HEINZ PROCEDURE',//,15X,'GRID FINENESS=',15,/,15X,'MACH00000740
2 NUMBER=',F11.6,/,15X,'AXIAL MODE # =',I3,/,15X,'AMPLITUDE=',F10
3.5,/,15X,'RADIUS TO LENGTH RATIC=',F10.5,/)
102 FFORMAT(F10.5)
103 FFORMAT(0,
1,R,145,U,T60,V,T75,CP,/)
STOP
END

```

```

00000500
00000510
00000520
00000530
00000540
00000550
00000560
00000570
00000580
00000590
00000600
00000610
00000620
00000630
00000640
00000650
00000660
00000670
00000680
00000690
00000700
00000710
00000720
00000730
00000740
00000750
00000760
00000770
00000780
00000790
00000800
00000810

```

```

SUBROUTINE GENFPT
GENFPT COMPUTES THE FLOW QUANTITIES IN THE GENERAL FLOW FIELD.
DIMENSION X(200,2),R(200,2),U(200,2),V(200,2),CP(200)
COMMON/BLK1/X,R,U,V,ISWITCH,JSWITCH,IHAVEP,CP
COMMON/BLK3/BETA,PI,H0,XM,RC
COMMON/BLK4/KOUNT,DELTAX,DELTAY
I=IHAVEP+1
RETA=(R(IHAVEP,ISWITCH)+R(I,ISWITCH))/2.0
RZETA=(R(I,JSWITCH)+R(I,ISWITCH))/2.0
A=V(IHAVEP,ISWITCH)-V(I,JSWITCH)+BETA*(RETA*U(IHAVEP,ISWITCH)+RZETA*U
1(I,JSWITCH))
B=BETA*(RZETA+RETA)

```

```

00000820
00000830
00000840
00000850
00000860
00000870
00000880
00000890
00000900
00000910
00000920
00000930
00000940
00000950

```









```

C      SUBROUTINE COMXPX
C      CCMPXR COMPUTES THE X,R POSITION OF THE GRIC POINT AND DETERMINES
C      THE VALUE OF X AND R AT THE INTERSECTION OF THE RIGHT- RUNNING
C      MACH LINE WITH THE SURFACE.
C
C      REAL MANGL
C      DIMENSION X(200,2),R(200,2),U(200,2),V(200,2),CP(200),DELX(200),DE
1LR(200)
C      CCMMON/BLK1/X,R,U,V,ISWITCH,JSWITCH,IHAVEP,CP
C      CCMMON/BLK3/BETA,PI,HO,XM,RC
C      CCMMON/BLK4/KOUNT,DELTAX,DELTAY
C      CCMMON/BLK5/MANGL
C
C      CHECK WHETHER POINT IS ON THE INITIAL MACH LINE.
C
C      IF(IHAVEP.EQ.0)GO TO 1
C      I=IHAVEP+1
C
C      CHECK WHETHER THIS IS A SURFACE POINT.
C
C      IF(IHAVEP.EQ.KOUNT)GO TO 2
C      X(I,ISWITCH)=X(IHAVEP,ISWITCH)+DELX(IHAVEP)
C      R(I,ISWITCH)=R(IHAVEP,ISWITCH)-DELR(IHAVEP)
C      RETURN
1  X(1,ISWITCH)=X(1,JSWITCH)+DELTAX
C      R(1,ISWITCH)=R(1,JSWITCH)+DELTAY
C      RETURN
C
C      COMPUTE THE POINT OF INTERSECTION.
C
2  YO=2.0*KOUNT*DELTAY
C      XMAX=X(IHAVEP,ISWITCH)
3  F=-TAN(MANGL)*XMAX-HO*SIN(XM*PI*XMAX)+YO
C      FP=-TAN(MANGL)-HO*XM*PI*COS(XM*PI*XMAX)
C      FAC=F/FP
C      XMAX=XMAX-FAC
C      IF(ABS(FAC).GT.0.00001)GO TO 3
C      X(I,ISWITCH)=XMAX
C      R(I,ISWITCH)=HO*SIN(XM*PI*XMAX)+RO
C      DELX(KOUNT)=XMAX-X(IHAVEP,ISWITCH)
C      DELR(KOUNT)=R(IHAVEP,ISWITCH)-R(I,ISWITCH)
C      RETURN
C      END
C
00001410
00001420
00001430
00001440
00001450
00001460
00001470
0000001480
00001490
00001500
00001510
00001520
00001530
00001540
00001550
00001560
00001570
00001580
00001590
00001600
00001610
00001620
00001630
00001640
00001650
00001660
00001670
00001680
00001690
00001700
00001710
00001720
00001730
00001740
00001750
00001760
00001770
00001780
00001790
00001800
00001810
00001820
00001830
00001840

```



C  
C  
C

# METHOD OF SINGULARITIES FOR TWO-BLADE CASCADE WITH SUBSONIC LEADING EDGE LCCU

```

REAL M
DIMENSION PNR(2), PNI(2)
COMMON/BLK1/PHIR,PHIL,PHIXR,PHIXI,RF
READ(5,100)M,RF,GRDFN,Y,STGR
WRITE(6,101)M,RF,GRDFN,Y,STGR
WRITE(6,104)
BETA=SQRT(M**2-1.0)
D=0.00001
N=0
DU=1.0/GRDFN
X=Y*BETA
STGR=STGR*0.01745
4 CONTINUE
DC 2 J=1,2
FOR=0.0
FOI=0.0
FOS=0.0
FOT=0.0
U=0.0
AA=BETA*Y
IF(J.EQ.1)GO TO 3
X=X-Y*TAN(STGR)
ARGC=0.0
ARGD=0.0
IF(X.EQ.0.0)GO TO 12
IF(X.LT.0.0001)GO TO 7
AA=0.0
3 CONTINUE
FAC=X-AA
XX=FAC/DU+1.0
LIMIT=XX
LIMX=XX-LIMIT
IF(XX.GE.0.5)LIMIT=LIMIT+1
ARGA=(X-U)*RF**M**2/BETA**2
ARGB=(RF*M/BETA**2)*SQRT(ABS((X-U)**2-AA**2))
ARGC=X*RF**M**2/BETA**2
ARGD=RF**M**SQRT(ABS(X**2-AA**2)/BETA**2)
IF(LIMIT.LE.1)GO TO 12
8 CALL BESJ(ARGB,N,BJ,D,IER)
A1=SIN(ARGA)*BJ*RF
B1=SIN(ARGA)*BJ*RF
C1=COS(ARGA)*BJ*RF
D1=COS(ARGA)*BJ*RF
9 DC 1 I=2,LIMIT
00000010
00000020
00000030
00000040
00000050
00000060
00000070
00000080
00000090
00000100
00000110
00000120
00000130
00000140
00000150
00000160
00000170
00000180
00000190
00000200
00000210
00000220
00000230
00000240
00000250
00000260
00000270
00000280
00000290
00000300
00000310
00000320
00000330
00000340
00000350
00000360
00000370
00000380
00000390
00000400
00000410
00000420
00000430
00000440
00000450
00000460
00000470
00000480

```



```

00000490
00000500
00000510
00000520
00000530
00000540
00000550
00000560
00000570
00000580
00000590
00000600
00000610
00000620
00000630
00000640
00000650
00000660
00000670
00000680
00000690
00000700
00000710
00000720
00000730
00000740
00000750
00000760
00000770
00000780
00000790
00000800
00000810
00000820
00000830
00000840
00000850
00000860
00000870
00000880
00000890
00000900
00000910
00000920
00000930
00000940
00000950
00000960

```

U=U+DU  
ARGA=(X-U)\*RF\*M\*\*2/BETA\*\*2  
ARGB=(RF\*M/BETA\*\*2)\*SQRT(ABS((X-U)\*\*2-AA\*\*2))  
CALL BESJ(ARGB,N,BJ,D,IER)  
A2=RF\*(-RF\*U\*COS(ARGA)+SIN(ARGA))\*BJ  
B2=BJ\*SIN(ARGA)\*RF  
C2=RF\*( RF\*U\*SIN(ARGA)+COS(ARGA))\*BJ  
D2=BJ\*COS(ARGA)\*RF  
FCR=FOR+(A1+A2)\*DU/2.0  
FOI=FOI+(B1+B2)\*DU/2.0  
FCS=FCS+(C1+C2)\*DU/2.0  
FCT=FCT+(D1+D2)\*DU/2.0  
A1=A2  
B1=B2  
C1=C2  
D1=D2  
CONTINUE  
1 CALL BESJ(ARGD,N,BJ,D,IER)  
PNR(J)=FOR+FOI+COS(ARGC)\*BJ  
PNR(J)=FOS+FOT-SIN(ARGC)\*BJ  
PNR(J)=PNR(J)/BETA  
PNI(J)=PNI(J)/BETA  
IF(J.EQ.2)GO TO 6  
GC TO 2  
PNR(2)=0.0  
PNI(2)=0.0  
PHIR=0.0  
PHII=0.0  
PHIXR=0.0  
PHIXI=0.0  
VSR=0.0  
VSI=0.0  
X=X+Y\*TAN(STGR)  
GC TO 1  
CALL POTEN(X,VSR,VSI,M,BETA,STGR,Y,GRDFN)  
PN3R=PHIXR-RF\*PHII  
PN3I=PHIXI+RF\*PHIR  
PRESI=PNR(1)+PNR(2)-PN3R  
PRESI=PNI(1)+PNI(2)-PN3I  
WRITE(6,103)X,PNR(1),PNI(1),PNR(2),PNI(2),PHIR,PHII,PHIXR,PHIXI  
WRITE(6,102)PN3R,PN3I,VSR,PRESI  
CONTINUE  
X=X+O.1  
IF(X.LE.Y\*(TAN(STGR)+BETA))GO TO 4  
FORMAT(5F10.5)  
100 FORMAT('1,1,10X,'MACH NUMBER=',F8.6,/,11X,'REDFRQ=',F7.2,/,11X,'GRI00000950'  
101 FORMAT('1,1,10X,'MACH NUMBER=',F8.6,/,11X,'ZN(ZETA)=ZETA',/,11X,'BET00000960'  
102 FINENESS='F7.2,/,11X,'Y=',F3.1,/,11X,'ZN(ZETA)=ZETA',/,11X,'BET00000960'



```

1A='F5.2//')
103 FFORMAT('0',T5,F4.2,T13,F10.5,T27,F10.5,T41,F10.5,T55,F10.5,T69,F10.5,T83,F10.5,T97,F10.5,T111,F10.5)
102 FFORMAT(' ',T13,F10.5,T27,F10.5,T41,F10.5,T55,F10.5,T69,F10.5,T83,F10.5,T97,F10.5,T111,F10.5//)
104 FFORMAT(' ',T7,'X',T16,'PNR(1)',T30,'PNI(1)',T44,'PNR(2)',T58,'PNI(12)',T72,'PHIR',T86,'PHIXR',T100,'PHIXI',T114,'PNR(3)',T130,'PNI(3)',T44,'VSR',T58,'VSI',T72,'PNR',T86,'PNI',/)
2 STOP
END
00000970
00000980
00000990
00001000
00001010
00001020
00001030
00001040
00001050
00001060

```

```

SUBROUTINE VSIGMA(Z,VSR,VSI,M,BETA,STGR,Y,GRDFN)
REAL M
COMMON/BLK1/PHIR,PHI1,PHIXR,PHIXI,RF
D=0.00001
N=1
DU=1.0/GRDFN
X=Z+Y*TAN(STGR)
CCONTINUE
4 FOR=0.0
FOI=0.0
U=0.0
ARGA=(X-U)*RF*M**2/BETA**2
ARGB=RF*M*SQR(ABS((X-U)**2-(BETA*Y)**2))/BETA**2
ARGC=Y*RF*M**2/BETA**2
CALL BESJ(ARGB,N,BJ,D,IER)
A1= COS(ARGA)*BJ/SQRT(ABS((X-U)**2-(BETA)**2))
B1=-SIN(ARGA)*BJ/SQRT(ABS((X-U)**2-(BETA)**2))
XX=(X-BETA*Y)/DU+1.0
LIMIT=XX
DXX=XX-LIMIT
IF(DXX.GE.0.5) LIMIT=LIMIT+1
DO 1 I=2,LIMIT
U=U+DU
ARGA=(X-U)*RF*M**2/BETA**2
ARGB=RF*M*SQR(ABS((X-U)**2-(BETA*Y)**2))/BETA**2
CALL BESJ(ARGB,N,BJ,D,IER)
A2=(RF*U*SIN(ARGA)+COS(ARGA))*BJ/SQRT(ABS((X-U)**2-(BETA*Y)**2))
B2=(RF*U*COS(ARGA)-SIN(ARGA))*BJ/SQRT(ABS((X-U)**2-(BETA*Y)**2))
FCR=FOR+(A1+A2)*DU/2.0
FCI=FOI+(B1+B2)*DU/2.0
A1=A2
B1=B2
1 CONTINUE
FCR=FOR*RF*M*Y/BETA
FCI=FOI*RF*M*Y/BETA
S=-RF*(X-Y*BETA)*SIN(ARGC)-COS(ARGC)
0001070
0001080
0001090
0001100
0001110
0001120
0001130
0001140
0001150
0001160
0001170
0001180
0001190
0001200
0001210
0001220
0001230
0001240
0001250
0001260
0001270
0001280
0001290
0001300
0001310
0001320
0001330
0001340
0001350
0001360
0001370
0001380
0001390
0001400
0001410
0001420

```





```

T=-RF*(X-Y*BETA)*COS(ARGC)+SIN(ARGC)
VSR=FOR+S
VSI=FOI+T
RETURN
END

```

```

00001430
00001440
00001450
00001460
00001470

```

```

SUBROUTINE POTEN(X,VSR,VSI,M,BETA,STGR,Y,GRDFN)
REAL M
COMMON/BLK1/PHIR,PHII,PHIXR,PHIXI,RF
U=0.0
DU=1.0/GRDFN
Z=0.0
ARGA=(X-U)*RF**M**2/BETA**2
ARGB=(X-U)*RF**M/BETA**2
A1=0.0
A2=0.0
B1=0.0
B2=0.0
B3=0.0
B4=0.0
XX=X/DU+1.0
LIMIT=XX
DXX=XX-LIMIT
IF(DXX.GE.0.5)LIMIT=LIMIT+1
N=0
CALL BESJ(ARGB,N,BJ1,D,IER)
N=1
CALL BESJ(ARGB,N,BJ2,D,IER)
CALL VSIGMA(Z,VSR,VSI,M,BETA,STGR,Y,GRDFN)
IF(LIMIT.LE.1)GO TO 2
PR1=(VSR*COS(ARGA)+VSI*SIN(ARGA))*BJ1
PR1=(VSI*COS(ARGA)-VSR*SIN(ARGA))*BJ1
PP1=(VSR*SIN(ARGA)-VSI*COS(ARGA))*BJ1
PP2=(VSR*CCS(ARGA)+VSI*SIN(ARGA))*BJ2
PP3=(VSR*CCS(ARGA)+VSI*SIN(ARGA))*BJ1
PP4=(-VSR*SIN(ARGA)+VSI*CCS(ARGA))*BJ2
DO 1 I=2,LIMIT
U=U+DU
Z=U
ARGA=(X-U)*RF**M**2/BETA**2
ARGB=(X-U)*RF**M/BETA**2
N=0
CALL BESJ(ARGB,N,BJ1,D,IER)
N=1
CALL BESJ(ARGB,N,BJ2,D,IER)
CALL VSIGMA(Z,VSR,VSI,M,BETA,STGR,Y,GRDFN)
PR2=(VSR*COS(ARGA)+VSI*SIN(ARGA))*BJ1

```

```

00001480
00001490
00001500
00001510
00001520
00001530
00001540
00001550
00001560
00001570
00001580
00001590
00001600
00001610
00001620
00001630
00001640
00001650
00001660
00001670
00001680
00001690
00001700
00001710
00001720
00001730
00001740
00001750
00001760
00001770
00001780
00001790
00001800
00001810
00001820
00001830
00001840
00001850
00001860
00001870
00001880

```



```

PI2=(VSI* COS(ARGA)-VSR* SIN(ARGA))*BJ1
PP5=(VSR* SIN(ARGA)-VSI* COS(ARGA))*BJ1
PP6=(VSR* COS(ARGA)+VSI* SIN(ARGA))*BJ2
PP7=(VSR* COS(ARGA)+VSI* SIN(ARGA))*BJ1
PP8=(-VSR* SIN(ARGA)+VSI* COS(ARGA))*BJ2
A1=A1+(PR1+PR2)*DU/2.0
A2=A2+(PI1+PI2)*DU/2.0
B1=B1+(PP1+PP5)*DU/2.0
B2=B2+(PP2+PP6)*DU/2.0
B3=B3+(PP3+PP7)*DU/2.0
B4=B4+(PP4+PP8)*DU/2.0
PR1=PR2
PI1=PI2
PP1=PP5
PP2=PP6
PP3=PP7
PP4=PP8
CONTINUE
PHIR=A1*(-1.0/BETA)
PHII=A2*(-1.0/BETA)
PHIXR=(M*B1+B2)*RF*M/(BETA**1.5)-(1.0/BETA)*VSR
PHIXI=(M*B3+B4)*RF*M/(BETA**1.5)-(1.0/BETA)*VSI
X=X+Y*TAN(STGR)
RETURN
END
1
2

```

```

0001890
00001900
00001910
00001920
00001930
00001940
00001950
00001960
00001970
00001980
00001990
00002000
00002010
00002020
00002030
00002040
00002050
00002060
00002070
00002080
00002090
00002100
00002110
00002120
00002130

```



### LIST OF REFERENCES

1. Bisplinghoff, R. L., Ashley, H., and Halfman, R. L., Aeroelasticity, Addison-Wesley, 1955.
2. Dowell, E. H., and Widnall, S. E., Generalized Aerodynamic Forces on an Oscillating Cylindrical Shell, MIT, 1966.
3. Teipel, I., "Ein Charakteristikenverfahren zur Berchnung der verallgemeinerten ebenen Flatterluftkrafte," Zeitschrift fur Flugwissenschaften, v. 10, p. 374-379, October, 1962.
4. Leonard, R. W., and Hedgepeth, J. M., "On Panel Flutter and Divergence of Infinitely Long Unstiffened and Ring-Stiffened Thin-Walled Circular Cylinders," NACA Report 1302, 1957.
5. Matsuzaki, Y. and Kobayashi, S., "Unsteady Supersonic Aerodynamic Forces on an Oscillating Circular Cylindrical Shell," AIAA Journal 9, No. 12, p. 2358-2362, December 1971.
6. Dowell, E. H., Panel Flutter: A Review of the Aeroelastic Stability of Plates and Shells, AIAA Journal, Vol. 8, No. 3, March 1970.
7. Platzer, M. F., Brix, C. W., Jr. and Webster, K. A., "A Linearized Characteristics Method for Supersonic Flow Past Vibrating Shells," to be published in AIAA Journal, submitted March 1973.
8. Snyder, L. E., "Supersonic Torsional Flutter in Cascades," Final Technical Report PWA-4701, 2 April 1973, Pratt and Whitney Aircraft, East Hartford, Conn.
9. Chalkley, H. G., A Study of Supersonic Cascade Flutter, Aeronautical Engineer's Thesis, Naval Postgraduate School, March, 1972.
10. Webster, K. A., A Study of Supersonic Flow Past Vibrating Panels and Shells, Master's Thesis, Naval Postgraduate School, March, 1972.
11. Sauer, R., and Heinz, C., Unpublished report, see "Gas-dynamics" by K. Oswatitsch, Academic Press, 1956, New York and London.



12. Garrick, I. E., and Rubinow, S. J., Flutter and Oscillating Air-Force Calculations for an Airfoil in Two-Dimensional Supersonic Flow, NACA Report 846, 1946.
13. Detroit Diesel Allison Report, "Aeroelasticity in Turbomachines," Proceedings of a workshop held at Detroit Diesel Allison, June 1-2, 1972. Project SQUID, Office of Naval Research.
14. Anderson, W. J., Oscillatory Pressure in an Idealized Boundary Layer with an Application to the Panel Flutter of Cylindrical Shells, AIAA Journal, Vol. 4, No. 5, May 1966.





INITIAL DISTRIBUTION LIST

	No. Copies
1. Defense Documentation Center Cameron Station Alexandria, Virginia 22314	2
2. Library, Code 0212 Naval Postgraduate School Monterey, California 93940	2
3. Professor R. W. Bell, Code 57Be Department of Aeronautics Naval Postgraduate School Monterey, California 93940	1
4. Assoc. Professor M. F. Platzter, Code 57Pl Department of Aeronautics Naval Postgraduate School Monterey, California 93940	15
5. LT C. W. Brix, Jr., USN GM DIV, Weapons Department USS Enterprise (CVAN-65) FPO San Francisco, California 96601	1
6. Dr. H. J. Mueller (AIR - 310) Naval Air Systems Command Washington, D. C. 20360	1
7. Professor M. H. Vavra, Code 57Va Department of Aeronautics Naval Postgraduate School Monterey, California 93940	1



UNCLASSIFIED

Security Classification

## DOCUMENT CONTROL DATA - R &amp; D

(Security classification of title, body of abstract and indexing annotation must be entered when the overall report is classified)

ORIGINATING ACTIVITY (Corporate author)

Naval Postgraduate School  
Monterey, California 93940

2a. REPORT SECURITY CLASSIFICATION

UNCLASSIFIED

2b. GROUP

REPORT TITLE

A Study of Supersonic Flow Past Vibrating Shells and Cascades

DESCRIPTIVE NOTES (Type of report and, inclusive dates)

Aeronautical Engineer's Thesis; June 1973

AUTHOR(S) (First name, middle initial, last name)

Christian W. Brix, Jr.

REPORT DATE

June 1973

7a. TOTAL NO. OF PAGES

133

7b. NO. OF REFS

14

CONTRACT OR GRANT NO.

9a. ORIGINATOR'S REPORT NUMBER(S)

PROJECT NO.

9b. OTHER REPORT NO(S) (Any other numbers that may be assigned this report)

DISTRIBUTION STATEMENT

Approved for public release; distribution unlimited.

SUPPLEMENTARY NOTES

12. SPONSORING MILITARY ACTIVITY

Naval Postgraduate School  
Monterey, California 93940

ABSTRACT

Supersonic flow past oscillating cylindrical shells and oscillating flat-plate cascades is analyzed distributions and generalized aerodynamic forces are computed for arbitrary radius-to-length ratios. Axial and circumferential wave numbers, Mach number, and reduced frequencies. Excellent agreement is obtained with a previous solution of the complete unsteady linearized potential equation by Dowell and Widnall using Laplace transform techniques. Also, pressure distributions are computed for flat-plate cascades with subsonic leading edge locus for arbitrary solidity, stagger angle, frequency, and interblade phase angle. For comparison, a two-blade solution is developed using the method of singularities. Good agreement is obtained for this special case.

FORM 1473

(PAGE 1)

132

UNCLASSIFIED

Security Classification

A-31408



Method of Characteristics

Supersonic

Cascade

Cylindrical Shell



Thesis

B80915

c.1

Brix

A study of supersonic  
flow past vibrating  
shells and cascades.

144296

Thesis

B80915

c.1

Brix

A study of supersonic  
flow past vibrating  
shells and cascades.

144296

thesB80915

A study of supersonic flow past vibratin



3 2768 002 08111 9

DUDLEY KNOX LIBRARY